THE UNIVERSITY OF ALBERTA

A MODEL STUDY OF AN UNCONSOLIDATED
SANDSTONE SYSTEM

A THESIS
SUBMITTED TO THE FACULTY OF GRADUATE STUDIES
IN PARTIAL FULFILLMENT OF THE REQUIREMENTS FOR THE
DEGREE OF MASTER OF SCIENCE IN PETROLEUM ENGINEERING

DEPARTMENT OF CHEMICAL AND PETROLEUM ENGINEERING

by

K.C.G. PRITCHARD

EDMONTON, ALBERTA

FEBRUARY, 1962

ABSTRACT

There is little data in the literature regarding the performance of a nine-spot water flood project. The ultimate objective of this research was to obtain such data, with special emphasis on oil recovery after water breakthrough.

Before such data was obtained, several preliminary investigations were undertaken on the sand-fluid system, utilizing synthetic core models. Good capillary pressure and effective permeability characteristics were obtained, although they deviated somewhat from literature results reported on unconsolidated sandstones. An investigation of the rate of injection at which oil recovery is rate independent was carried out. Results showed that this type of critical rate did not exist for this system but rather that there was an optimum rate with recovery declining at high rates: some attempt is made to account for this phenomenon.

Four well patterns were studied on the two dimensional sand models: confined five-spot, isolated five-spot, line drive, and nine-spot. Two models and two viscosity oils were used. High recoveries to breakthrough were experienced on all isolated floods run on the low viscosity oil and the small model. Some postulates regarding this are put forward. For three floods run on the same sand-fluid system, the line-drive was more efficient than the five-spot or nine-spot. Although a universal nine-spot correlation for areal sweep efficiency as a function of water injected was not obtained for a wide range of mobility ratio, several general conclusions are made regarding the performance of these floods.

ACKNOWLEDGEMENTS

The writer wishes to express his gratitude to Dr. D.L Flock, Department of Chemical and Petroleum Engineering, University of Alberta, under whose direction this research project was undertaken.

Thanks are also due to Mr. Frank Butz, Mr. Ray Kirby, and the technical staff of the Chemical and Petroleum Engineering shop for their assistance in the design and construction of equipment. The writer is also indebted to many friends and colleagues who gave of their time and knowledge in making helpful suggestions and construction criticisms regarding both the experimental techniques employed and the results obtained.

TABLE OF CONTENTS

LIST OF TABLES

iii

LIST OF FIGURES

1

INTRODUCTION

Many of the fundamental properties of an oil reservoir are evaluated by core analysis. The techniques and apparatus used have been readily adapted to studying the effects of water flooding in core specimens. While this work indicated many of the effects and phenomena of the process, it has proven difficult to apply the results of these linear investigations to a two dimensional oil field project except in the most qualitative manner.

In an attempt to introduce the concept of two dimensional flow, investigators utilized potentiometric, electrolytic, and mathematical models. Several analogies between electrical flow, heat flow, and fluid flow have been devised. However, in spite of this abundance of data, it became evident that if the many variables encountered in secondary recovery projects were to be adequately studied, laboratory equipment which more closely resembled the actual field operation must be used. This lead to the advent of the two dimensional geometric or flow model. Early work on these models utilized unit patterns (such as 1/4 of a five-spot pattern) and, by assuming symmetry, the drilled out pattern and its performance would be evaluated. Lately the trend has been to duplicate well patterns in their entirety and even whole fields on a single model.

Reservoir models have not been extensively scaled to field prototypes. However, several attempts at dimensional analysis and the use of dimensionless groupings of fundamental properties have been made. To date there is much controversy as to what properties should be scaled and which may be ignored. However, it is conceivable that, with time, the scaling of model

oil reservoirs will be as thoroughly undertaken as the scaling of hydraulic apparatus and transportation vehicles; with the same success in designing and interpretting the performance of the prototype.

The most important pattern on which secondary recovery is undertaken is the "five-spot". This refers to a unit of five wells located on a square pattern; one well at each corner and one in the center. In the isolated case, a central producing well surrounded by injection wells is the normal five-spot; a central injection well surrounded by producers is the inverted pattern. A similar pattern is referred to as the "nine-spot". It is a unit of nine wells on a square pattern, as above, except now there are wells midway along each of the sides of the square. Much research has been done on the five-spot pattern -- although the field is by no means exhausted. To the writer's knowledge little published work is available on the nine-spot pattern.

For this reason, the present research was set up to ultimately investigate the relationship between sweep efficiency and the volume of injection water for a nine-spot water flood project. Before this data was taken, however, it was thought desirable to investigate several preliminary properties of the sand-fluid system to be used in the model studies. A set of experiments, utilizing synthetis core models, was devised and investigations were undertaken of capillary pressure, effective permeabilities and critical rate.

From a literature review it was found that the term sweep efficiency was ambiguous in many cases. Indeed, several component efficiencies made up the efficiency of a water flood project. It was resolved to investigate these components to see if they could be evaluated separately. Sweep

efficiency data was obtained for each of three well patterns: five-spot, line drive, and nine-spot.

From the above preamble it can be seen that the study was carried out in two phases:

1. One dimensional flow studies through synthetic core models, and

2. Two dimensional flow studies through sand packed reservoir models.

<u>STUDY OF FUNDAMENTAL RESERVOIR PROPERTIES</u>

<u>CAPILLARY PRESSURE</u>

<u>Theory</u>

Capillary pressure is a combination of surface tension and wettability effects. It has been described as: "the capillary suction exerted by a wetting phase holding it within the interstices of the rock"[11]. The adhesion tension or attractive force between the rock and the fluids indicates which fluid will wet a given rock type. This leads to the concept of preferential wettability. Where two fluids are present with a solid phase, preferential wettability is measured as a function of the contact angle which the interface between the fluids makes with the rock. By definition the contact angle is measured through the denser liquid phase. This indicates that if the adhesive tension is large and the contact angle small, the denser phase will wet the rock surface.

For capillary tubes, the capillary pressure has been related to the surface tension and wetting angle by the relationship:

$$P_c = \frac{2\gamma \cos\theta}{r} \quad \ldots \ldots \ldots \ldots \ldots \ldots \ldots (1)$$

where P_c is the capillary pressure

γ is the surface tension

$\cos\theta$ is the wetting angle

r is the radius of the capillary tube

In a porous medium the fluids exist in spaces which are capillary in size so that the analogy between a bundle of capillaries has often been used. In an attempt to relate capillary pressure to wetting angle and inter-

facial tension for a porous medium Leverett[14, 15] proposed his "J-function". This J-function is a dimensionless grouping of surface tension, capillary pressure, wetting angle, porosity and permeability as follows:

$$J = \frac{\Delta \rho g h}{\gamma \cos \Theta} \qquad \frac{k}{\phi} \quad \ldots \ldots \ldots \ldots \ldots \ldots (2)$$

where $\Delta \rho$ is the difference in density between the fluids.

          g   is the acceleration of gravity

          h   is the height above some datum.

         P_c = $\Delta \rho$ g h, capillary pressure dynes/cm^2

         γ =   interfacial tensions, dynes/cm.

         k   =   permeability, cm^2

         ϕ =   fractional porosity

         Θ =   contact angle

This J-function was originally proposed as a universal correlation for porous media. Most unconsolidated sandstones do fall in the same range as Leverett's curve but work by Rose and Bruce[22] and Brown[3] indicates that there is considerable variation in the J-function for different porous media.

The problem was to obtain the capillary pressure characteristics for the 30-60 mesh Ottawa sand with which the various synthetic cores and models were constructed. More explicitly, it was to measure capillary pressure as a function of water saturation. Several methods have been devised. One is the Purcell mercury injection apparatus[20]; another is the porous plate, gravity drainage method[19]. For an unconsolidated sediment, neither of these methods can be used. The method which is particularly useful in this case utilizes a long vertical synthetic core or sand packed tube.

The pressure varies over the length of the sand pack, from top to bottom as the head of wetting fluid and after a long period of drainage or imbibition a wide range of saturations is present over the length of the core.

As indicated above, the capillary pressure at any point will be the height of the wetting phase above some datum (in this case the discharge end). The problem reduces to one of measuring the saturations of the wetting phase. Some attempts at this have utilized removable sections of core which could be weighed. However, using this technique, it is difficult to minimize loss of fluid.

A method which utilizes the relationship between resistivity and saturation has been used by some workers[15, 12]. Archie[2] has put forth the following empirical formula, which is widely used in logging work:

$$S_w = \left[\frac{R_O}{R}\right]^{1/n} \quad \ldots \ldots \ldots \ldots \ldots \ldots \ldots \ldots (3)$$

S_w is the water saturation

R_O is the resistivity of the formation when it is entirely saturated with water

R is the resistivity of the formation at water saturation S_w

n is the saturation exponent, generally assumed to be 2.0

Experimental Procedure and Apparatus

To evaluate the capillary pressure properties of the unconsolidated sandstone system, it was decided to use apparatus modified after Leverett[15] and Flock[12]. That is, a lucite tube was fitted with screen electrodes throughout its length (see Figure 1) and packed with the Ottawa sand to a maximum density. This maximum density pack was obtained by aggitating the sand as it was introduced under water.

Rather than use the empirical Archie equation, it was decided to calibrate the core by taking a series of resistance measurements at known saturations. An air-brine mixture was passed through the core (see Figure 1) until equilibrium had been attained. The resistance of each segment was then measured and recorded. The overall saturation of the core was obtained by weighing. If the core followed the Archie relationship, these data plotted on log-log paper should result in a straight line with slope of $1/n$.

Basically, the electrical apparatus consisted of a resistance box used in conjunction with a bridge (see Figure 2). A constant current input was maintained by means of an AC oscillator operating at 100 cps. The resistance box was adjusted until the same voltage reading was obtained in both circuits. As the water saturation of the core was reduced, the resistance of each core segment increased and correspondingly larger settings of the box were required.

Discussion of Results

Figure 3 shows the calibration points plotted on log-log paper. As can be seen, they do not fall on the straight line as expected although possibly some best fit straight line could be passed through them. Figure 4 shows the same data plotted on arithmetic paper. As a reasonably uniform curve can be fitted to these points, these curves were used as the calibration rather than the semi-empirical log-log plot. In order to eliminate end-effects, the end segments were calibrated separately.

To compare the results with those of Leverett, the drainage capillary pressure was converted into the J-function (see Tables 3 and 4). The results are plotted in Figure 5. As can be seen, the J-function of the sand pack is not identical to Leverett's. The points are lower in all cases, although the general shape of the curve is the same.

1/4" TOGGLE VALVE

1/4" PIPE TO PIPE NIPPLE (BRASS)

STAINLESS STEEL SCREEN ELECTRODES

LUCITE CYLINDER

BRONZE PLATE (POROUS)

"O-RING" SEAL

BRASS BOLT

1/4" NYLON TUBING

1/4" PIPE TO TUBING NIPPLE (NYLON)

SAND PACK

SOLDER CONNECTION

BRASS BOLT

VALVE ASSEMBLY AS OTHER SIDE

NOTE: PACK CONTAINS 10 SCREEN ELECTRODES AT 1 1/4" SPACING AND 1 1/4" SPACING FROM BRONZE PLATES
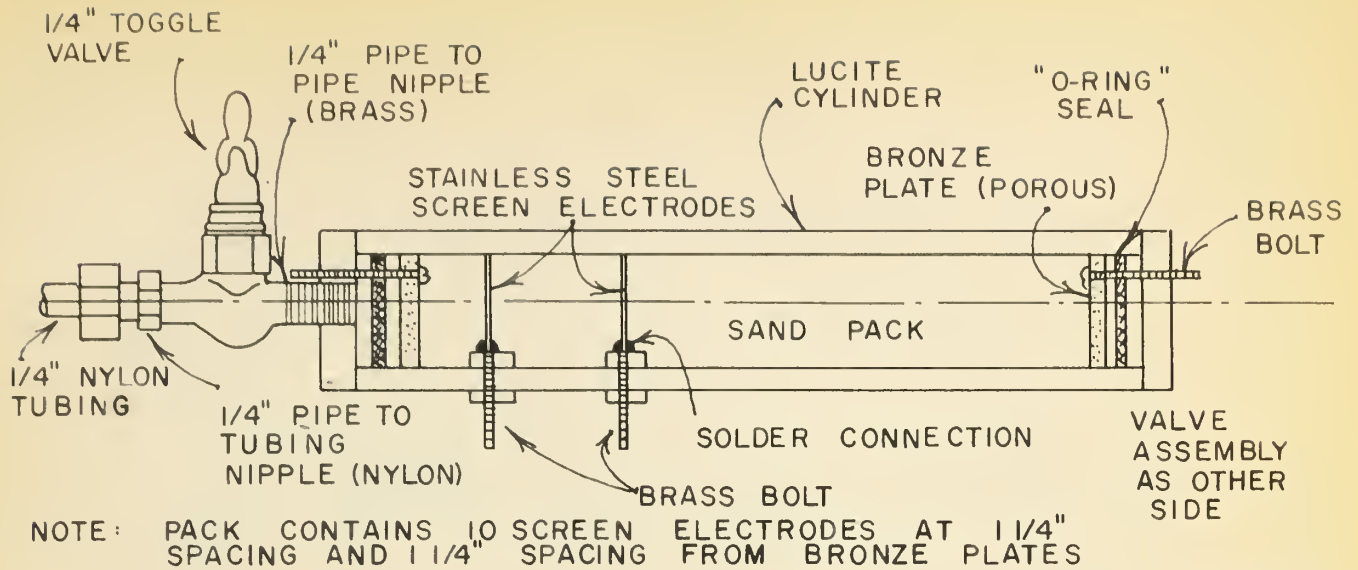
DETAIL OF THE SYNTHETIC CORE

CALIBRATION APPARATUS (TWO-PHASE, AIR-BRINE FLOW)

TO AIR SUPPLY

PRESSURE REGULATOR

BRINE CYLINDER

FLOW

ELECTRODES, WIRING AS PER FIG. 2

DISCHARGE LINE

FLOW

NEEDLE VALVES

CORE (AS ABOVE)

LENGTH OF GRADUATED TRANSPARENT TUBING
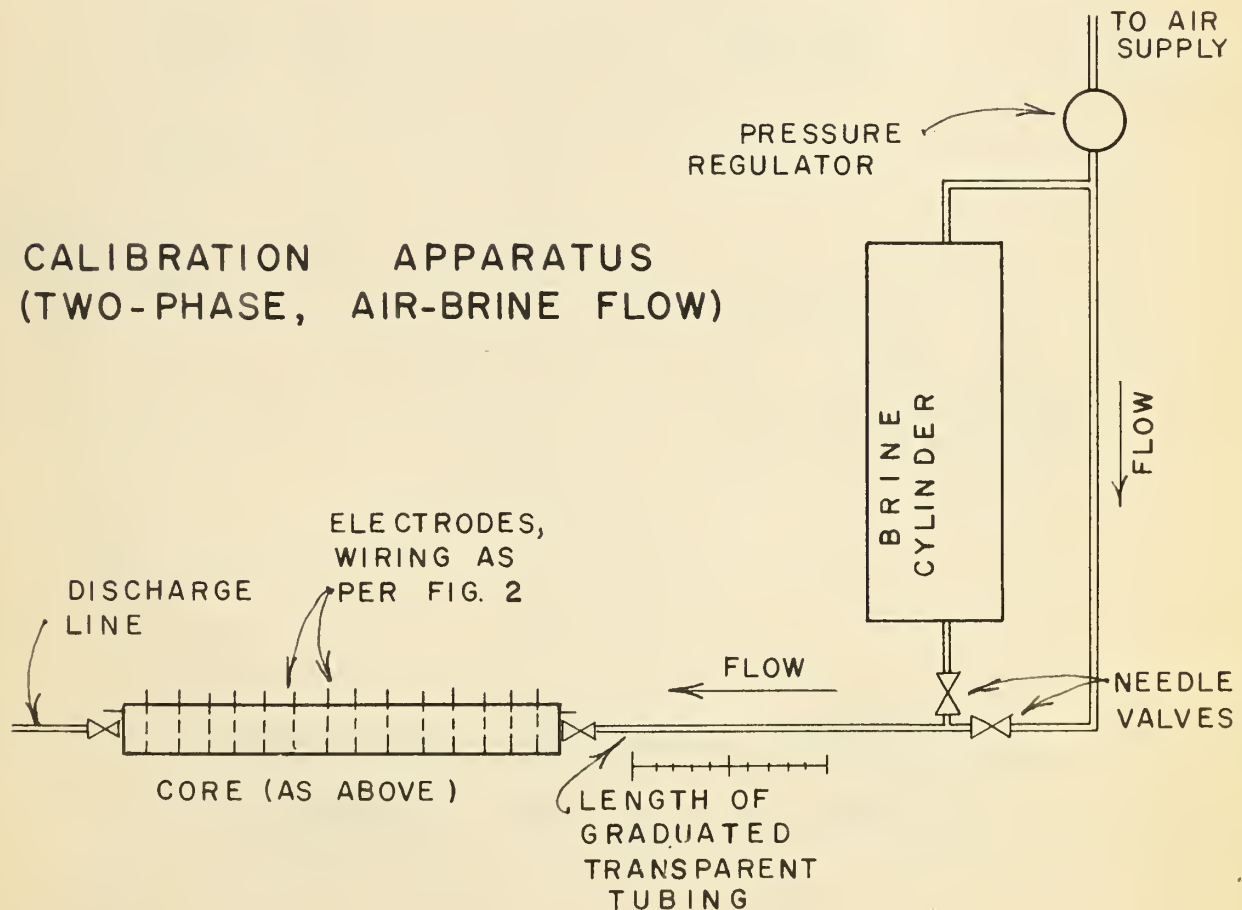
FIG. I   CAPILLARY PRESSURE APPARATUS   DETAIL OF THE SYNTHETIC CORE   AND CALIBRATION SET-UP
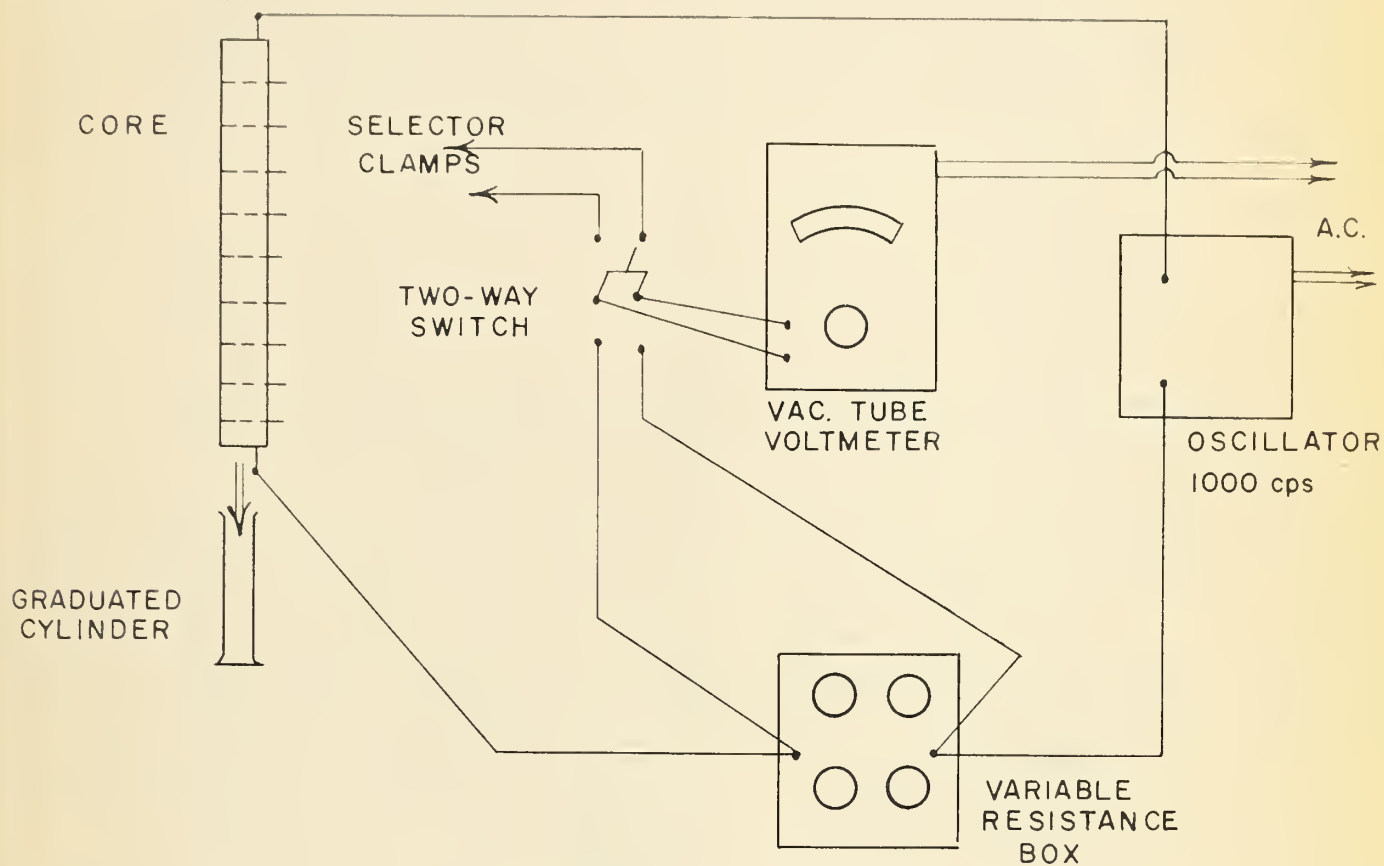
FIG. 2   CAPILLARY PRESSURE APPARATUS   GRAVITY
         DRAINAGE   SET-UP   AND   WIRING   DIAGRAM
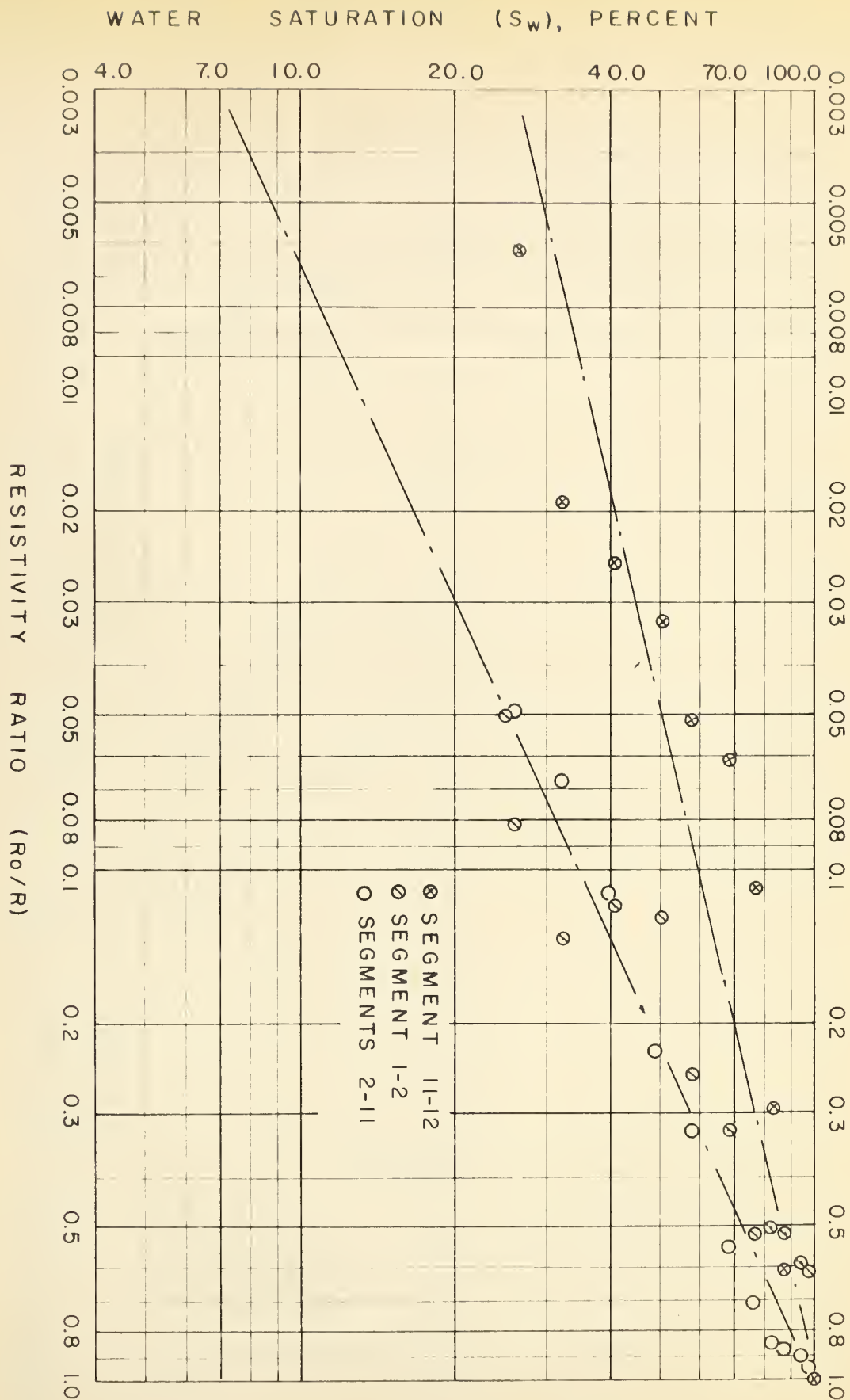
FIG. 3 CALIBRATION POINTS (Ro/R VS. Sw) ON A
LOG-LOG PLOT

FIG. 4   CALIBRATION   POINTS
(Ro/R) vs. (S$_w$) ON AN ARITHMETIC
PLOT

RESISTIVITY   RATIO   (Ro/R)

WATER   SATURATION   (S$_w$),   PERCENT

● TOTAL CORE
⊗ SEGMENT 11-12
⊘ SEGMENT 1-2
○ SEGMENTS 2-11
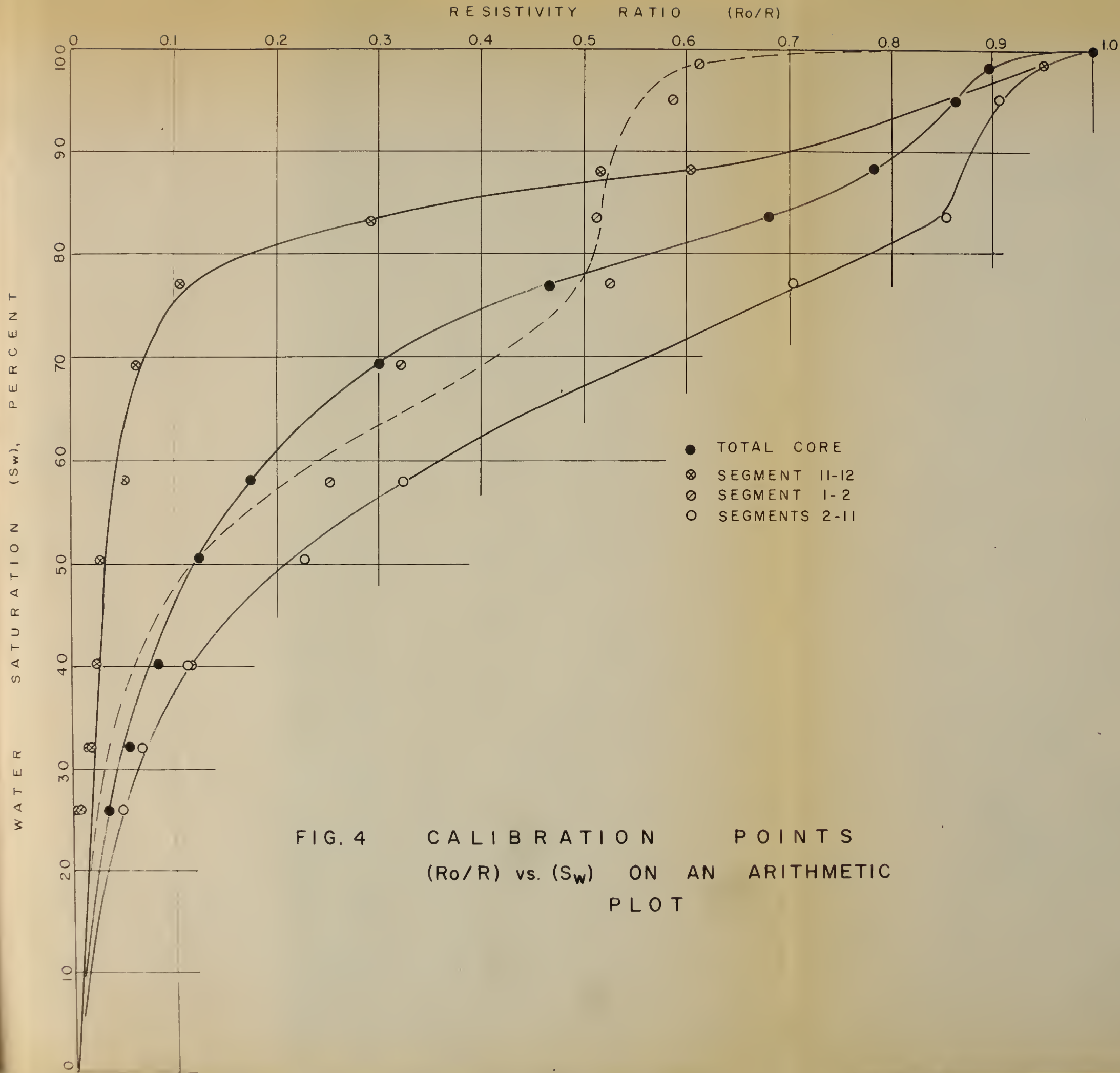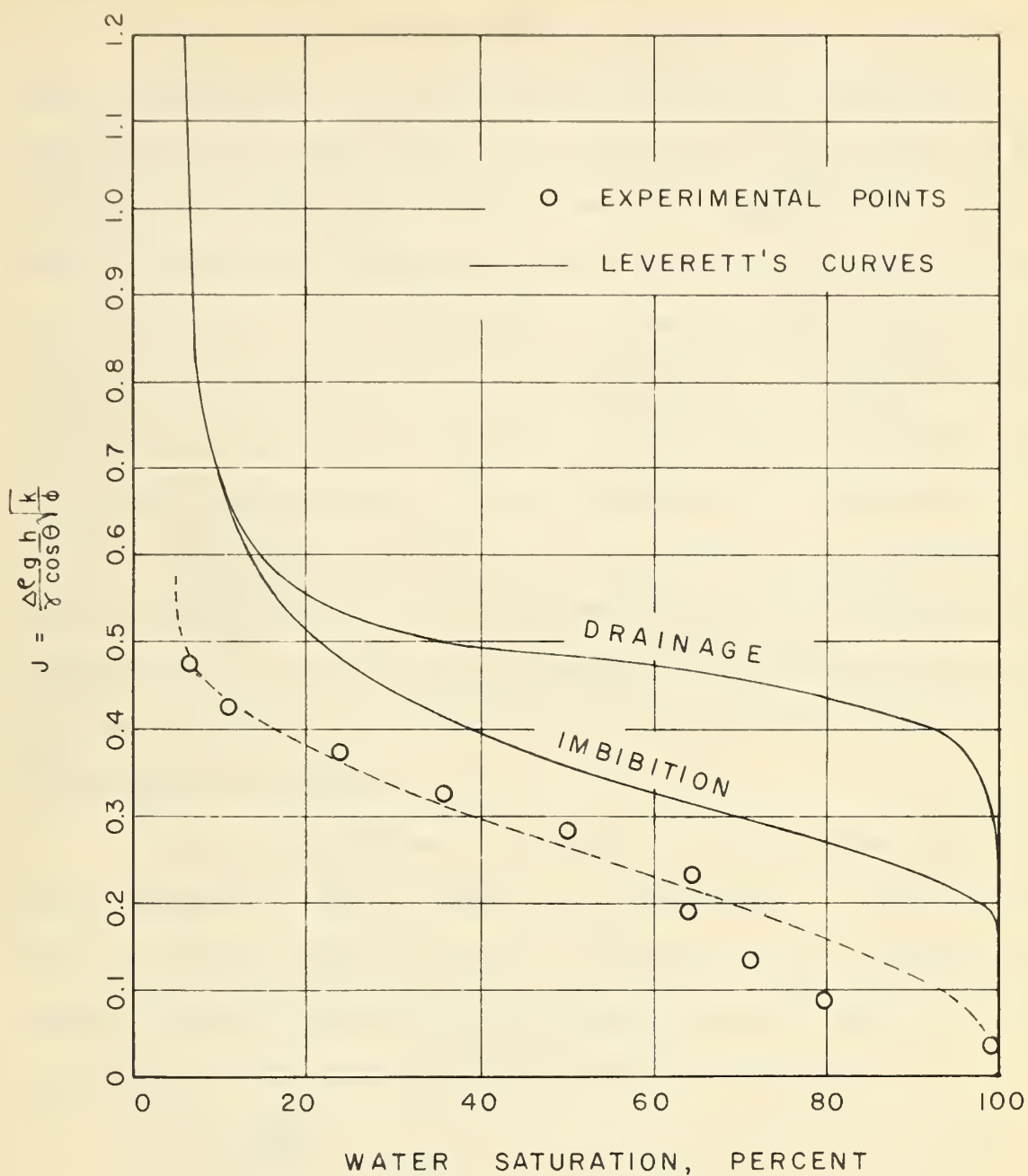
FIG. 5   CAPILLARY   PRESSURE   RESULTS
COMPARED TO LEVERETT'S J-FUNCTION

ABSOLUTE, EFFECTIVE, AND RELATIVE PERMEABILITY

Multi-phase flow in porous media has lead to the concept of effective permeability. In this concept each fluid is considered to be independent of the other fluids in the flow network. The fluids are also considered immiscible so that Darcy's law may be applied to each phase. Absolute permeability refers to a porous medium which is fully saturated with a homogeneous, single phase fluid. It has been found, experimentally, that the absolute permeability varies widely with the effective permeability even when the second phase is immobile, as in the case of a connate water or a residual oil saturation. Relative permeability is the ratio of the effective permeability to the absolute permeability, at any saturation. Relative permeability may also be expressed as the ratio of effective oil permeability at the connate water saturation; or for the water phase, as the ratio of the effective permeability to the effective permeability at the residual oil saturation.

The apparatus (Figure 6) consisted of a sand packed lucite tube used in conjunction with two Ruska constant rate pumps. It was possible to inject two liquids simultaneously but at different rates. A mercury manometer was used to measure pressures. The effective permeabilities were obtained by evaluating the Darcy equation for each phase, at each point.

$$k = \frac{Q \mu L}{A \Delta P} \quad \dots \dots \dots \dots \dots \dots \dots \dots \dots \quad (4)$$

where k is the effective permeability, darcies

   Q is the flow rate of the phase in question, cc/sec.

   μ is the viscosity of the phase in question, centipoise.

   L is the length of the core, cm.

A   is the cross-sectional area, cm^2.

ΔP is the pressure differential, atmospheres.

The results are presented in Tables 5 and 6, and are plotted as Figure 7. Saturations were obtained by keeping a close material balance of fluids injected and produced.

The relative permeability, as a ratio to the absolute permeability was computed (see Table 7). Relative permeabilities were also calculated using the effective permeabilities to oil and water at the connate water saturation and residual oil saturation respectively. Both sets of curves are compared to Leverett's in Figure 8.

These same data were used to construct an experimental fractional-flow curve (Table 8). These experimental points are compared to a calculated curve (see Figure 9). The calculated points were obtained (Table 9) from the fractional flow formula:

$$f_W = \frac{1}{1 + \dfrac{k_O\,\mu_W}{k_W\,\mu_O}} \quad \ldots \ldots \ldots \ldots \ldots \ldots \ldots (5)$$

where f_W = the fraction of water flowing

k_O = effective permeability to oil

k_W = effective permeability to water

μ_O = oil viscosity

μ_W = water viscosity

The above equation ignores the capillary and gravity terms. The effective permeabilities were read from Figure 7. As can be seen from Figure 9, the calculated curve verifies the experimental data as all the experimental points fit the curve closely.

CRITICAL RATE

Rapoport and Leas[21] found that for a linear flood recovery varied with length, rate, and viscosity of the displacing phase; for a given porous medium and a given water-oil viscosity ratio. They also found that for floods with the same $Lv\mu_W$ product, the production behavior was similar and that equal injection volumes resulted in equal recoveries. This resulted in their proposal of $Lv\mu_W$ as a general scaling coefficient for model tests. They further discovered that at some critical value of $Lv\mu_W$ recovery was independent of this factor; this is referred to as the critical scaling coefficient. The use of $\dfrac{Lv\mu_W}{\gamma \cos \Theta}$ as a dimensionless scaling factor has been proposed (13). However, difficulty exists in obtaining accurate contact angle and interfacial tension data, so that the scaling coefficient is usually used in its original form.

The same experimental set-up as for the effective permeability tests was used (Figure 6). As length and water viscosity were constant for all tests, it remained only to determine the critical rate. Recovery and water-oil ratios were recorded for a variety of different rates. The production histories of these several tests are presented in Table 10 and Figure 10. The relationship between recovery and rate, with producing water-oil ratio as a parameter, was obtained by cross-plotting Figure 10 and is presented as Figure 11.

As can be seen, recovery increases with rate to a maximum as expected. However, beyond this point there is a decrease in recovery with increasing rate. The phenomenon is much more pronounced at breakthrough but at high water-oil ratios the system behaves more closely to the Rapoport data.

The increase of recovery with rate is generally attributed to capillary forces. From their laboratory results, Rapoport and Leas[21] developed the following unsteady state equation for flow through porous media:

$$\frac{\partial S}{\partial T} + \frac{\partial F}{\partial S}\frac{\partial S}{\partial X} - \frac{k}{C\,Lv\mu_W}\frac{\partial}{\partial X}\left[k_0 F\,\frac{\partial Pc}{\partial S}\frac{\partial S}{\partial X}\right] = 0 \quad \ldots \ldots \ldots \ldots (6)$$

where $T = \frac{tv}{L\phi}$; the accumulated injection at time t expressed as a fraction of total pore volume.

$X = x/L$; distance expressed as a fraction of length.

S = saturation of the wetting phase.

C = viscosity ratio μ_O/μ_W

$F = 1 +$ the mobility ratio; $1 + \dfrac{k_O}{C\,k_W}$

All other terms as defined previously.

It can be seen that as $Lv\mu_W$ increases and approaches infinity, the third term becomes negligible so that at some rate (assuming L and μ_W as constant):

$$\frac{\partial S}{\partial T} + \frac{\partial F}{\partial S}\frac{\partial S}{\partial X} = 0 \quad \ldots \ldots \ldots \ldots \ldots \ldots \ldots \ldots (7)$$

This indicates that if the rate is large enough the capillary pressure term becomes negligible. At rates below this, it is probable that capillary pressure gradients result in water flowing preferentially ahead of the front. Such gradients are the result of changes in saturation at the flood front, degree of preference of the sand to be water wet, pore size and geometry, and the interfacial tension between oil and water.

Little data is available regarding the relationship between recovery and rate of displacement at high rates. Some possible explanations for the phenomenon are:

1. Capillary Pressure

From Figure 11, it can be seen that the deviation in recovery
with rate is much more pronounced at breakthrough. At high water-oil ratios,
where the saturation of the core is approaching that of the residual oil,
the effect is much smaller. A casual examination of the fractional flow
formula indicates that this is to be expected:

$$f_w = \frac{1 - \frac{k_o}{\mu_o\,q_t}\left[\frac{\partial P_c}{\partial L} + g\,\Delta\rho\,\sin\alpha\right]}{1 + \frac{k_o\,\mu_w}{k_w\,\mu_o}} \qquad \ldots \ldots \ldots (8)$$

where q_t is the rate of the total flow stream.

α is the angle of dip.

All other terms as defined previously.

As q_t increases the capillary pressure term in the numerator
decreases. At high water-oil ratios or as the saturation of the system
approaches that of the residual oil, the capillary pressure effects become
negligible. Possibly at breakthrough, saturations and total recovery are
low enough so that capillary pressure gradients result in preferential water
production even at high displacement rates.

2. Turbulence

It has been recognized that for gas flow through a porous medium,
turbulence does occur in the vicinity of the well bore. However, for liquid
flow through porous media, only flow in the laminar region has been reported.
Possibly at very high rates, turbulence does exist and the decline in recovery
at high rates is a result of the onset of turbulence.

3. Instability of the Flood Front

It is well known, especially in miscible floods, that fingering can occur at the flood front. Scheidegger[23] gives the following definition of fingering: "Protuberences may arise which shoot through the porous medium at relatively great speed, leaving behind large amounts of the liquid intended to be displaced. This phenomenon is commonly referred to as fingering". Scheidegger further concludes that the initial growth of fingers is conditioned by two effects: the rate of starting of fingers due to heterogenieties of the porous medium and prevailing flow potentials. It is possible that at high rates both these conditions are of sufficient magnitude to cause fingering and hence the low oil recoveries.

4. Equipment Design

The fluids were injected into the core through a point source. Immediately ahead of this inlet is a porous bronze plate which is to disperse the fluid over the entire cross-sectional area of the core. It is possible that, at high rates, the injection fluid enters the core as a jet and displaces fluid only over a cross-sectional area of the same magnitude as the orifice. This could account for the early breakthrough to water at high rates.
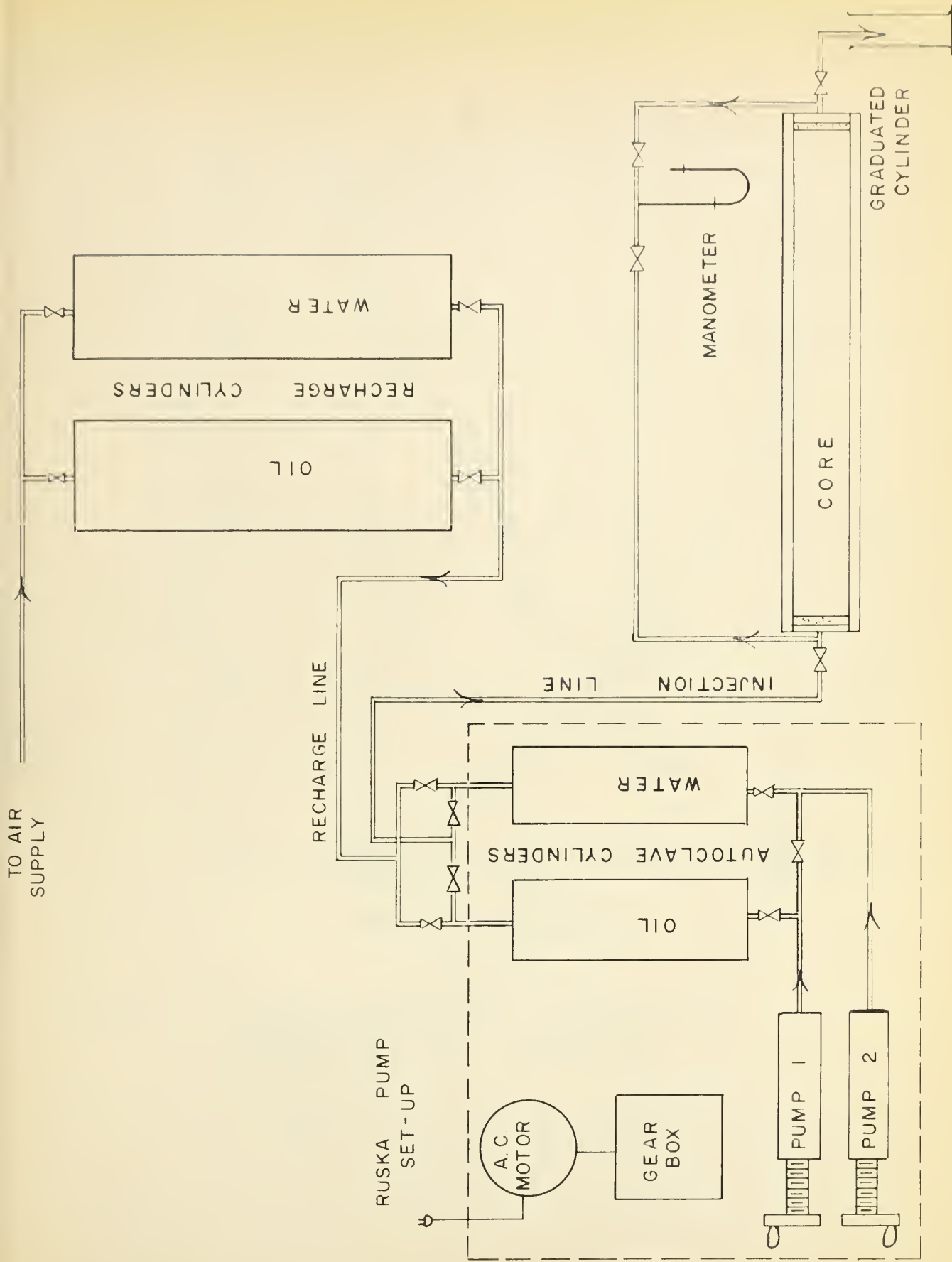
FIG. 6   EFFECTIVE PERMEABILITY AND CRITICAL RATE APPARATUS

FIG. 7   EXPERIMENTAL   EFFECTIVE
PERMEABILITY   CURVES

NOTE: THESE ARE NOT TRUE RELATIVE PERMEABILITIES BUT ARE CALCULATED RELATIVE TO THE EFFECTIVE PERMEABILITIES AT THE IRREDUCIBLE SATURATIONS

WATER SATURATION, FRACTION OF PORE SPACE
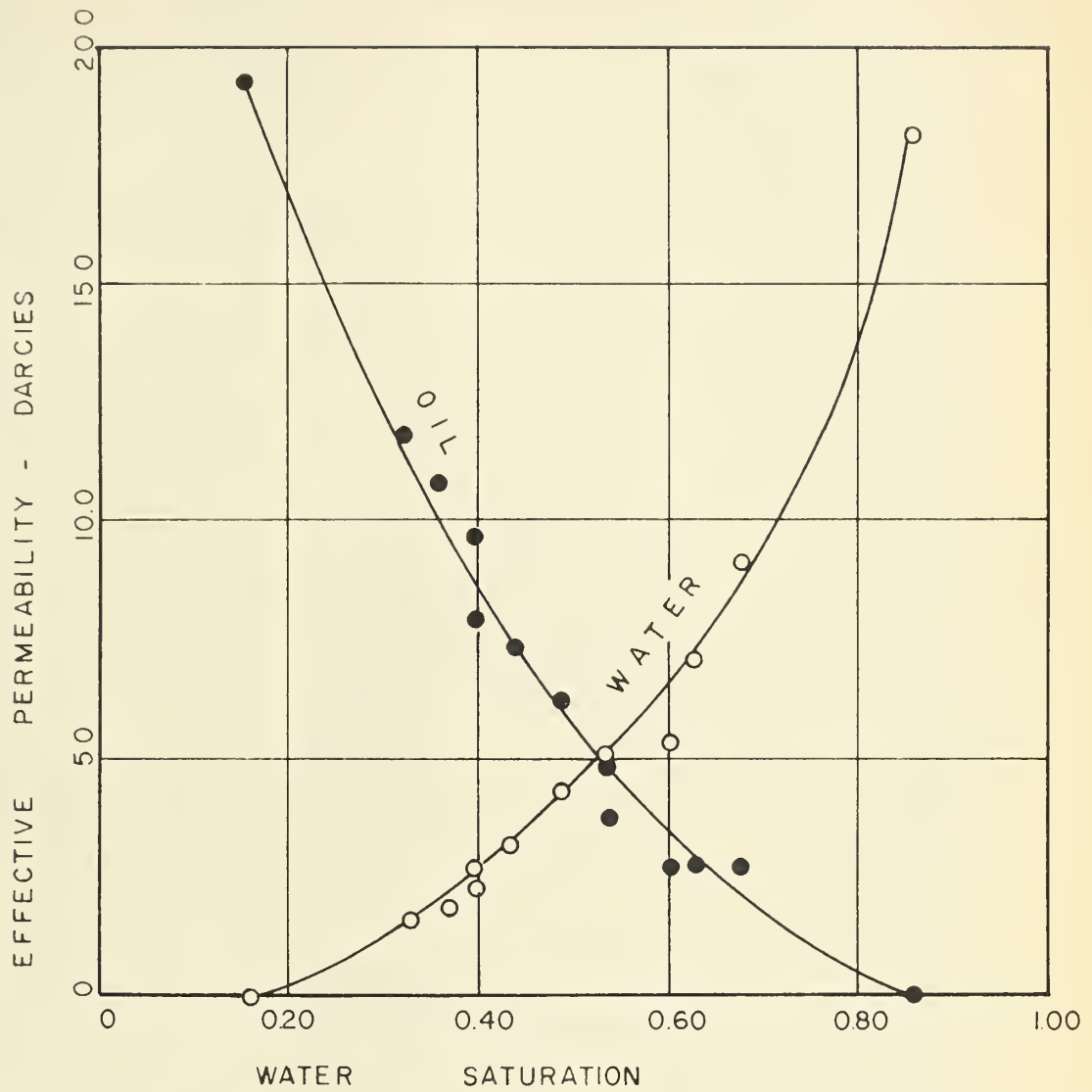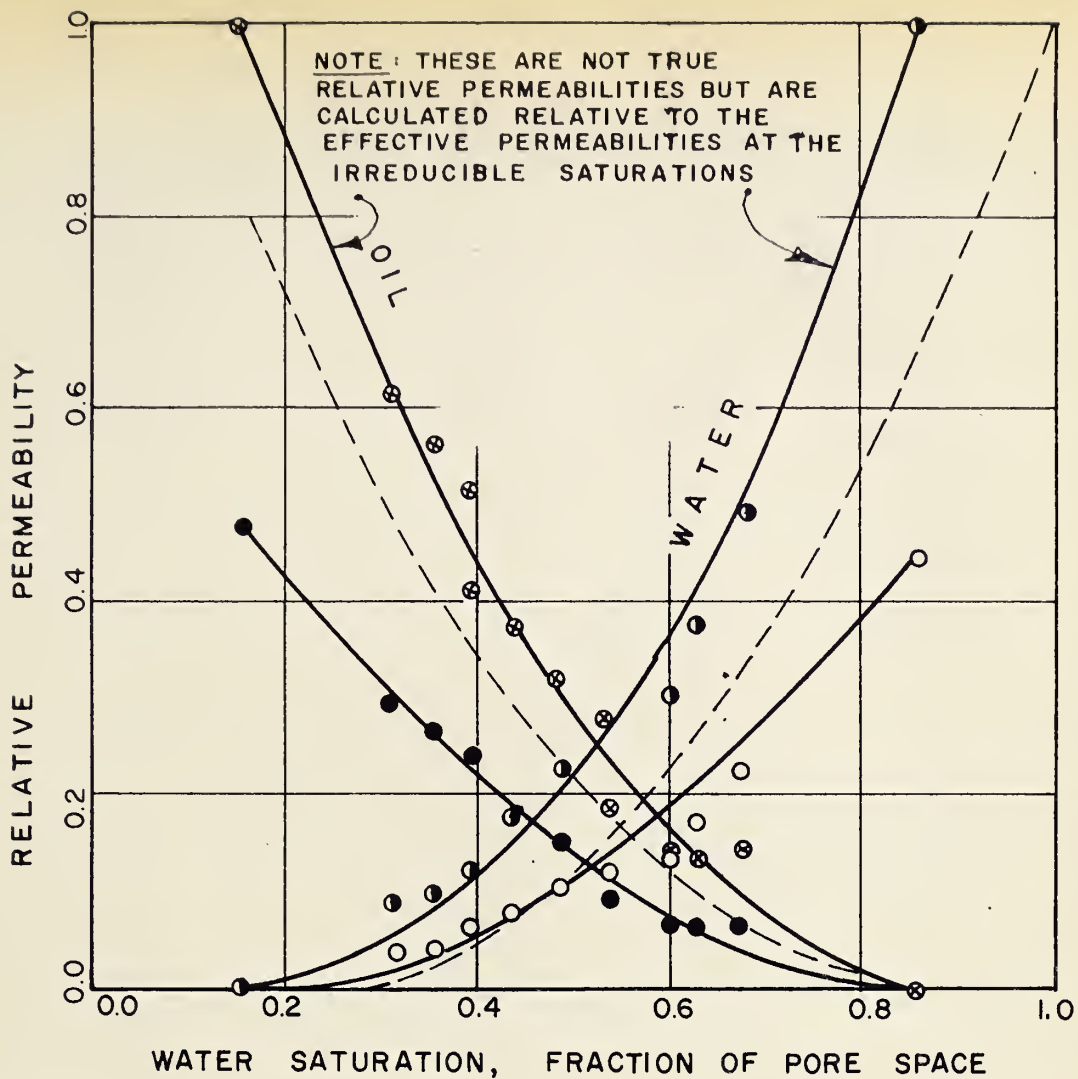
O ABSOLUTE   PERMEABILITY = 40.7 d
● ABSOLUTE   PERMEABILITY = 40.7 d
◑ EFFECTIVE   PERMEABILITY = 18.2 d
⊗ EFFECTIVE   PERMEABILITY = 19.3 d
——— LEVERETT'S   CURVES

FIG. 8   RELATIVE   PERMEABILITIES
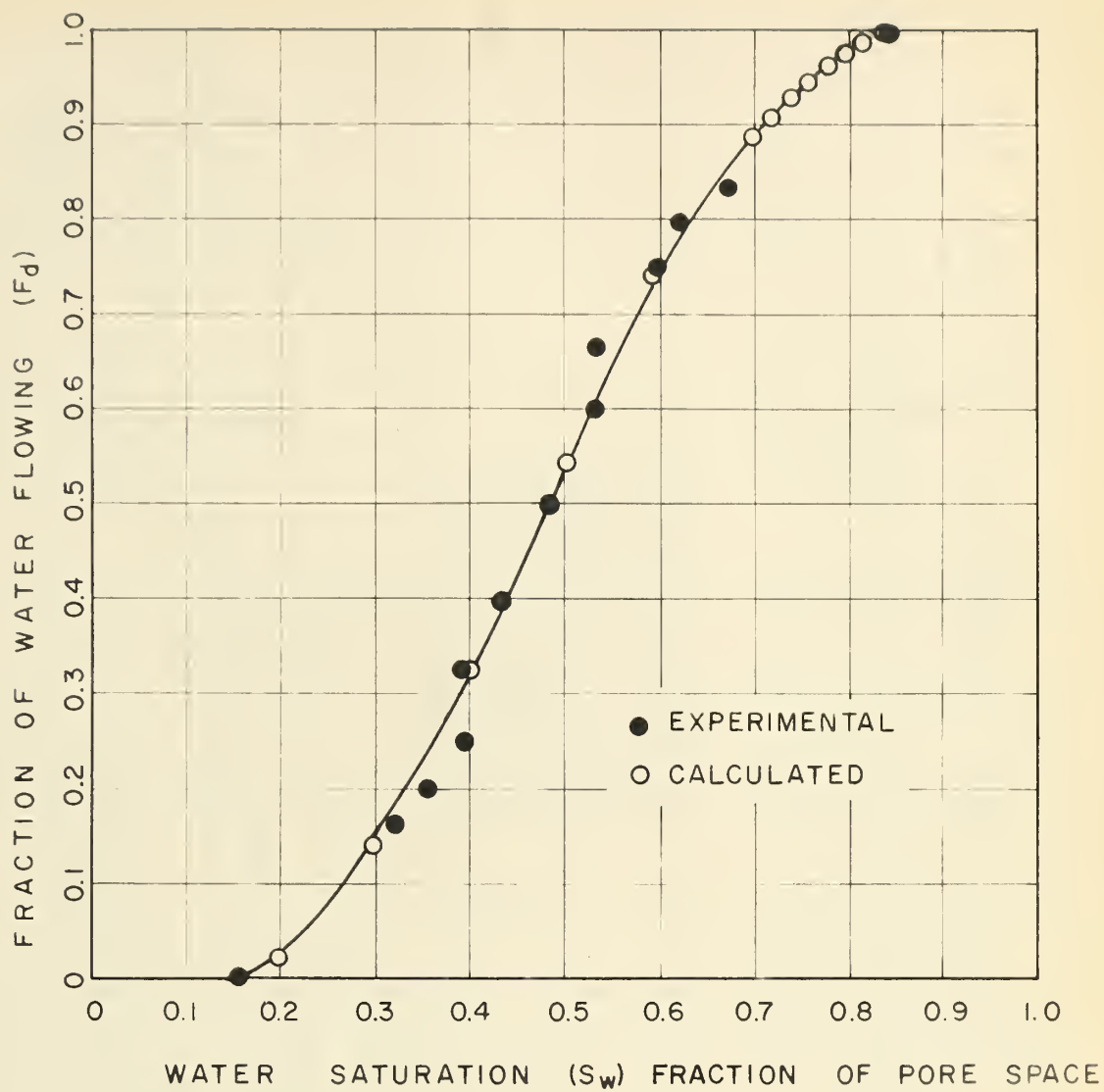
FIG. 9   EXPERIMENTAL AND CALCULATED
FRACTIONAL-FLOW DATA
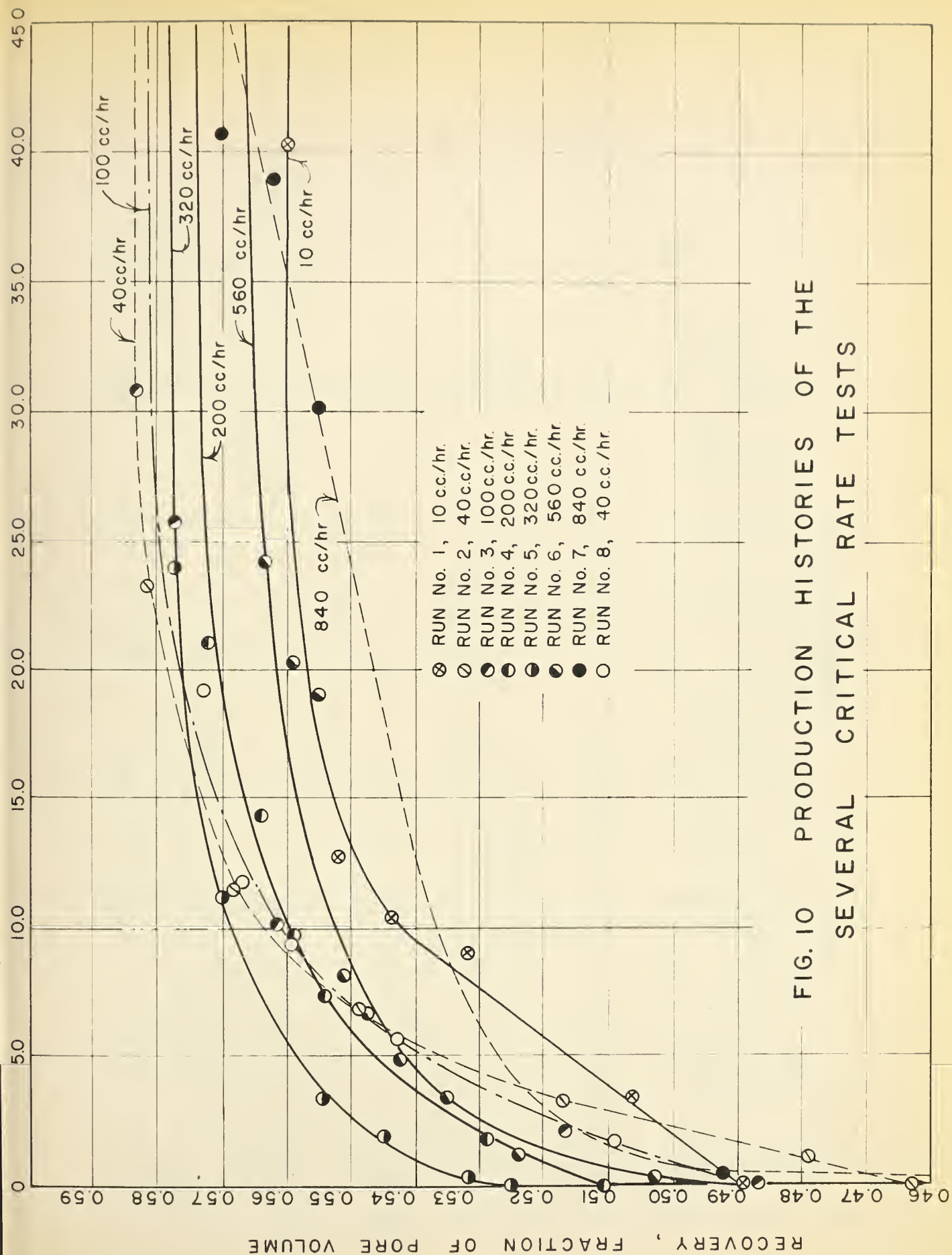
FIG. 10   PRODUCTION HISTORIES OF THE
SEVERAL CRITICAL RATE TESTS

RUN No. 1,   10 c.c./hr.
RUN No. 2,   40 c.c./hr.
RUN No. 3, 100 c.c./hr.
RUN No. 4, 200 c.c./hr.
RUN No. 5, 320 c.c./hr.
RUN No. 6, 560 c.c./hr.
RUN No. 7, 840 c.c./hr.
RUN No. 8,   40 c.c./hr.

RECOVERY, FRACTION OF PORE VOLUME
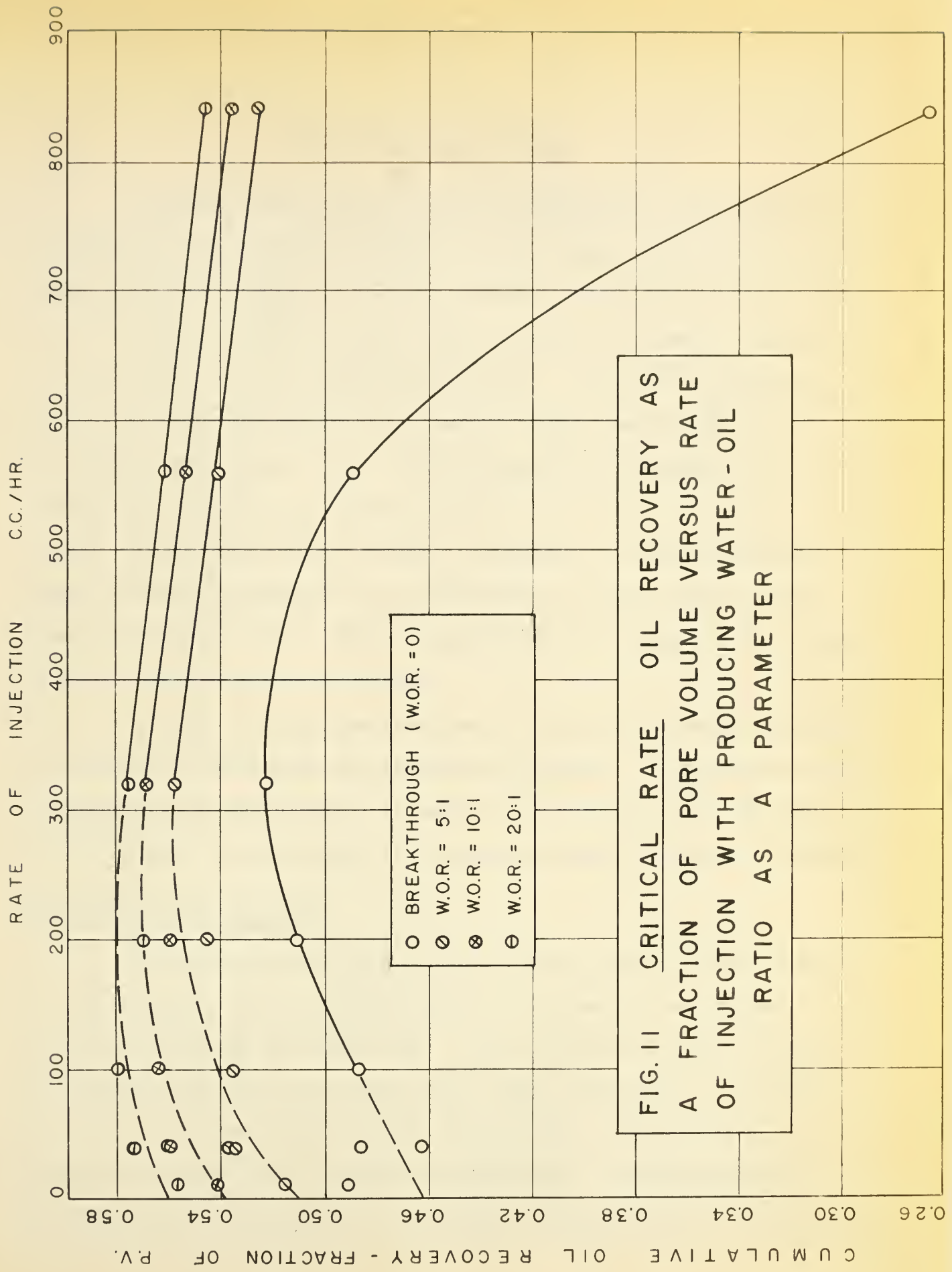
FIG. II CRITICAL RATE OIL RECOVERY AS
A FRACTION OF PORE VOLUME VERSUS RATE
OF INJECTION WITH PRODUCING WATER-OIL
RATIO AS A PARAMETER

MODEL WATER-FLOOD STUDIES

Two models were used and shall be referred to as "the large model" and "the small model" for the remainder of this report. Dimensions and other data are included in Table 11. It was originally hoped that the flood front might be visually observed by using a water soluble dye. However, attempts using dyed water met with only moderate success. The use of a fluorescene tracer dye and an ultraviolet lamp resulted in only a vague suggestion of the location of the flood front. A more successful dye was used on the large model. In this case, although the front was visible and could be mapped, the sand pack retained the dye -- resulting in a one run process. Figure 12 shows the location of the flood front at various times as it was observed during this test. The dark pattern around the injection well is due to the dye being adsorbed on the sand.

Data taken on the model consisted of records of the water injected, oil and water produced, and producing water-oil ratios. These data were later converted to total sweep efficiency, areal sweep efficiency, and the ratio of the volume of water injected to the volume of water injected to breakthrough.

Description of the Apparatus

The models are basically a maximum density sand bed packed between two lucite plates. Nine simulated oil wells are located on an isolated pattern in the center (see Figure 13). Figure 13 also shows the injection and producing wells for the various patterns that were studied. There are also wells in the four outside corners of the models. Injection was maintained by means of the constant rate Ruska pump. A mercury manometer was fitted to the injection line as a pressure measuring device. The producing

wells discharged to atmospheric pressure. The bed was initially evacuated from the four corner wells and saturated with water from the center well. By measuring the amount of water injected to fully saturate the bed, the porosity was calculated. Permeability data from the synthetic core studies were used in any subsequent calculations.

To initially establish the connate water saturation, the water saturated bed was driven down with oil until no more water was produced. The bed was then ready for a water flood test which was continued to a producing water-oil ratio of 20:1 or higher. The connate water was re-established by the same procedure subsequent to each test.

Definition of Efficiency Terms

While it would appear that only the total efficiency or the amount of oil produced in relation to the amount of oil in place is of main concern, several other efficiency terms are widely used in reservoir engineering. The total efficiency of a water-flood program is the product of three efficiencies: the vertical sweep efficiency, the areal sweep efficiency, and the displacement efficiency. The vertical sweep efficiency refers to that portion of a vertical section of reservoir which is encountered by the injection fluid at any time as compared to the total reservoir thickness. It is a function of permeability layering or stratification. Several methods have been devised to deal with vertical sweep efficiency, most notably that of Stiles[25], which attempts to break the reservoir into several layers each of which is approximately homogeneous. In a reservoir which is homogeneous throughout its vertical section, the vertical sweep efficiency is 100%. This is the case of the sand packed reservoir models and for this reason vertical sweep efficiency is not considered in the model studies.

Areal sweep efficiency may be considered as the measure of the area of reservoir which is contacted by the injection fluid at any time as compared to the unit area of the pattern. It is a term restricted to a pattern flood; if the flood is linear as in the case of a core, the areal sweep efficiency is 100%.

Displacement efficiency refers to the fraction of oil which is swept from the individual pores as compared with the amount of oil originally in the pore. It refers to the amount of oil produced by stripping action or subordinate recovery which is obtained from that portion of the reservoir which has already been encountered by the injection fluid. Because a certain residual oil remains, even at a producing water-oil ratio of infinity, the displacement efficiency must always be less than 100%.

A. Saturating the evacuated sand bed with water.
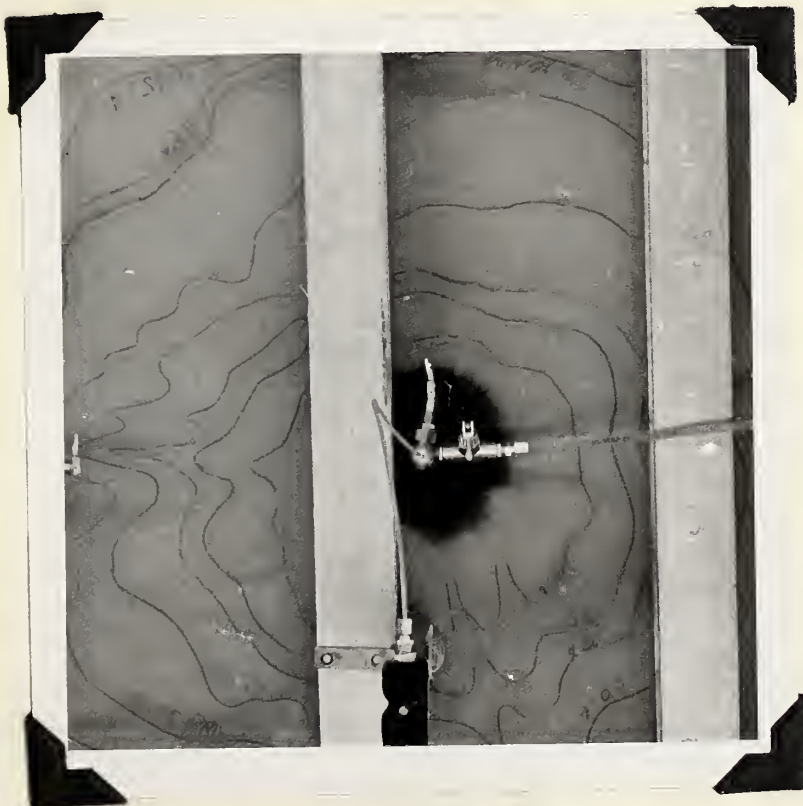
B. Location of the flood front during a water-flood test.

FIG. 12   PHOTOGRAPHS OF THE FLOOD FRONT
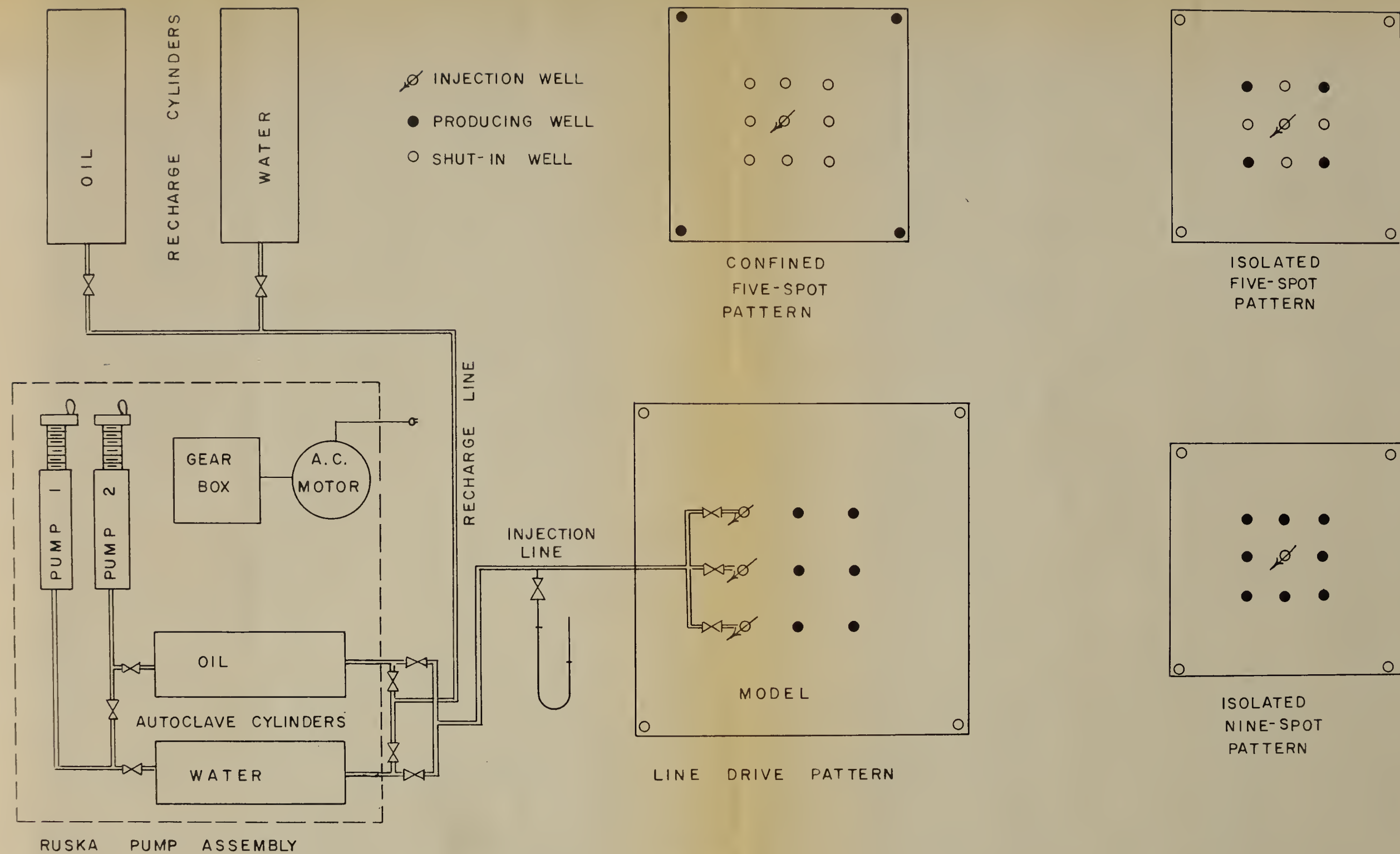
FIG. 13   SCHEMATIC   DIAGRAM   OF   THE   TWO   DIMENSIONAL   MODEL   APPARATUS
SHOWING   THE   WELL   PATTERNS   USED   FOR   THE   WATER-FLOOD   TESTS

LITERATURE REVIEW

Various methods have been devised to study the sweep efficiencies of an oil-water-porous medium system. One of the early methods involved the use of the potentiometric analogue. This type of a laboratory analysis is based on the analogy between Ohm's law and Darcy's law, which in their simplest form are:

$$I = E/R \quad\ldots\ldots\ldots\ldots\ldots\ldots\ldots\ldots (9)$$

where   I   is the current

E   is the potential or voltage

R   is the resistance

And $$Q = \frac{k}{\mu}\frac{A}{L}\Delta P \quad\ldots\ldots\ldots\ldots\ldots\ldots (10)$$

All terms as defined previously

That is, pressure drops may be equated to voltage drops; flow rates to current rates; and the other parameters may be equated to resistances.

The model is a pool of water containing an electrolyte whose depth is proportional to the reservoir thickness and whose areal geometry and well locations are similar to the reservoir it represents. Currents are adjusted proportional to existing or proposed production or injection rates. By using a voltage measuring device the isopotential lines may be mapped. The position of the flood front (which is, in effect, a constant time line) is obtained as follows: The relative time of travel between two isopotential lines is directly proportional to the distance ΔX and inversely proportional to the voltage gradient $\Delta E/\Delta X$, so that

$$\Delta t = \frac{\Delta X}{\Delta E/\Delta X} = \frac{(\Delta X)^2}{\Delta E} \quad\ldots\ldots\ldots\ldots\ldots (11)$$

$$t \; = \; \sum \Delta t \; = \; \sum (\frac{\Delta X}{\Delta E})^2 \quad \ldots \ldots \ldots \ldots \ldots \ldots \ldots \; (12)$$

The front for any relative time is found by joining points of equal relative time along the several flow lines.

Figure 14 shows results obtained by Wykoff, Botset, and Muskat[27] using a potentiometric model of 1/4 of a confined five-spot pattern. The drawback of this method is that it is impossible to simulate two-phase fluid properties. Hence the assumption of unit mobility ratio (i.e. invading and invaded fluid have the same flow properties) is inherent in the solution. The concept of displacement efficiency is also not considered and as a result these solutions assume a displacement efficiency of 100%.

The electrolytic model works on the same analogy as the potentio-metric model but flow actually takes place through a physical porous medium. To simulate the porous medium, investigators have used either blotting paper or an agar geletin. The process consists of observing the advance of a colored liquid (usually copper-ammonium) into a colorless liquid (zinc ammonium). The ions move under voltages applied to electrodes inserted at well locations and the advance of the front is observed visually or photo-graphed at various intervals. Both geometric and electrical scaling is necessary. The effect of a variety of mobility ratios may be taken into account by the use of different fluids. As the flow takes place through an actual porous media, displacement efficiency will be accounted for, at least in so far as it is defined by the blotting paper or agar gelatin.

Mathematical solutions have often been referred to as the mathematical model. Two such approaches have been devised by Muskat[17] and Bruce[4]. Even for very simple systems the equations are quite complex and difficult to

solve. They are not included in this report but are readily available from the literature.

The geometric model is the most versatile method for the laboratory investigation of water-flood efficiencies. This type of model allows almost unlimited variation of the factors which effect the reservoir performance. Slobod and Caudle[24] were the early workers in this field. They developed a procedure using the X-ray shadowgraph. The reservoir unit was a porous plate or rock specimen sealed on the top, bottom, and edges. Liquids were injected and produced through various well patterns. Variation in mobility ratio may be studied by using fluids of different viscosities. The injection fluid was rendered more strongly absorbant to X-rays than the reservoir fluid by the addition of some X-ray absorbing material such as iodobenzene or potassium iodide.

Most of the above papers considered only areal sweep efficiency up to breakthrough. Production after breakthrough was not taken into account. The following table[23] gives the results of several investigations of areal sweep efficiency for a confined five-spot, mobility ratio of one, at breakthrough.

Muskat (early electroytic model)	75%
Muskat (early mathematical solution)	72.3
Hurst (mathematical solution)	72.6
Muskat (later mathematical solution)	71.5
Fay and Prats (numerical solution)	73
Aronofsky (potentiometric model)	72.2

Work at the University of Alberta by Neilson[18] obtained the following results from an isolated, inverted five-spot pattern at a mobility

ratio of 0.423.

Breakthrough	110% areal sweep efficiency
W.O.R. = 0.5:1	305
W.O.R. = 1.0:1	410
W.O.R. = 20:1	655

As can be seen this investigation took into account recovery and increase in areal sweep efficiencies after breakthrough. Original thought was that areal sweep efficiencies of such high magnitude were unreasonable. However, a mathematical treatment by Bruce[4] has resulted in the configuration of isopotentials and flow lines for an isolated, inverted five-spot pattern. These are presented as Figure 15. The location of the flood front at various water-oil ratios are after Neilson.

Work by Caudle, Erickson, and Slobod[6] and by Dalton, Rapoport, and Carpenter[9] also tend to substantiate Neilson's results. These two papers are concerned with additional production to be realized from undrilled boundary areas of an oil field. Both sets of data were obtained from geometric models and both show that considerable area outside the well pattern is swept. The parameter which controls the magnitude of this additional area was found to be mobility ratio. They also found that results of a pilot flood (such as an isolated five-spot) and a drilled out (or confined) pattern did not correspond. It is therefore apparent that Neilson's work should not be compared to previous confined five-spot studies but rather to isolated or pilot studies.

As mentioned above, much of the work done on areal sweep efficiencies has only been concerned with sweep efficiency to breakthrough. Work by Dyes, Caudle and Erickson[10] has taken into account additional sweepout efficiency

with production after breakthrough. Work along a similar line was done by Craig, Geffen and Morse[8]. The following remarks refer to these investigations where they pertain to the five-spot pattern.

The Dyes et al investigation was carried out on models cut from alundum plates and flooded with fluids at a wide range of mobility ratios. The injected and displaced phases were miscible in all proportions. Fluids were injected at constant rates via a constant rate pump. Tracings of areal sweep were obtained from X-ray shadowgraphs and plotted versus the number of displacable volumes injected, with mobility ratio as a parameter. Figure 16 shows the graphical results of this investigation.

The Craig et al investigation also utilized the X-ray shadowgraph technique. Their models were cut from outcrop samples of sandstone and the fluids used were immiscible water and oil. They found good agreement between their investigation and that of Dyes et al for areal sweep efficiencies at breakthrough for the same mobility ratios. Mobility ratio was calculated in the following manner:

1. The average saturation behind the flood front is obtained from the fractional-flow versus saturation curve. This is done by utilizing the Welge[26] modification to the Buckley and Leverett procedure[5]: a straight line whose origin is the displacing fluid saturation is drawn tangent to the curve and extended to f_d = 1.0. This is the saturation of the invading fluid behind the flood front.

2. The effective permeability to water at this saturation is read from the experimental effective permeability curve.

3. The effective permeability to oil, k_o, is the value corresponding to the oil saturation at the flood front. If there is no gas phase, this will

be the connate water saturation.

4. The values are substituted along with the respective viscosities
into the equation:

$$M = \frac{k_o \mu_w}{k_w \mu_o} \quad \ldots \ldots \ldots \ldots \ldots \ldots \ldots \ldots (13)$$

Where M is the mobility ratio and all other terms are as defined previously.

The results of the Craig et all investigation are presented (see
Figure 17) as areal sweep efficiency versus the ratio of the volume of water
injected to the volume of water injected to breakthrough for various mobility
ratios at breakthrough. Dyes et al results may be converted to this form
by cross plotting his curves at a constant mobility ratio and converting
D_v to Q/Q_{bt} by $D_v/D_{v_{bt}}$. One such curve is included in Figure 17.

CALCULATION OF DISPLACEMENT EFFICIENCY

As the Buckley Leverett theory[5] was developed for linear flow, the areal sweep efficiency is 100%. Recovery is merely a measure of the displacement efficiency of the system. On the strength of the close correlation between calculated and experimental fractional-flow curves (Figure 9), calculated fractional-flow curves were constructed for the two viscosity oils which were used in the model tests (see Figure 18). In this case, displacement efficiency is the oil produced over the oil in place. The oil produced at any time is the water saturation at that time minus the connate water saturation. The problem is to obtain the average saturation of the invaded section after breakthrough. To do this the Welge modification[26] to Buckley Leverett theory was utilized. That is, tangents were drawn to the fractional-flow curve at various water cuts (f_W) and extended to $f_W = 1.0$. The intercept of this tangent is the average water saturation of the formation. The results of these calculations are tabulated in Table 12 and plotted in Figures 19 and 20.

PRODUCING
WELL

INJECTION
WELL

——————— FLOOD FRONTS

——— -- —— ISOPOTENTIAL LINES
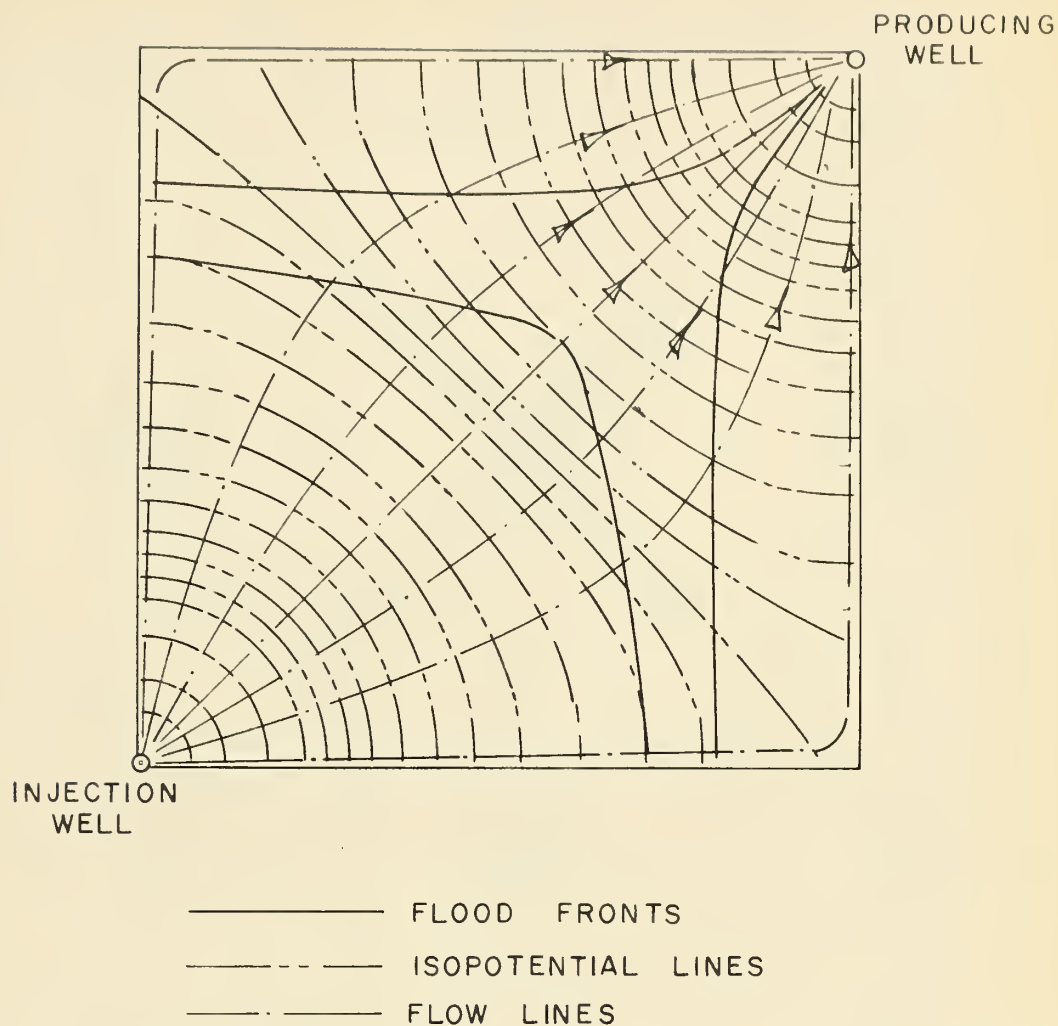
——— · —— FLOW LINES

FIG. 14   POTENTIOMETRIC   MODEL   RESULTS   FOR
1/4 OF A FIVE-SPOT PATTERN (AFTER
WYCKOFF,   BOTSET   AND   MUSKAT)

W.O.R = 20
W.O.R = 2.0
W.O.R = 0.5
B.T.

— — — — — FLOOD FRONTS (AFTER NEILSON)
———— · ———— FLOW LINES (AFTER BRUCE)
————— — ————— ISOPOTENTIAL LINES (AFTER BRUCE)
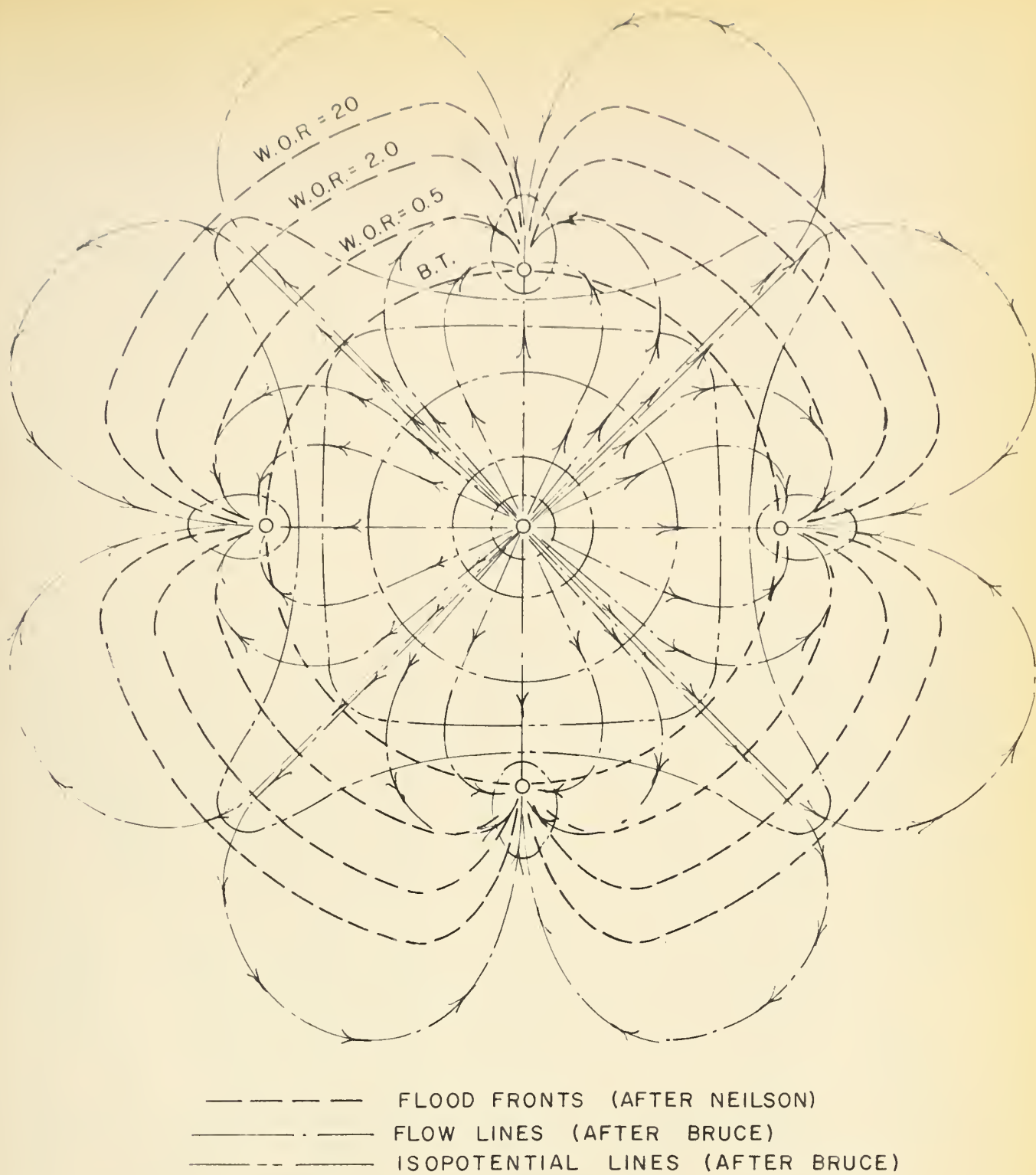
FIG. 15   ISOLATED, INVERTED FIVE-SPOT FLOOD
FRONTS, FLOW LINES, AND ISOPOTENTIALS
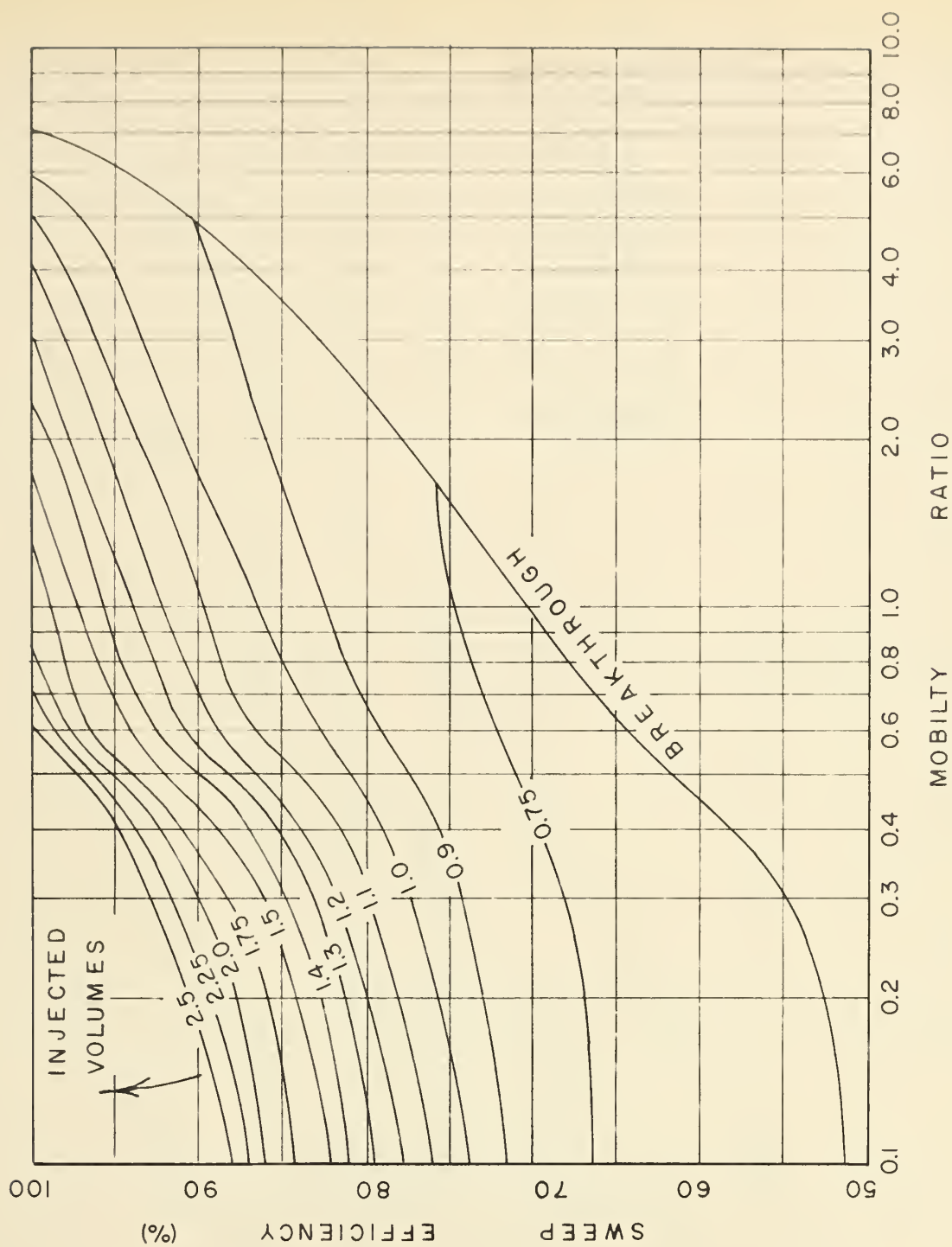
SWEEP EFFICIENCY VERSUS MOBILITY RATIO
WITH INJECTED VOLUMES AS A PARAMETER
(AFTER DYES ET AL)

FIG. 16
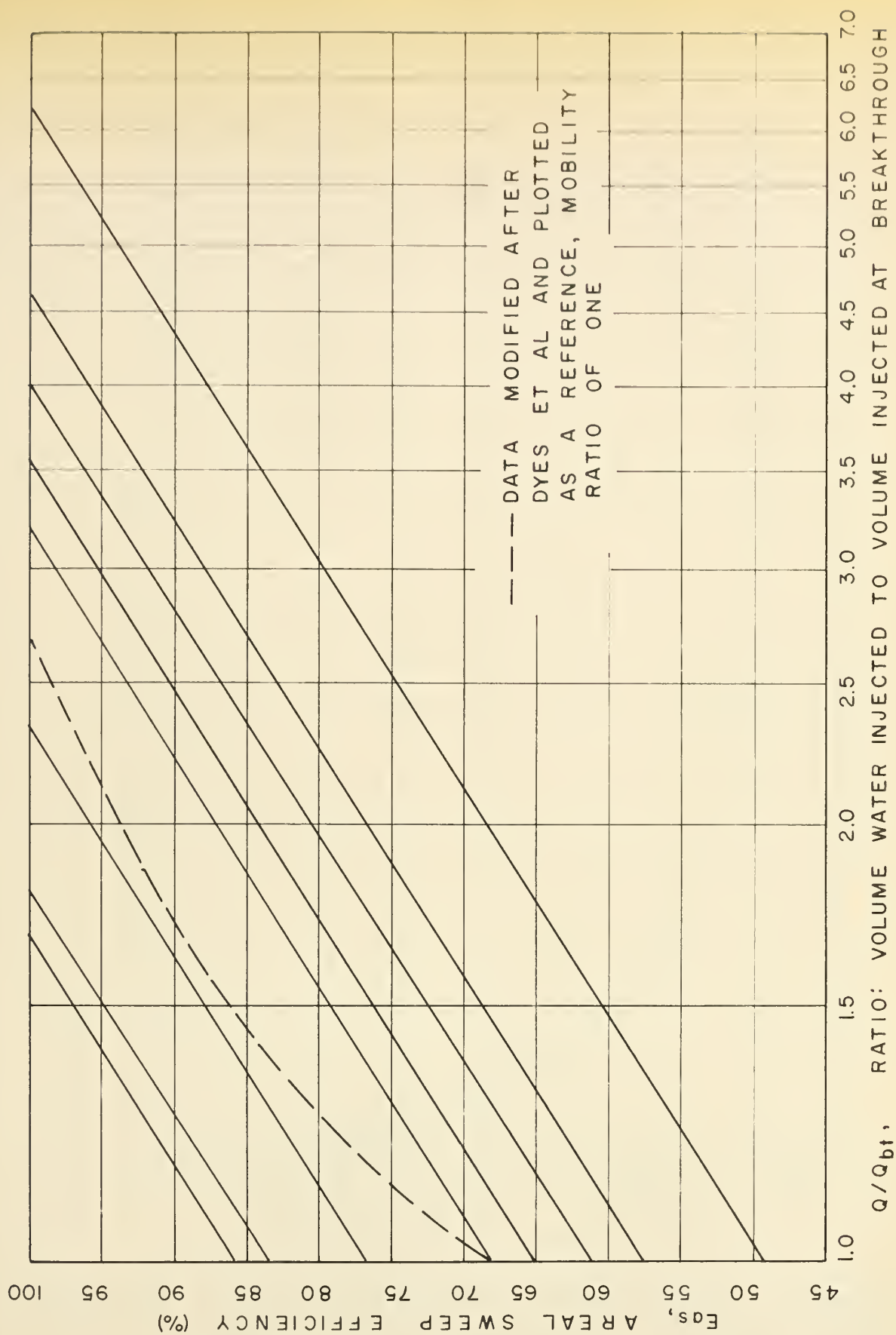
FIG. 17 THE RATIO OF THE VOLUME OF WATER INJECTED TO THE VOLUME INJECTED AT BREAKTHROUGH VERSUS THE AREAL SWEEP EFFICIENCY FOR A VARIETY OF MOBILITY RATIOS (AFTER CRAIG ET AL)
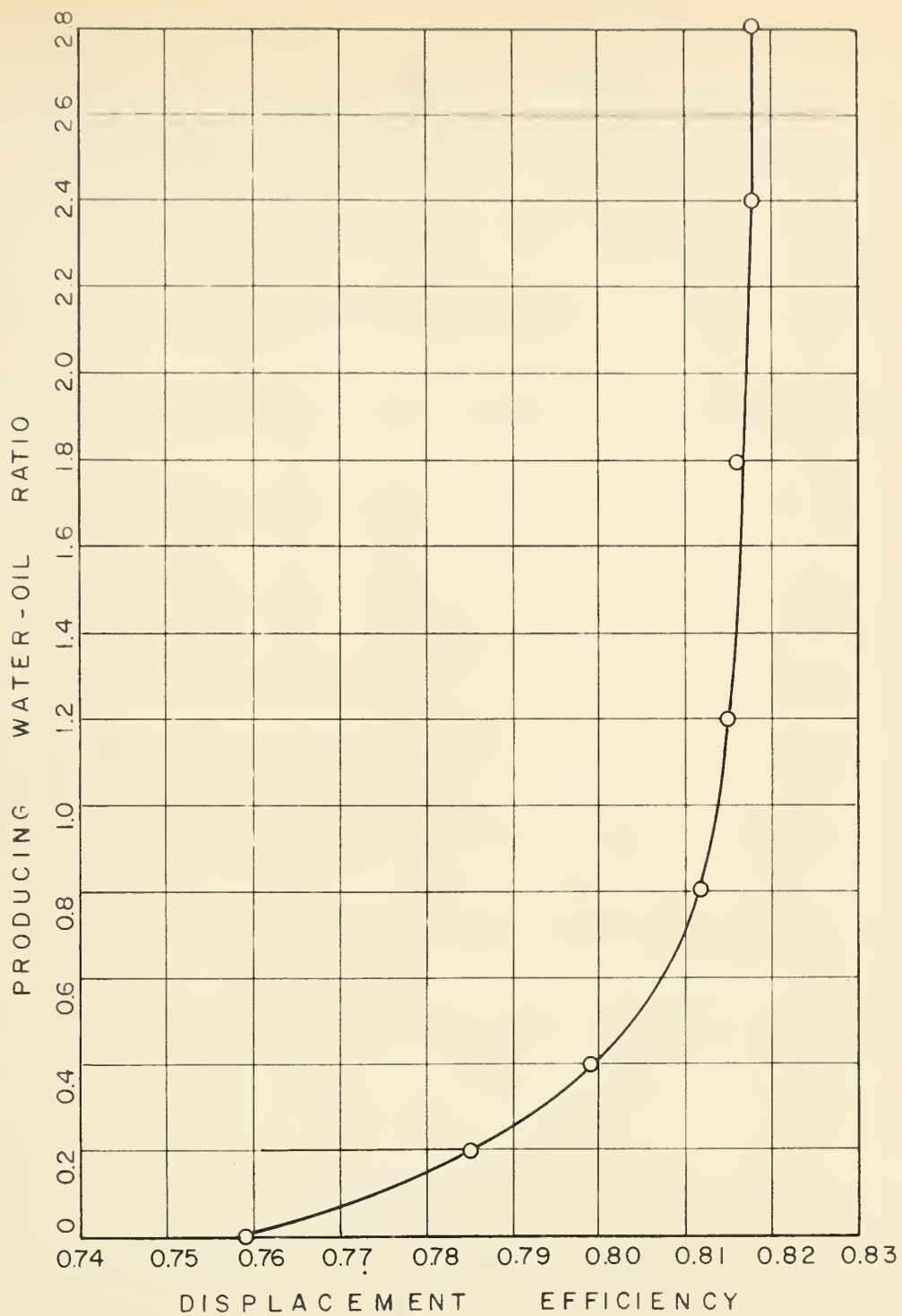
FIG. 19 DISPLACEMENT EFFICIENCY VERSUS
PRODUCING WATER-OIL RATIO, LOW
VISCOSITY OIL
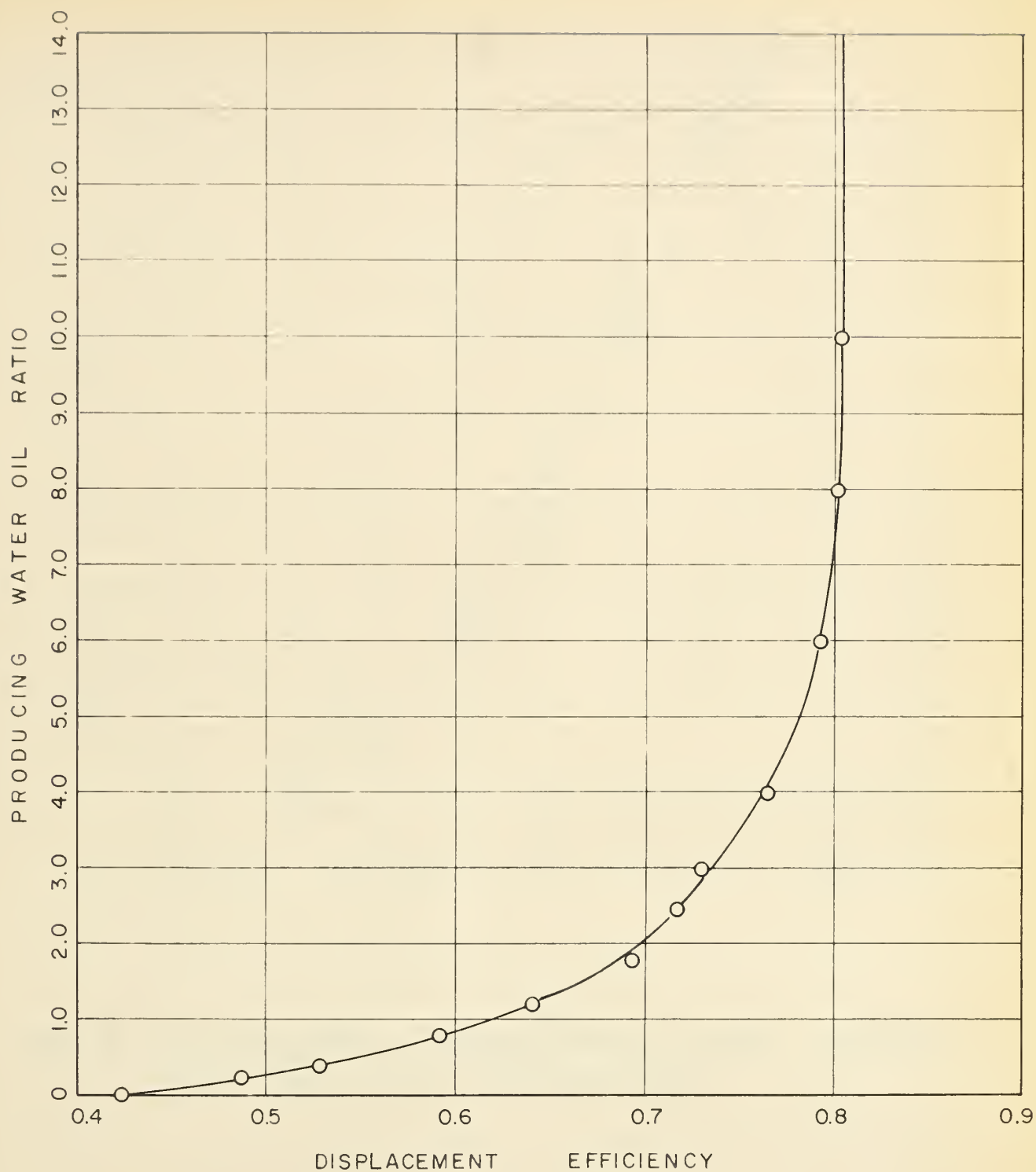
FIG. 20   DISPLACEMENT   EFFICIENCY   VERSUS
PRODUCING   WATER-OIL   RATIO, HIGH
VISCOSITY   OIL
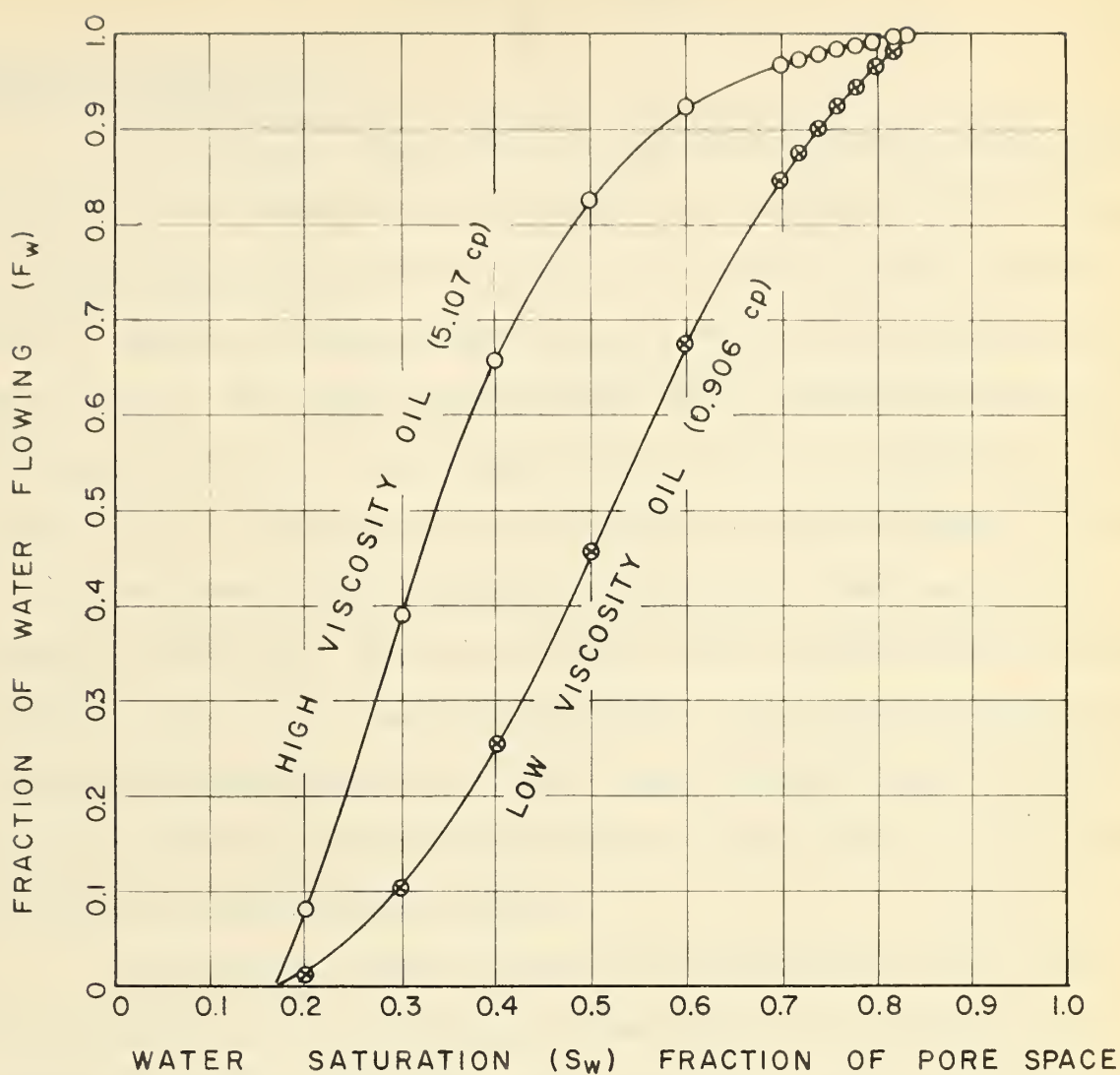
FIG. 18 CALCULATED FRACTIONAL-FLOW CURVES
FOR TWO OIL VISCOSITIES

EXPERIMENTAL RESULTS

CONFINED FIVE-SPOT FLOOD

By injecting in the center well and producing from the four outside corner wells, the small model was converted to a confined five-spot pattern (see Figure 13). The production history of the tests is given in Table 14. Figure 21 shows the producing water-oil ratio versus the oil recovered and the water injected. The total sweep efficiency of the system was calculated by dividing values from the oil produced curve by the oil in place of the unit pattern (70.8 cc). The areal sweep efficiency was then calculated by dividing the total efficiency by the displacement efficiency. These curves are presented in Figure 22. The two curves are roughly parallel with the deviation increasing as the life of the test progressed. The curves are convex up and it appears that limiting values of total sweep efficiency and areal sweep efficiency of 80.5% and 98.5% respectively have been reached. Areal sweep efficiency at breakthrough was 68.0%.

An attempt to compare the data with that of Dyes et al[10] and Craig et al[8] was made as follows: The mobility ratio of the flood, at breakthrough, was 1.235 (see Table 13). According to Craig this should result in an areal sweep efficiency of 71.5%. The Craig curve with this origin is plotted in Figure 23. The Dyes data for this mobility ratio was cross-plotted and is presented on the same figure, also with 71.5% as origin. The experimental total efficiency data was then transposed to this datum and also plotted in Figure 23. These are the points shown as modified by assumption one. Points modified by assumption two were obtained by applying the displacement efficiency correction to this data and transposing the resulting curve to the datum. These points are also plotted on the same figure. As

can be seen from Figure 23, points modified by assumption one closely approximate the Dyes curve while those of assumption two lie someplace between it and the Craig curve. Again both experimental curves seem to be approaching a maximum; 100% for assumption one and 93% for assumption two.

ISOLATED FIVE-SPOT FLOOD

The producing and injection wells are shown in Figure 13. Production history of this test is presented in Table 16 while Table 17 gives the calculation of total sweep efficiency, areal sweep efficiency, and the injection ratio. These parameters are presented graphically as Figure 25.

As can be seen from Figure 24, the general configuration of the production and injection history curves is normal but the recovery to breakthrough is 7.35 times the initial oil in place of the unit area. Areal sweep efficiency was 9.68 times the unit area, at breakthrough. Both efficiency curves (Figure 25) are roughly parallel and approach limiting values of 12.5 and 10.2 for total sweep and areal sweep efficiency respectively. There is some suggestion of an "S-shape" configuration of the curves.

Again an attempt was made to compare the data to the Dyes and Craig curves. The calculation was similar to that described above and is presented in tabular form as Table 17. Results are plotted along with the literature curves as Figure 26. As can be seen, points modified by assumption one closely approximate the Dyes curve while those obtained by assumption two fall between the two curves. The points appear to be approaching maximum values as in the previous case (99.5% and 92.0% respectively), while the literature curves do not.

DISCUSSION OF THE TWO ASSUMPTIONS

The first consists of essentially assuming all the recovery to be due to areal sweep, and breakthrough recovery to be 71.5% of the oil in place for the unit area. The close approximation to Dyes results may indicate that miscible data can be modified and utilized in immiscible (i.e. water-flood) studies.

The second assumption involves the displacement efficiency correction and the transposition to 71.5% areal sweep efficiency at breakthrough. The elimination of displacement efficiency should correct the data to the Craig curve. In both cases it does not. This indicates that the displacement correction is inadequate or that the Craig data is not applicable to this system.

Both the actual efficiency curves and the corrected ones seem to be approaching maximum values in direct contrast to the literature results. It can be postulated that for an infinite reservoir the sweep efficiency would continue to increase with the injection ratio. However, for a confined system of any type, a maximum efficiency is to be expected as the reservoir saturation approaches that of the residual oil. This seems to be the situation exhibited in the above results.

LINE DRIVE FLOOD

One set of line drive data, with one row of injection wells and two rows of producing wells, was run. The pattern used is shown in Figure 13. The production and injection history is presented as Figure 27 and Table 18. The unit area was isolated. Table 19 and Figure 28 give the actual results, processed as total sweep efficiency, areal sweep efficiency and the ratio of water injected to water injected to breakthrough. Recovery at breakthrough

was 9.82 times the oil in place while breakthrough areal sweep efficiency

was 12.94 times the unit pattern area. The ultimate total sweep efficiency

and areal sweep efficiency were 11.6 and 14.2 respectively. No attempt to

correct for the high breakthrough recovery was made as no data for comparison

were readily available from the literature.
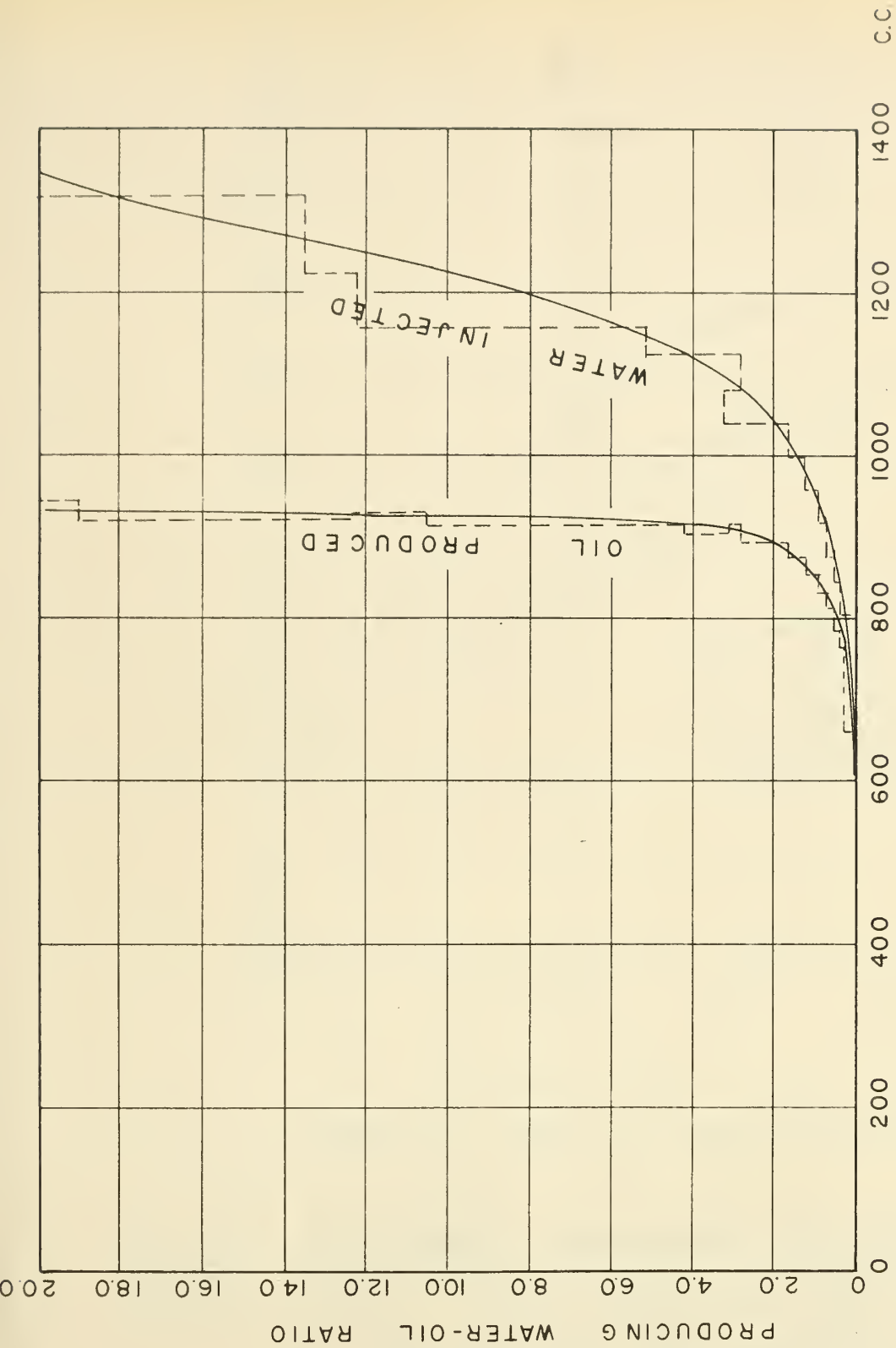
FIG. 21   CONFINED   FIVE-SPOT   FLOOD   PRODUCING   WATER-OIL
RATIO VERSUS OIL RECOVERED   AND WATER INJECTED
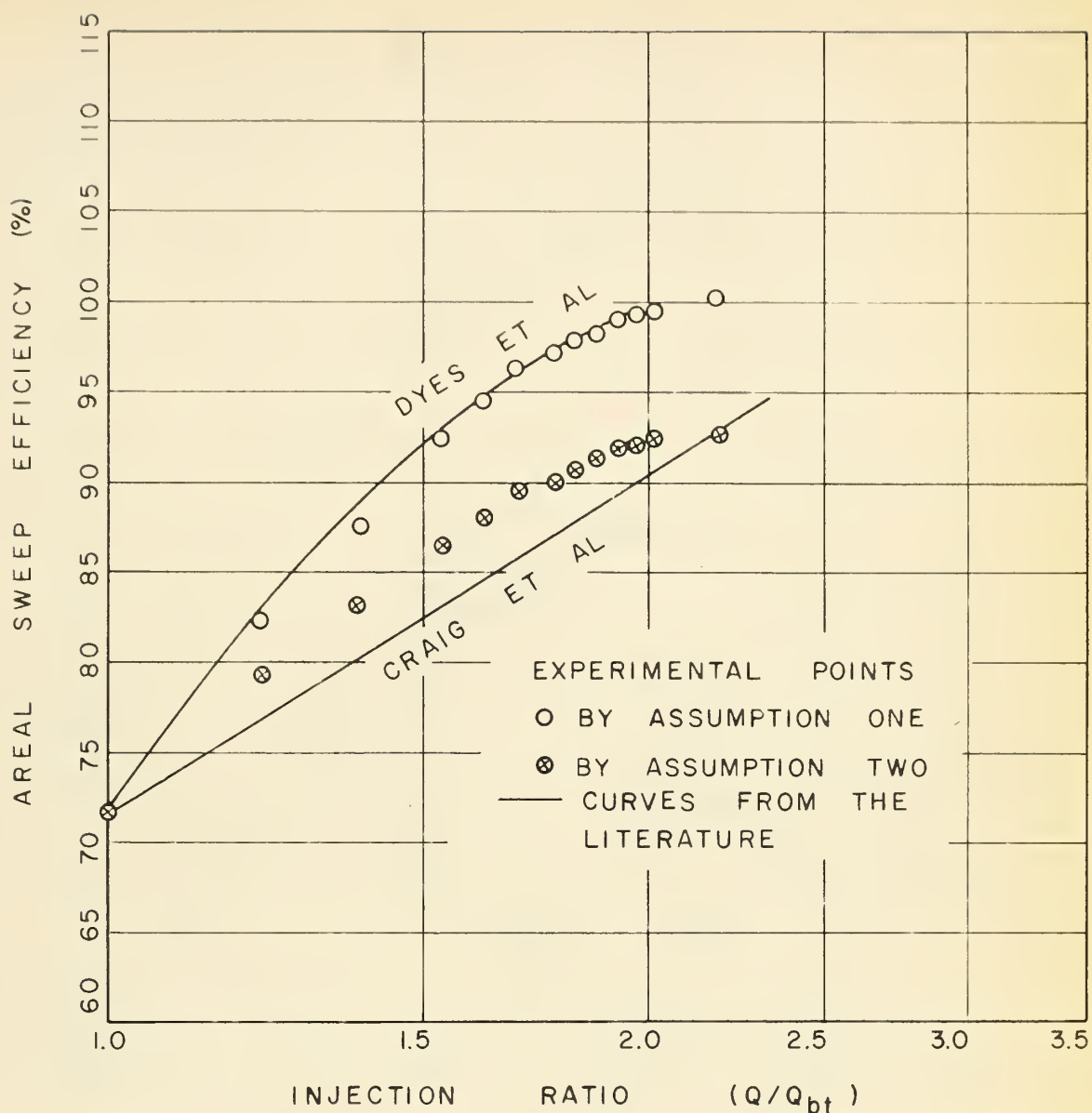
VISCOSITY RATIO μ_w/μ_o = 0.94881

MOBILITY RATIO, AT BREAKTHROUGH $\dfrac{k_o \mu_w}{k_w \mu_o}$ = 1.235

FIG. 23 CONFINED FIVE-SPOT FLOOD AREAL SWEEP EFFICIENCY VERSUS INJECTION RATIO. EXPERIMENTAL DATA MODIFIED AND COMPARED TO DYES ET AL AND CRAIG ET AL
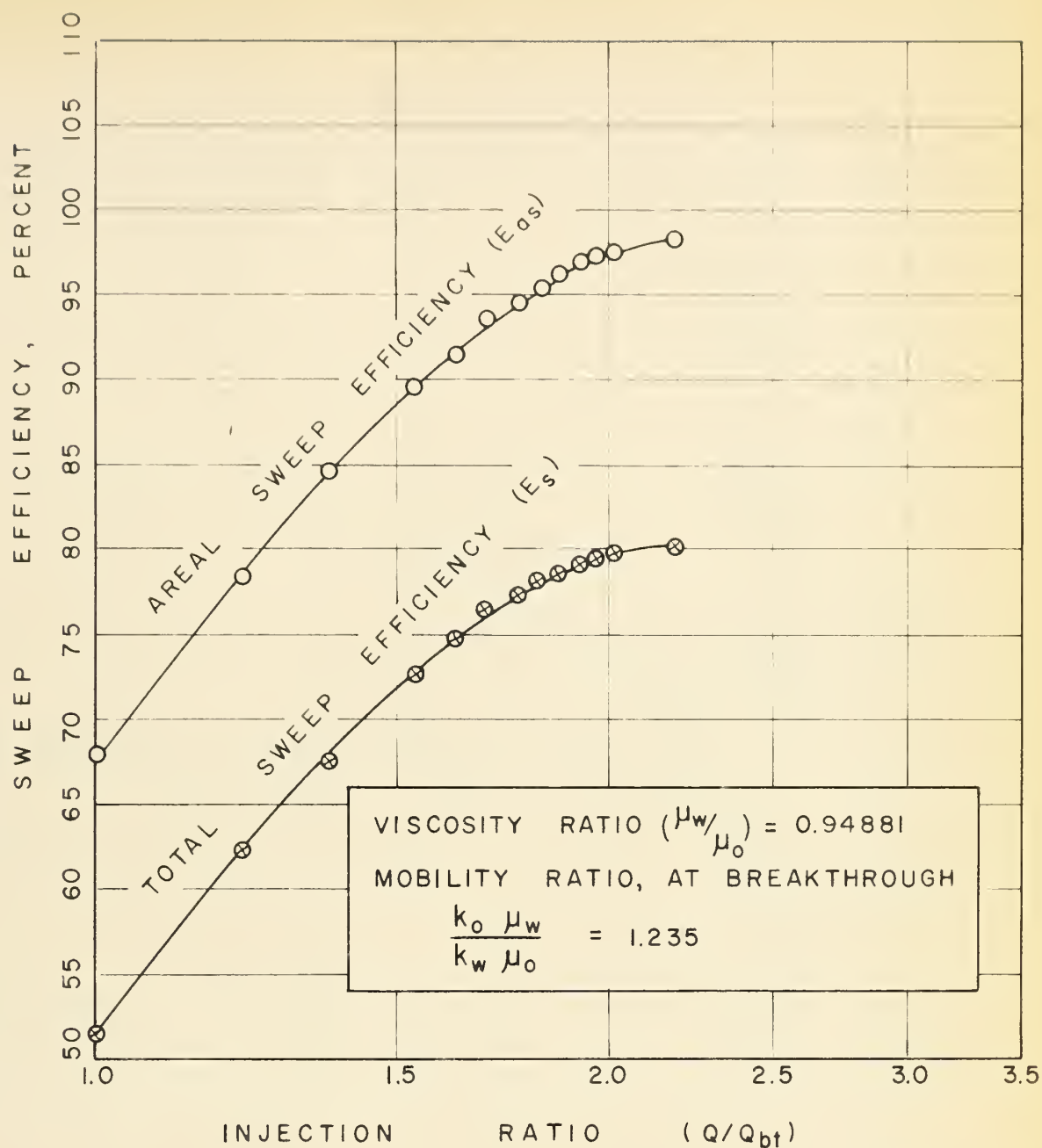
FIG. 22 CONFINED FIVE-SPOT FLOOD TOTAL AND AREAL SWEEP EFFICIENCIES (E_s, E_{as}) VERSUS THE RATIO OF THE VOLUME OF WATER INJECTED TO THE VOLUME OF WATER INJECTED TO BREAKTHROUGH
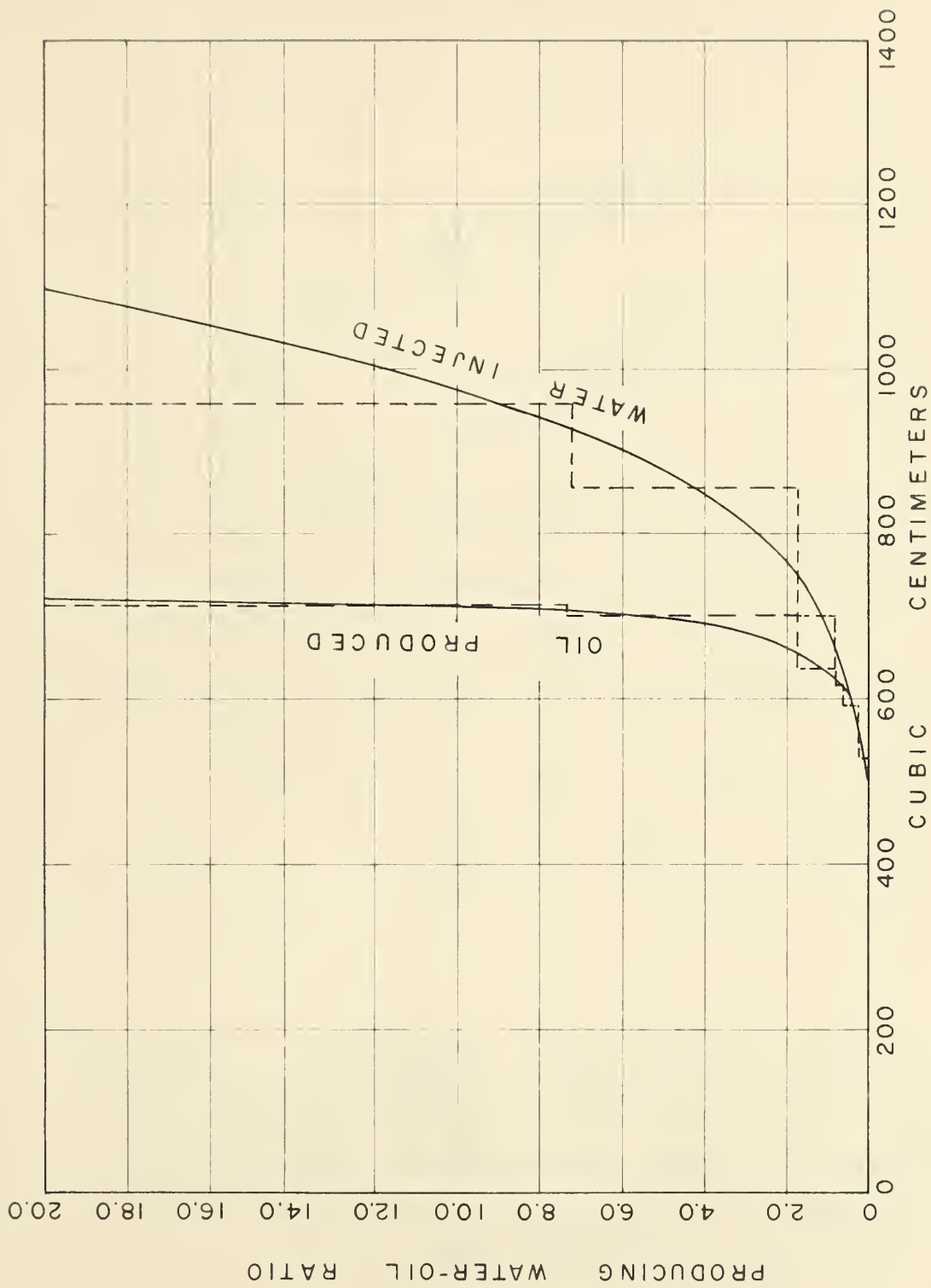
FIG. 24   ISOLATED FIVE-SPOT FLOOD PRODUCING WATER-
OIL RATIO VERSUS OIL RECOVERED AND WATER
INJECTED
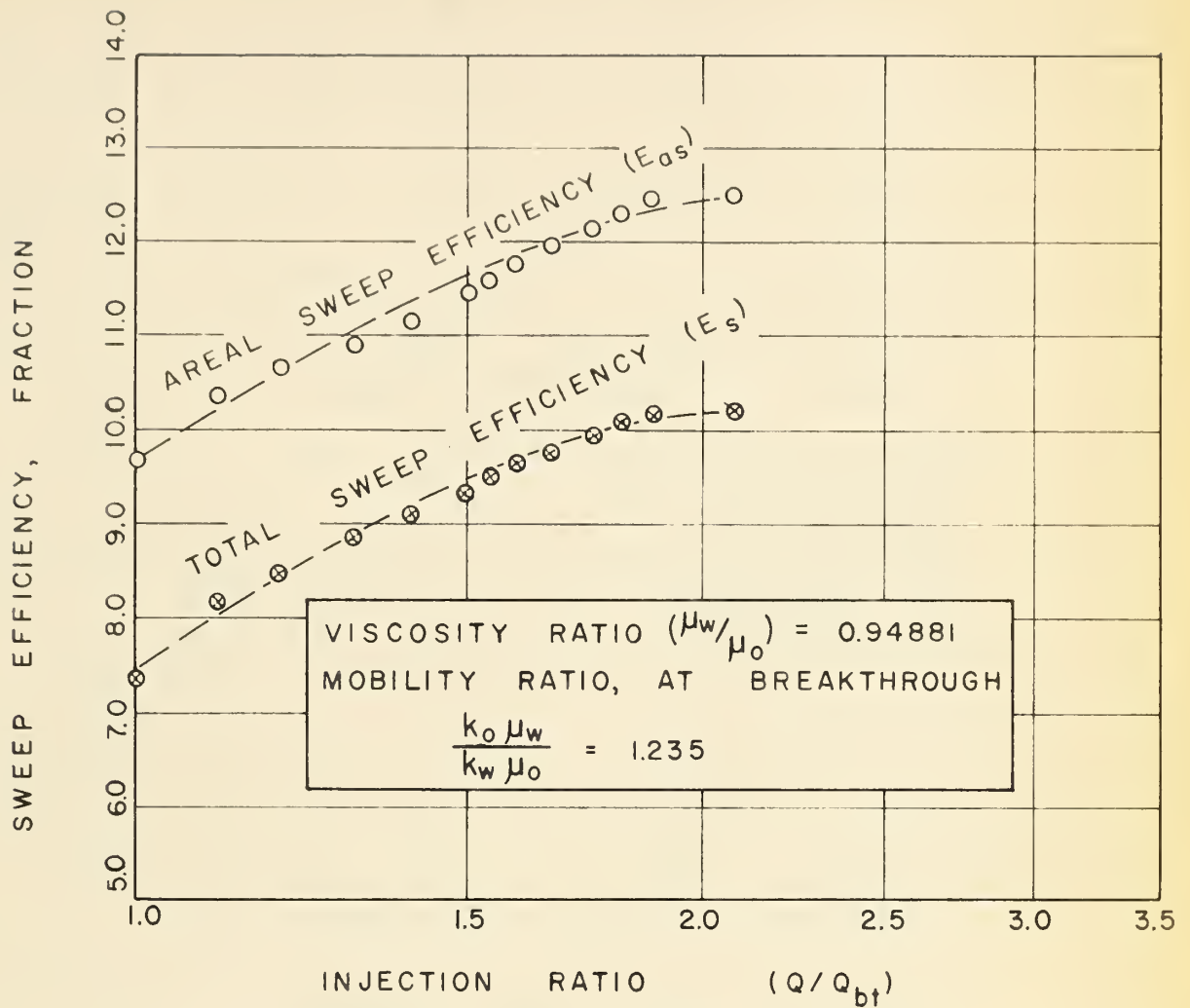
FIG. 25   ISOLATED FIVE - SPOT FLOOD   TOTAL
AND AREAL SWEEP EFFICIENCIES (E_s, E_{as})
VERSUS THE RATIO OF THE VOLUME OF WATER
INJECTED TO THE VOLUME OF WATER INJECTED
TO BREAKTHROUGH (Q/Q_{bt})
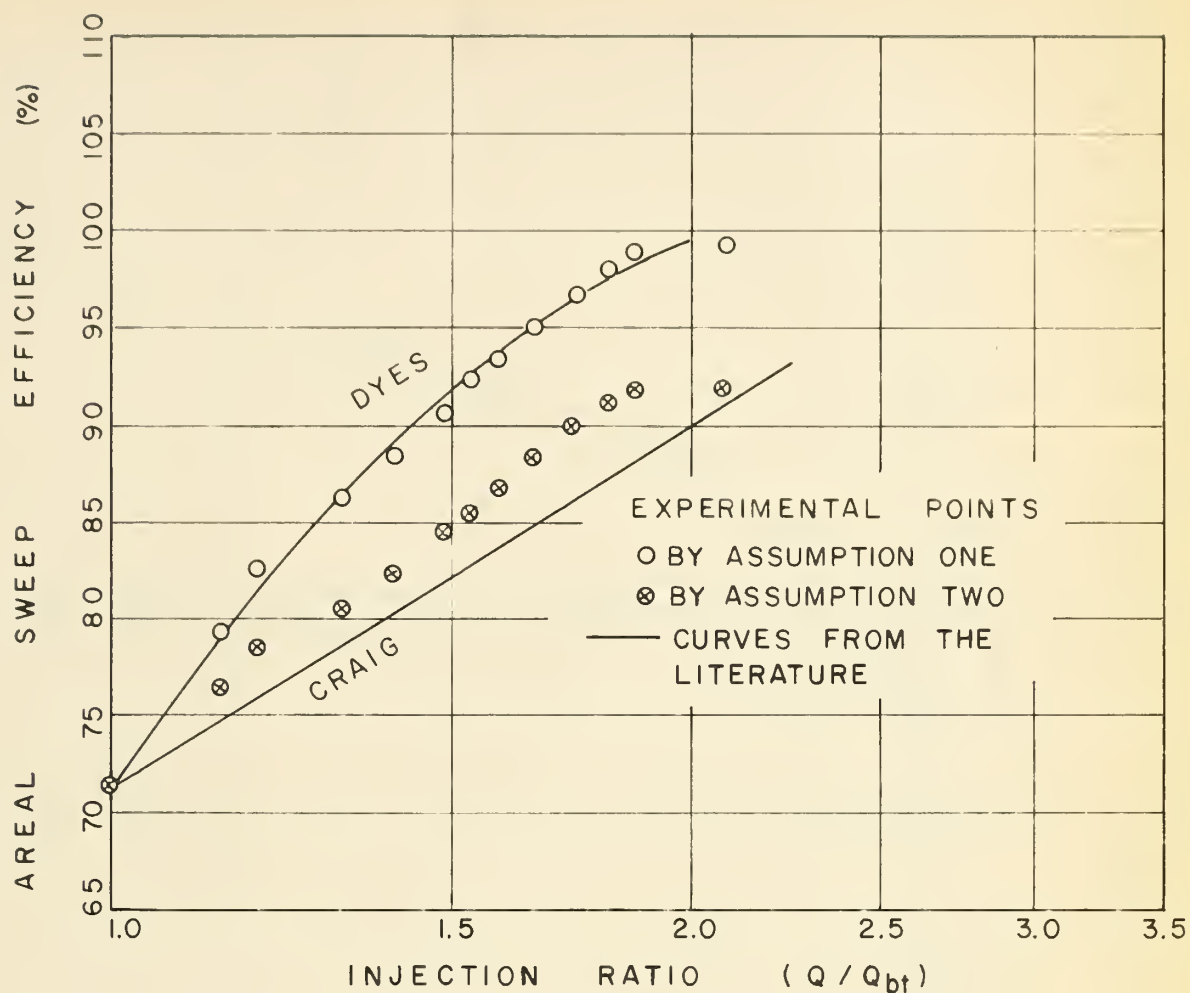
VISCOSITY RATIO μ_w/μ_o = 0.94881

MOBILITY RATIO, AT BREAKTHROUGH, $\dfrac{k_o\,\mu_w}{k_w\,\mu_o}$ = 1.235

FIG. 26   ISOLATED   FIVE-SPOT   FLOOD   AREAL
SWEEP   EFFICIENCY   VERSUS   INJECTION
RATIO - EXPERIMENTAL   DATA   MODIFIED   AND
COMPARED   TO   DYES   ET   AL   AND   CRAIG   ET   AL
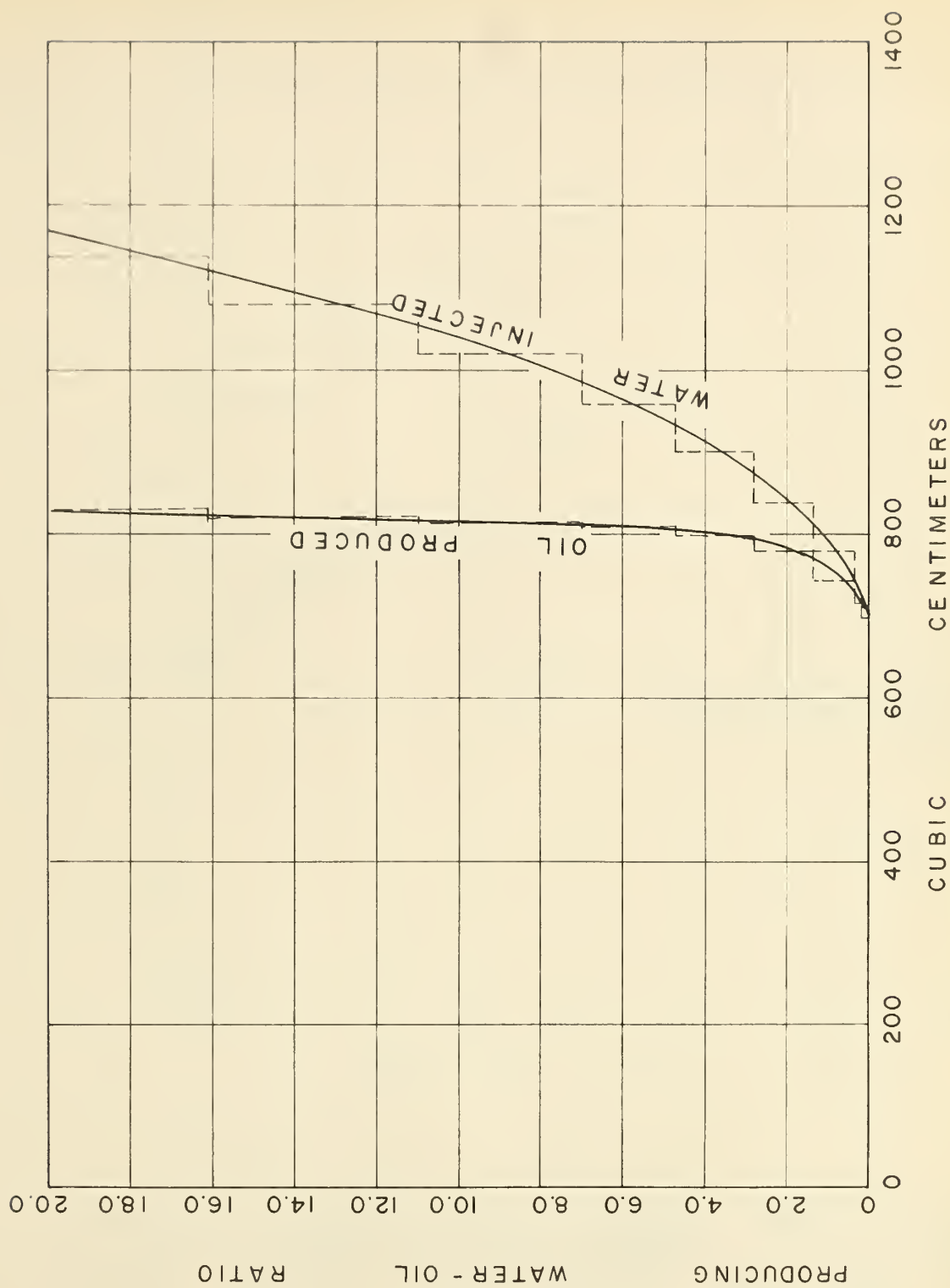
FIG. 27   LINE-DRIVE FLOOD PRODUCING WATER-OIL RATIO
VERSUS OIL RECOVERED AND WATER INJECTED
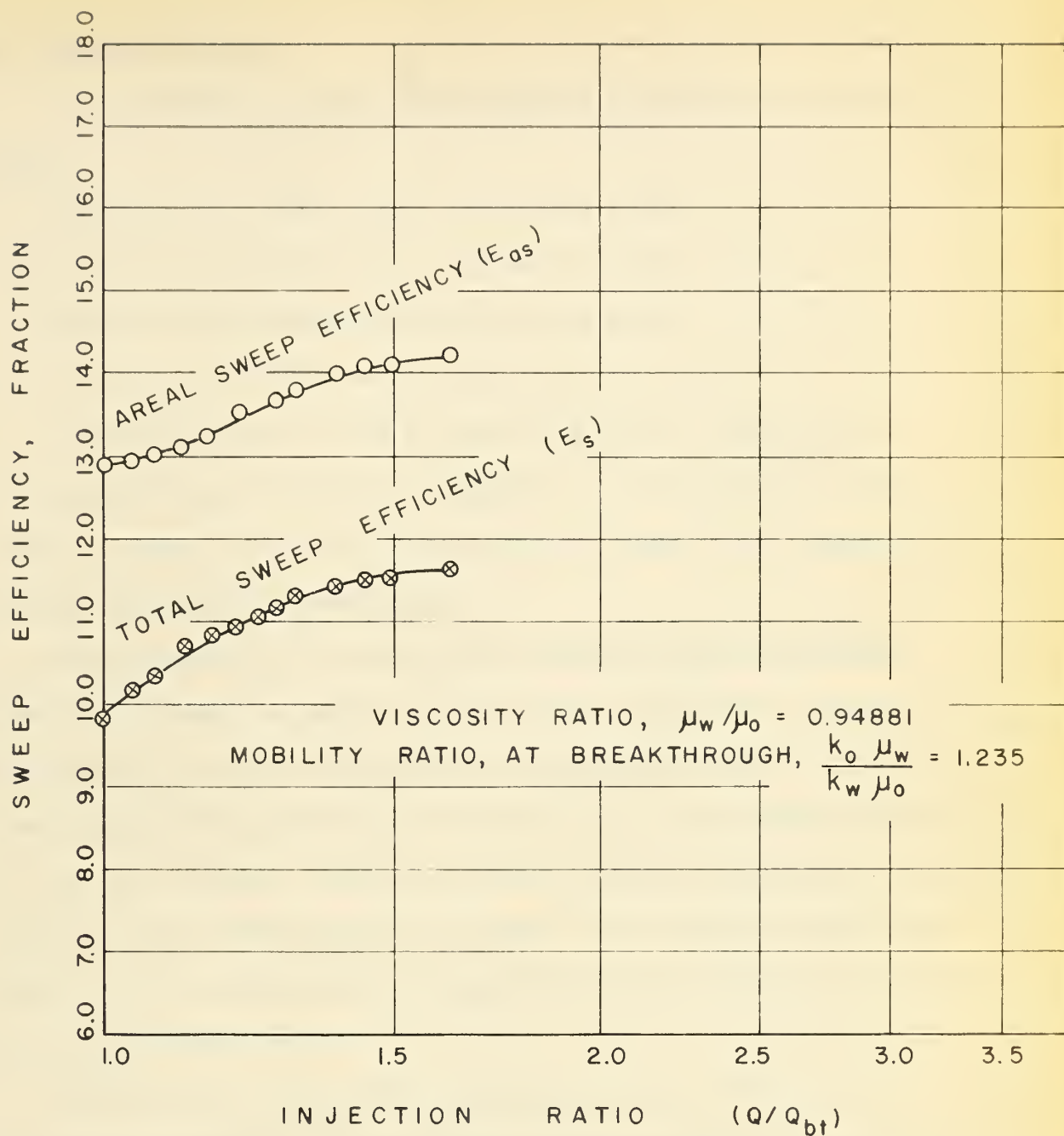
FIG. 28   LINE   DRIVE   FLOOD   TOTAL   AND
AREAL   SWEEP   EFFICIENCIES (E_s , E_{as}) VERSUS
THE   RATIO OF THE   VOLUME   OF   WATER   INJECTED
TO THE VOLUME OF WATER INJECTED TO BREAKTHROUGH

ISOLATED NINE-SPOT FLOODS

Four isolated nine-spot water floods were run and are identified
as follows:

Flood No. 2-1; large model, low viscosity oil

Flood No. 2-2; small model, low viscosity oil

Flood No. 2-3; small model, low viscosity oil

Flood No. 2-4; small model, high viscosity oil

Flood No. 2-3 was run as a repeat of Flood No. 2-2 as only a
limited amount of production data was collected in the latter test. For
this reason, results of Flood No. 2-2 have not been used in any computations
and are only referred to quantitatively.

Nine-spot floods 2-2 and 2-3 both exhibited high breakthrough
recoveries of 9.04 and 7.06 times the oil in place respectively. These
high breakthrough recoveries are similar to those experienced from the line
drive and isolated five-spot tests. On Flood No. 2-1 breakthrough recovery was
52.2% of the oil in place. When this was corrected for displacement efficiency,
the resulting areal sweep efficiency was 74.0%. The ultimate recovery was
2.28 times the oil in place and the ultimate areal sweep efficiency was 2.84
times the pattern unit area.

Flood No. 2-4, on a 5.107 centipoise oil, also did not exhibit the
high breakthrough recovery. In this case breakthrough recovery was 89.2% of
the oil in place while the areal sweep efficiency was 210%.

Production and injection histories of tests 2-1, 2-3, and 2-4 are
shown in Figures 29, 31 and 33 respectively. The conversion of this data to
total sweep efficiency, areal sweep efficiency and the injection ratio (Q/Q_{bt})
is tabulated as Tables 23, 29, and 33. The resulting curves are plotted in
Figures 30, 32, and 34.

Injection ratio values over a much greater range were obtained
for Flood No. 2-4 than for either of the other two floods. This is the result
of the much greater subordinate production (i.e. production after breakthrough)
of Flood No. 2-4. As can be seen from all three sets of curves, the total
efficiency and areal sweep efficiency parallel each other although they
deviate more over the high efficiency portion of the curves. This may be
considered a function of the higher displacement efficiency in this range.
In all cases the efficiencies appear to be approaching a maximum.

A comparison of Figure 20 (Flood No. 2-1) and Figure 34 (Flood
No. 2-4) shows that both curves exhibit the same characteristic "S-shape"
although the injection ratio (Q/Q_{bt}) and efficiency values for Flood No.
2-4 cover a much greater range. Shortly after breakthrough both curves are
slightly concave up, although they approximate a straight line. This indicates
that the relationship between sweep efficiency and the injection ratio is
essentially the same as for Craig's five-spot flood; i.e. the sweep efficiency
varies directly with the logarithm of Q/Q_{bt}. Following the straight line
portion of the curve is a section of increasing slope, passing through an
inflection point to a decreasing slope, and finally approaching a maximum.

This latter portion of the curve (i.e. that which deviates from
the straight line) might be interpretted as due to boundary effects. Up
until this point the bed has acted essentially as an infinite reservoir.
The injection of more and more fluid has swept more and more area in what may
be visualized as essentially a circular pattern. At the point where the edges
have been contacted, only unswept area in the corners is available. Now
most of the injection fluid enters these areas, accounting for the increased
slope of curve. When these areas have been swept there is no more reservoir

available for flooding so the curve approaches a maximum efficiency for any
particular flood.

Flood No. 2-3 was run on the same fluid-sand system as Flood No.
2-1; but on a different model. As mentioned above, the breakthrough recoveries
did not compare. In an attempt to compare the data from Flood No. 2-3 to
that of Flood No. 2-1, a correction similar to that of the five-spot was made.
That is, the areal sweep efficiency at breakthrough was assumed to be 74.0%,
the same as for Flood No. 2-1. The resulting curve is plotted in Figure 35
along with the actual result of Flood No. 2-1. As can be seen, the curves
coincide over the early life of the flood but deviate greatly over the
later life of the flood.

COMPARISON OF THE THREE ISOLATED PATTERNS

Figure 36 shows the areal sweep efficiency versus the injection
volume ratio for the five-spot, nine-spot and line drive patterns. All three
tests were run on the same model using the low viscosity oil, the same rate
of injection and the same pattern unit area. All floods were taken to a pro-
ducing water-oil ratio of 20:1. The only variation was in the well pattern used.

As can be seen, results of the five-spot and nine-spot patterns
coincide closely; the five-spot having slightly higher areal sweep efficiencies
over the life of the flood but a lower ultimate areal sweep efficiency. The
line drive system exhibits higher areal sweeps over its entire history with a
much smaller change in areal sweep over this period.
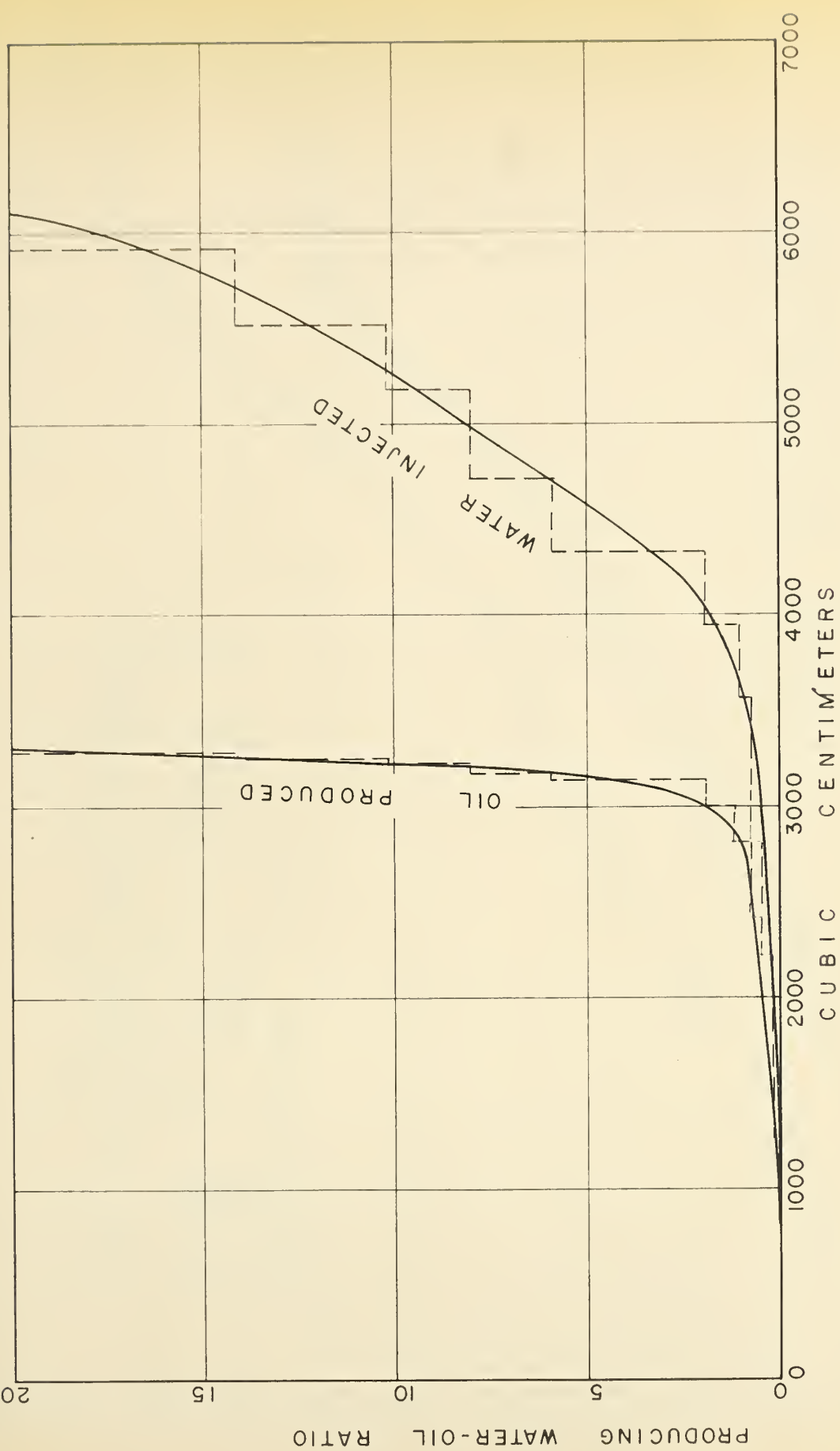
FIG. 29   NINE-SPOT FLOOD NO. 2-1   PRODUCING   WATER-OIL
RATIO VERSUS OIL RECOVERED AND WATER INJECTED

FIG. 30 NINE-SPOT FLOOD NO. 2-1
TOTAL AND AREAL SWEEP EFFICIENCIES (E_s, E_{as}) VERSUS THE RATIO OF THE VOLUME OF WATER INJECTED TO THE VOLUME OF WATER INJECTED TO BREAKTHROUGH (Q/Q_{bt})

VISCOSITY RATIO μ_w/μ_o = 0.94881
MOBILITY RATIO, AT BREAKTHROUGH,
$$\frac{k_o}{k_w}\frac{\mu_w}{\mu_o} = 1.235$$

AREAL SWEEP EFFICIENCY (E_{as})

TOTAL SWEEP EFFICIENCY (E_s)

SWEEP EFFICIENCY, PERCENT

INJECTION RATIO (Q/Q_{bt})
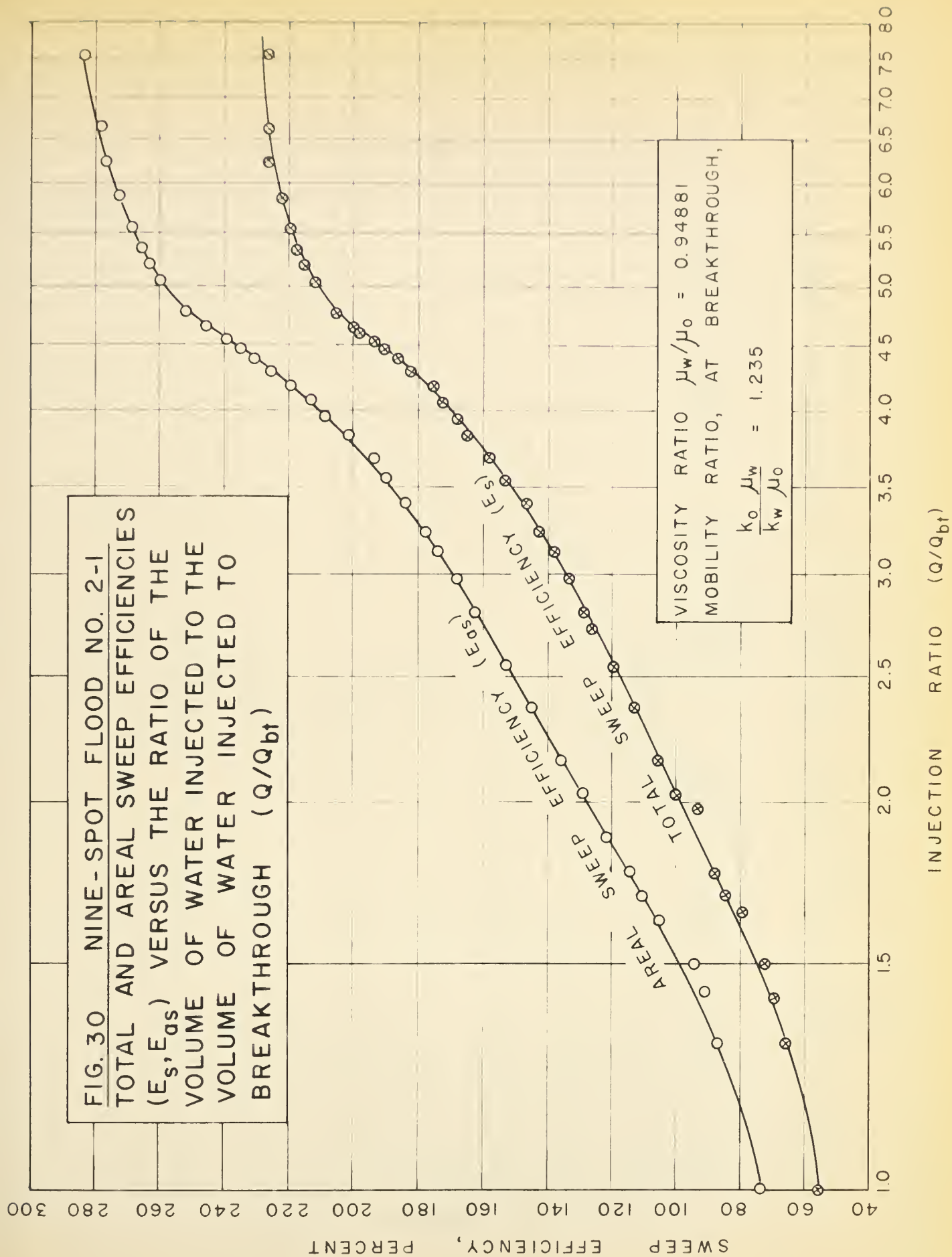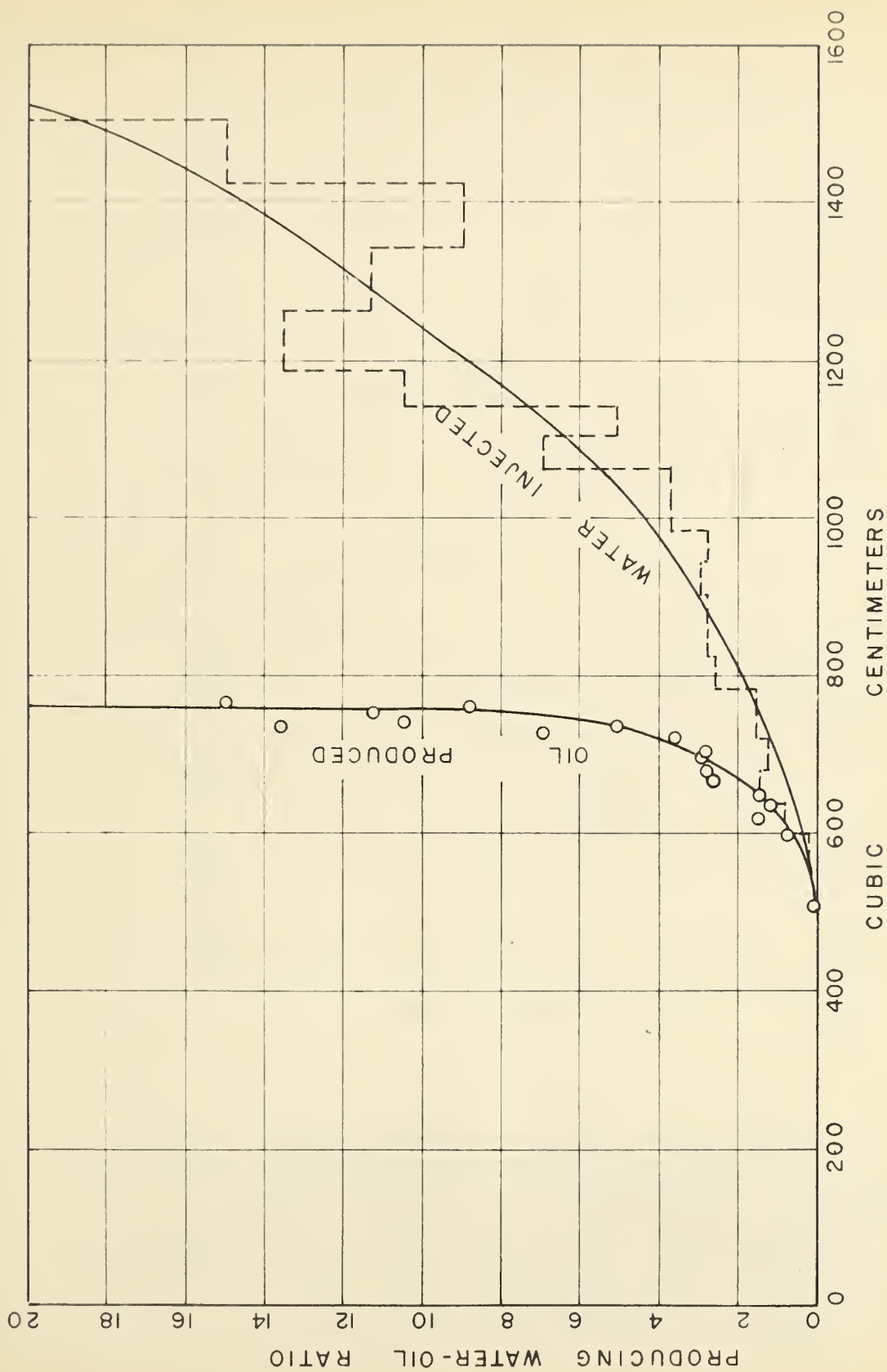
FIG. 31   NINE-SPOT FLOOD NO. 2-3   PRODUCING WATER-OIL
RATIO VERSUS OIL RECOVERED AND WATER
INJECTED
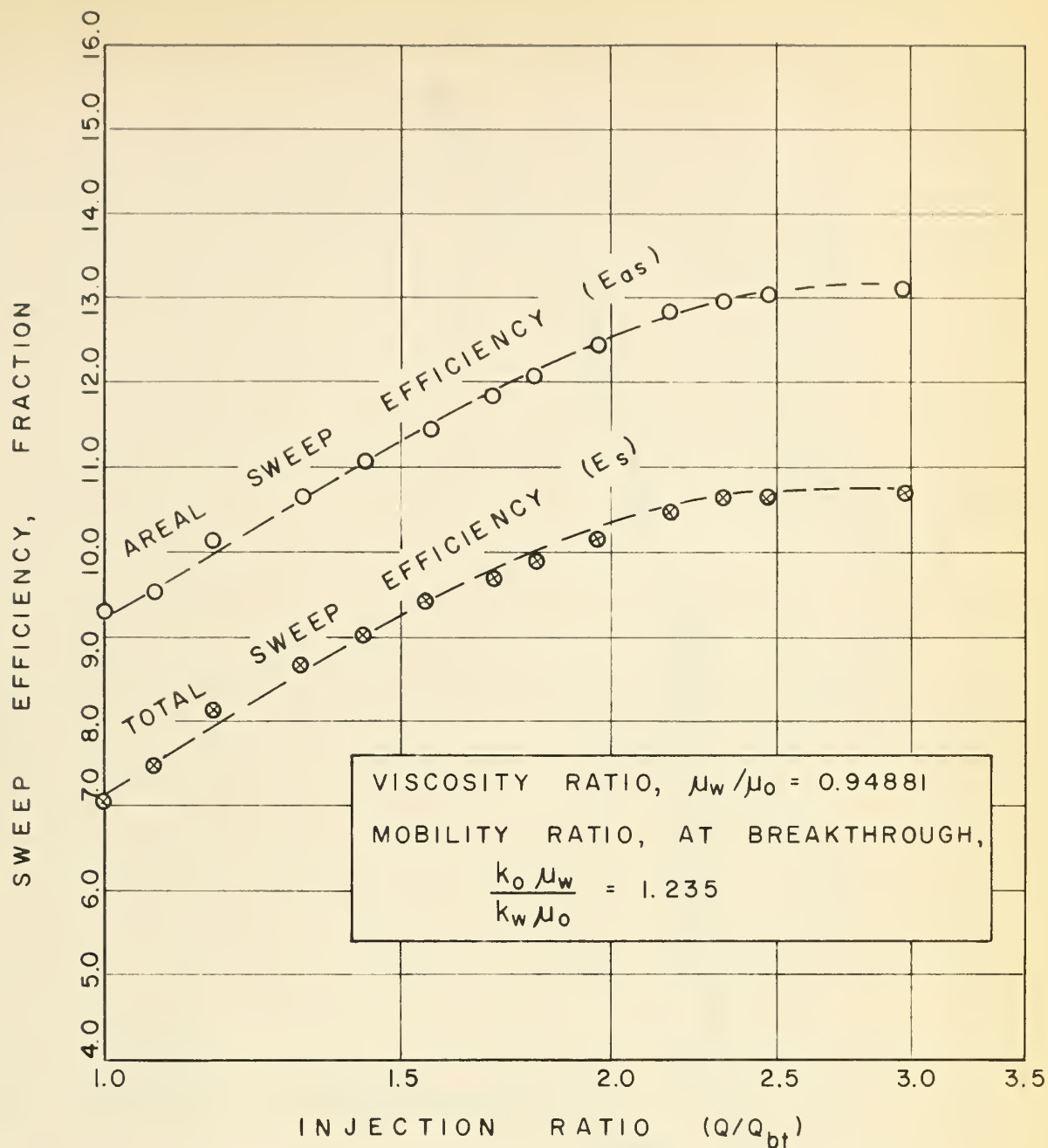
FIG. 32   NINE-SPOT   FLOOD   NO. 2-3   TOTAL
AND   AREAL   SWEEP   EFFICIENCIES (E_s, E_{as})
VERSUS   THE   RATIO   OF   THE   VOLUME   OF   WATER
INJECTED   TO   THE   VOLUME   OF   WATER   INJECTED
TO   BREAKTHROUGH (Q/Q_{bt})
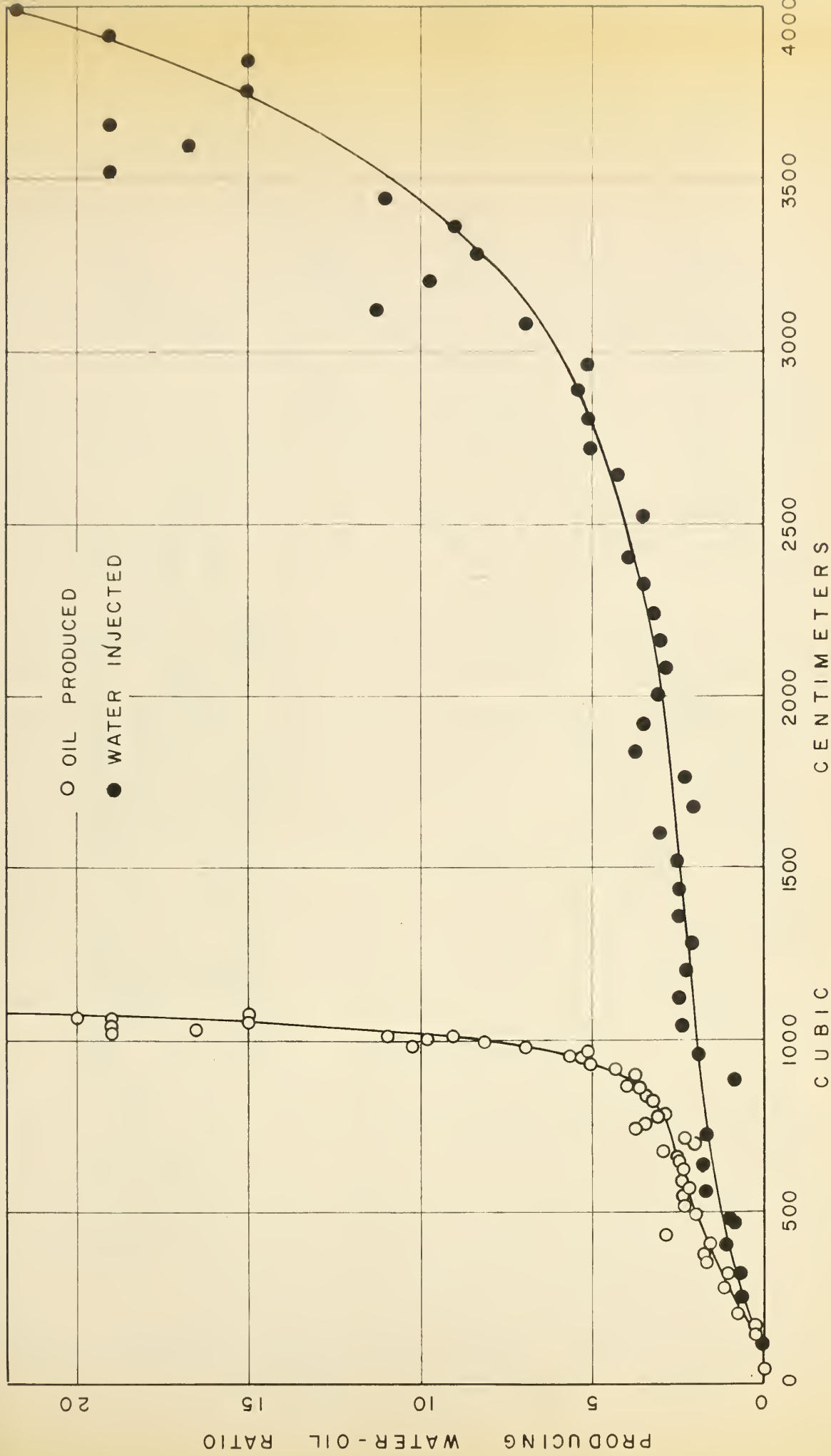
FIG. 33   NINE-SPOT FLOOD NO. 2-4   PRODUCING WATER-OIL
RATIO VERSUS OIL RECOVERED AND WATER INJECTED

FIG. 34 NINE-SPOT FLOOD NO. 2-4 TOTAL AND AREAL SWEEP EFFICIENCIES (E_s, E_{as}) VERSUS THE RATIO OF THE VOLUME OF WATER INJECTED TO THE VOLUME OF WATER INJECTED TO BREAKTHROUGH (Q/Q_{bt})

VISCOSITY RATIO $\mu_w/\mu_o = 0.16840$

MOBILITY RATIO, AT BREAKTHROUGH,

$$\frac{k_o\,\mu_w}{k_w\,\mu_o} = 0.667$$

INJECTION RATIO (Q/Q_{bt})

SWEEP EFFICIENCY, FRACTION

AREAL SWEEP EFFICIENCY (E_{as})

TOTAL SWEEP EFFICIENCY (E_s)
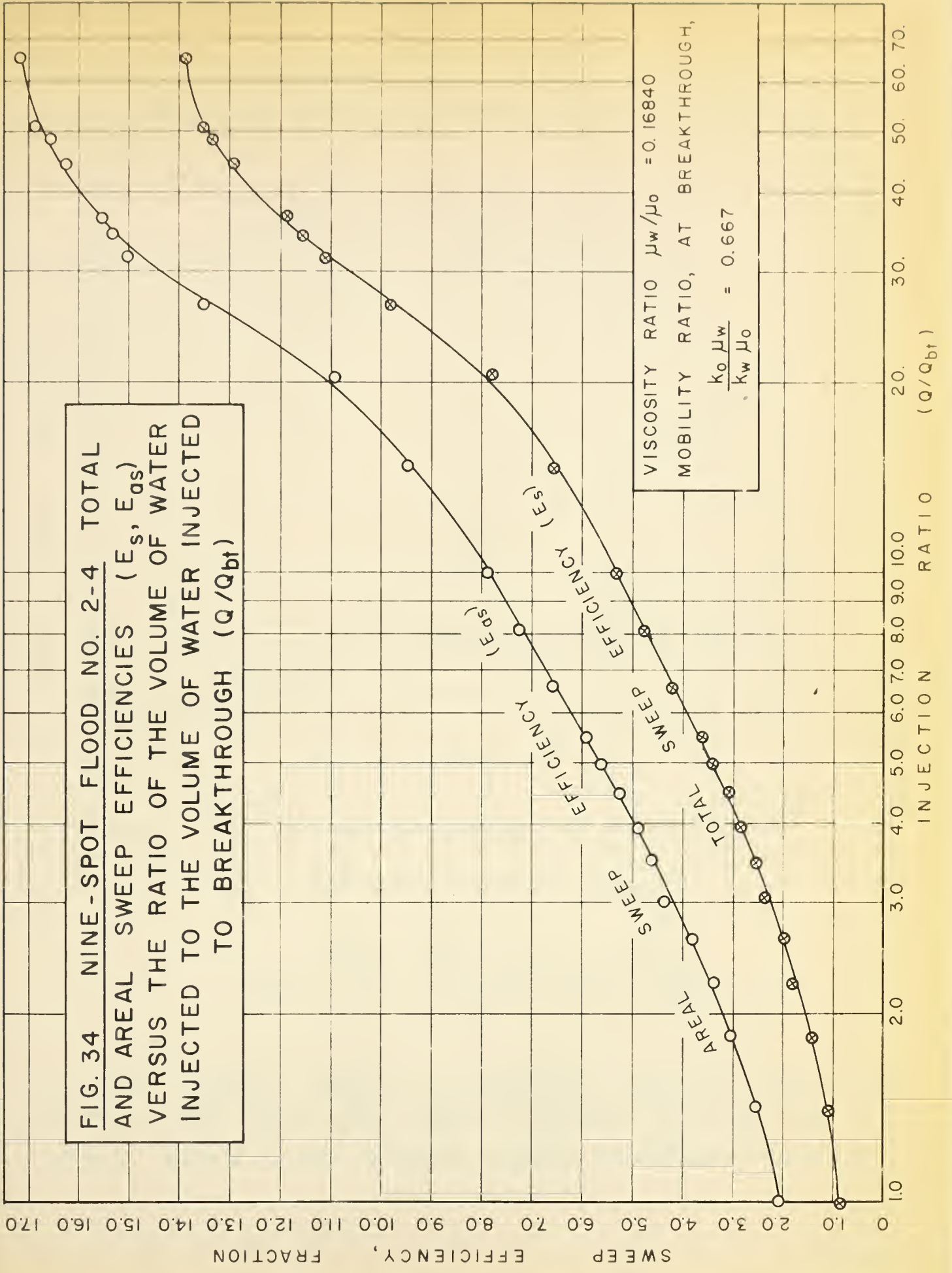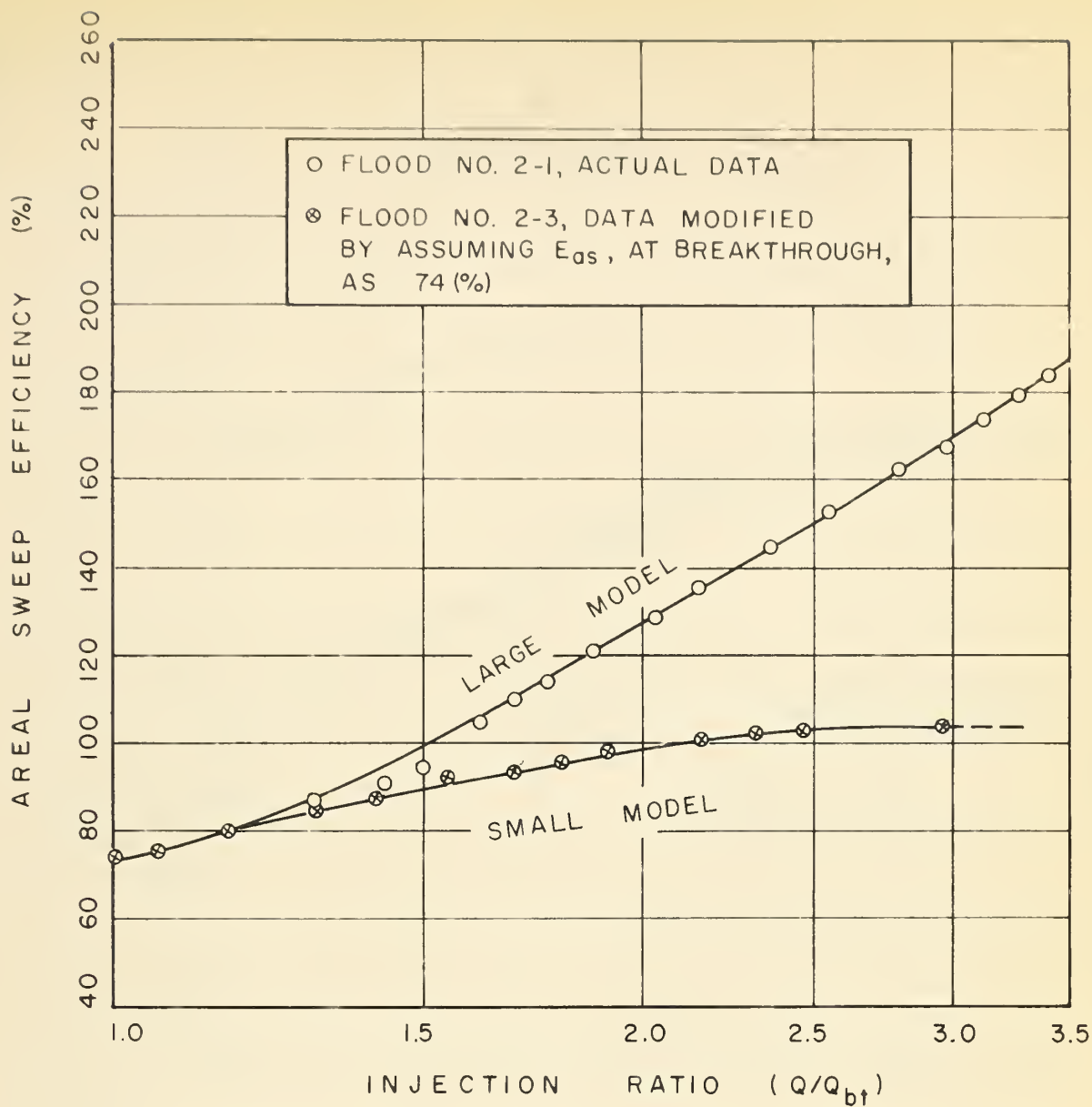
VISCOSITY RATIO $\mu_w/\mu_o = 0.94881$

MOBILITY RATIO, AT BREAKTHROUGH, $\dfrac{k_o\mu_w}{k_w\mu_o} = 1.235$

FIG. 35   AREAL SWEEP EFFICIENCY VERSUS INJECTION
RATIO   FOR   TWO   NINE-SPOT FLOODS   RUN   ON   THE
SAME   SAND-FLUID SYSTEM USING DIFFERENT MODELS
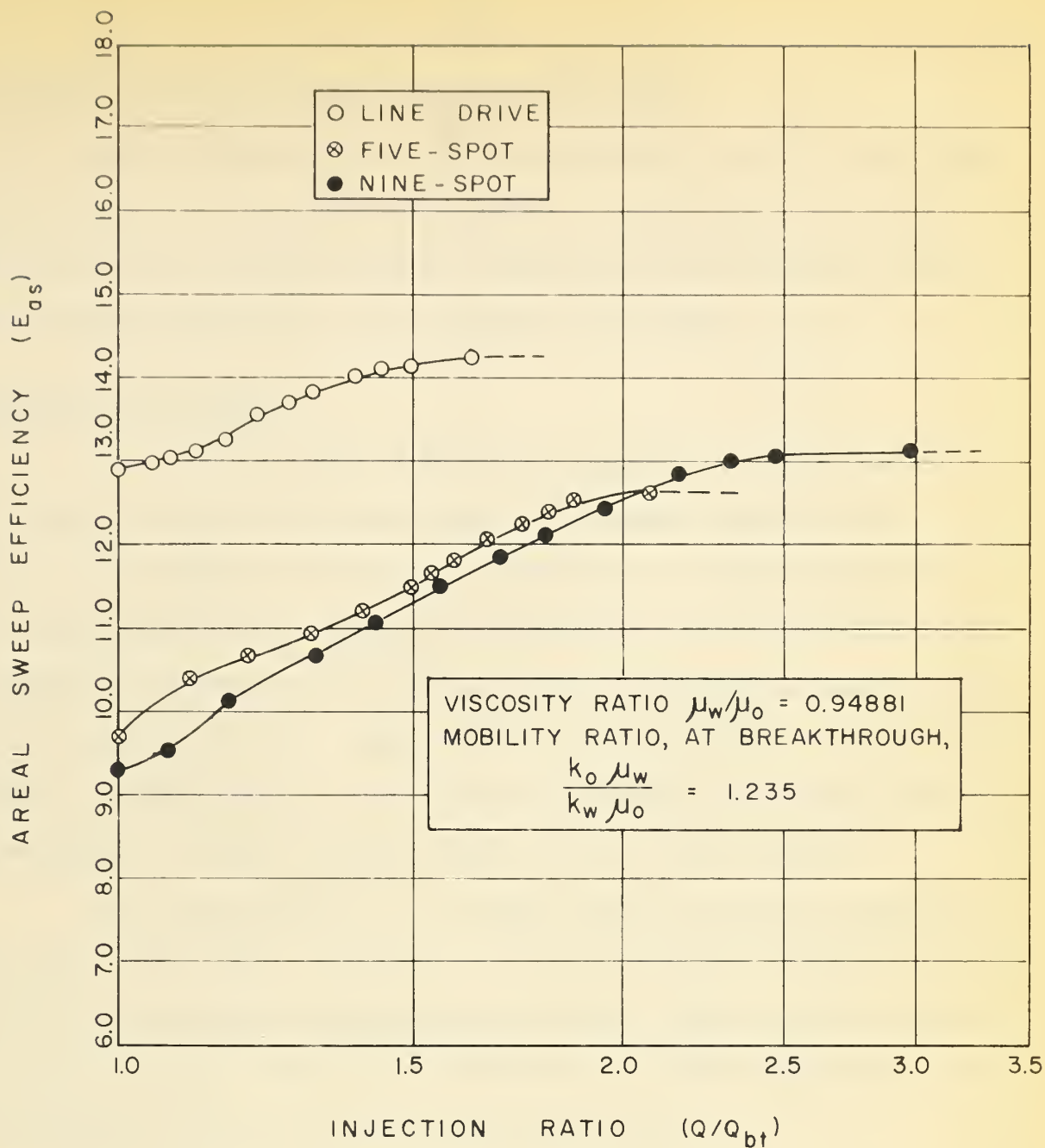
FIG. 36   AREAL   SWEEP   EFFICIENCY   VERSUS
INJECTION   RATIO   FOR   THREE   DIFFERENT
WELL PATTERNS RUN ON THE SAME SAND-
FLUID   SYSTEM

POSTULATES REGARDING THE HIGH BREAKTHROUGH RECOVERIES

From the forgoing, it can be noted that all tests run on the small model with the low viscosity oil resulted in extremely high breakthrough recoveries. The writer has arrived at two possibilities which may account for these high recoveries. Each are briefly put forward.

Imbibition Into the Sand

In a water wet sand, if there is a capillary pressure gradient in the direction of flow, displacement will be increased because of this gradient. The process is referred to as imbibition. Mattax and Kyte[16] have illustrated that a permeability discontinuity in the system will result in imbibition taking place more rapidly in the less permeable portion of the reservoir at certain rates. They conducted their experiments on a fractured limestone and found that at rates below their critical, water would invade and displace oil in the limestone itself; but not in the fracture.

In the small model, it is possible that the well bores exhibited this larger permeability condition so that injection water actually by-passed the well bore to imbibe into additional reservoir. When the entire reservoir was flushed to some critical water saturation, the easiest water path would be through the well bore and breakthrough would occur.

Well Design

One of the main differences between the large model (Flood No. 2-1) and the small model was the design of the well bore. The basic difference is that the large model well utilizes a perforated sleeve while the other consists of two large perforations at right angles with a screen sleeve liner in the upper perforation. This screen is of smaller mesh size so that the sand cannot

be produced with the liquid flow stream.

It is not known if the screen is preferentially water wet or oil wet but for the balance of this discussion it will be assumed oil wet.

An oil wet screen, due to capillary forces and wetting attractive forces, retains oil on the members and in the mesh voids. An outside force or a pressure differential is required to move this oil. At some maximum or critical pressure differential (and hence and injection rate) the capillary force will be over-come and all the oil flushed from the mesh, except for a residual which cannot be removed due to the screen being oil wet (analogous to the connate water saturation in a porous rock). Using this reasoning, it is possible that at certain pressures an oil wet screen could pass oil and not water. It was noticed that just before breakthrough the pressure increased slightly. Possibly there is a critical water saturation at which production through the screen occurred; as a constant rate pump was used the only noticeable effect would be a slight increase in pressure.

From the above postulate it can be imagined that the screen, included in the well design, acted as a water filter up to a critical saturation at which time water broke through and was produced.

General Notes

Both of the above postulates depend on flow below the critical rate and on capillary pressure effects; in the first case these parameters apply to the screen sleeve; in the second to the sand bed itself.

The phenomenon was not exhibited in Flood No. 2-1 nor Flood No. 2-4. As can be seen from Darcy's law (eqn. 10), the injection rate is a function of the sand permeability, liquid viscosity, differential pressure, and dimensions of the system. Flood No. 2-1 was run on the large model at the

same rate, on the same viscosity oil. Because of the larger dimensions a larger pressure differential resulted so that the flood took place at pressures above the capillary pressure of the system. High breakthrough recoveries were not exhibited in Flood No. 2-4 for similar reasons. A higher viscosity oil was used which resulted in a larger pressure differential for the same rate. Again this larger operating pressure was above the capillary pressure of the system.

THE APPLICABILITY OF THE DISPLACEMENT EFFICIENCY CORRECTION

In the two dimensional, model water floods the relationship between total sweep efficiency, displacement efficiency, and areal sweep efficiency are defined by the simple equation:

$$E_s = E_d E_{as} \quad \ldots \ldots \ldots \ldots \ldots \ldots \ldots \ldots \ldots \quad (14)$$

If E_s is known as in the present case, E_{as} may be calculated by substituting the appropriate E_d term. For a linear system the displacement efficiency can be calculated from the fractional-flow curve as it was this type of data that Buckley and Leverett used in developing the theory.

The question is whether or not this theory may be used to calculate the displacement efficiency of a two dimensional flood.

Let us consider a simple, two well, confined system as shown in Figure 37. Area 1 indicates area flooded at time 1; area 2 indicates additional area flooded at time 2. Oil production during the time interval comes from both area 1 (by displacement or stripping action) and from area 2 by areal sweep. In this case does the producing water cut result in the proper saturation value from the fractional-flow curve? If area 1 was the only area swept and all the injection fluid passed through it, then the resulting oil production would be due only to displacement. However, in this case some of

the injection fluid goes into the newly swept area and results in what
appears to be a lower water cut figure than would occur in the linear flood.

No attempt was made to prove or disprove the applicability of the
correction as it now stands. The above dissertation merely illustrates the
problem. Some suggestion as to setting up experimental procedures
for verifying the correction are included in the following section.
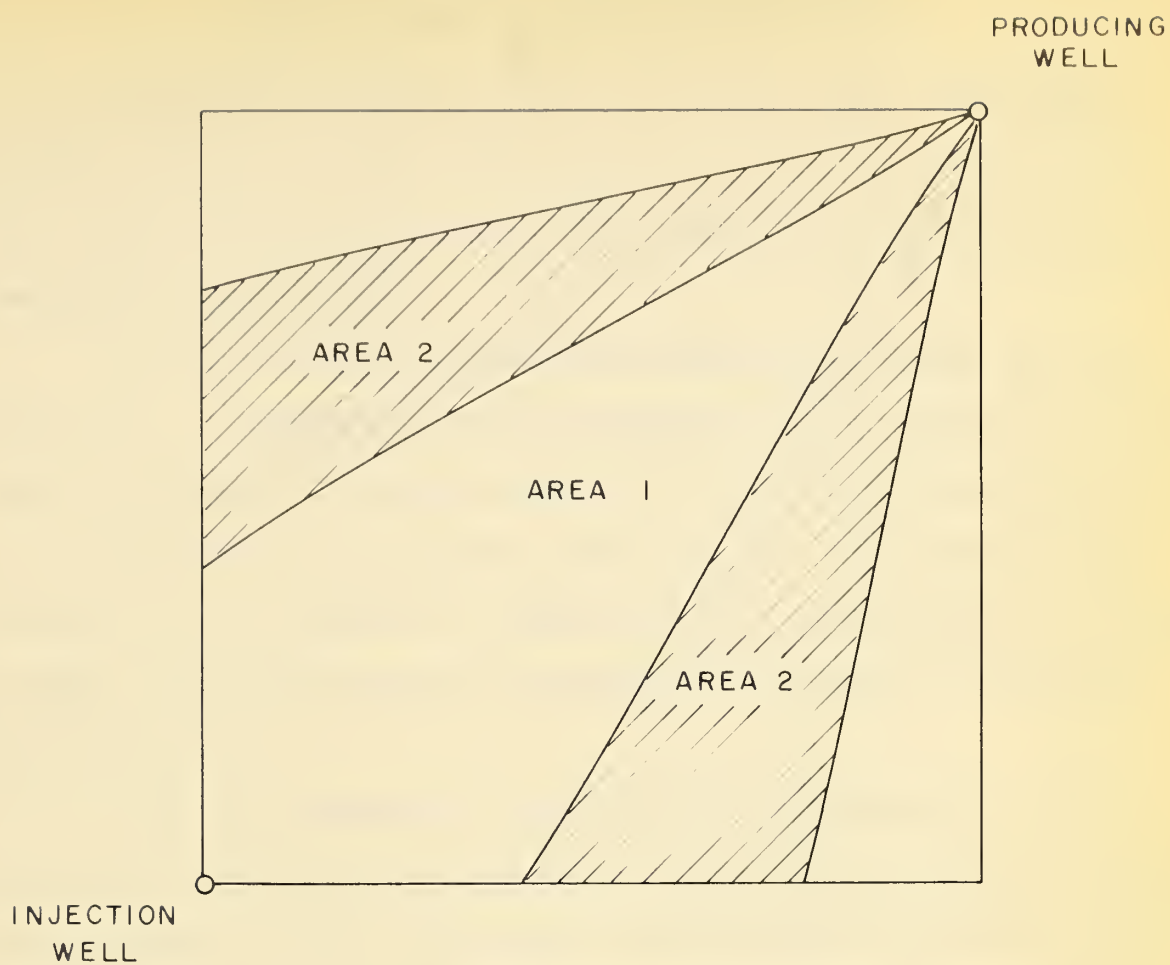
FIG. 37   SCHEMATIC   DRAWING   OF   AN   HYPOTHETICAL
TWO   WELL   CONFINED   SYSTEM

RECOMMENDATIONS FOR FUTURE INVESTIGATIONS

What was originally thought to be a fairly simple experimental procedure resulted in several difficulties and unusual effects. For this reason, further work on the nine-spot study should be delayed until some of these problems are overcome.

Some investigation of the high breakthrough recoveries should be carried out. By substituting wells of a different design the well bore effect could be evaluated. If the well design is not the cause, the problem becomes one of investigating the properties of the sand bed. This could possibly be carried out as a critical rate study; that is, using the same oil, to flood the model at different rates and to determine if the effect is overcome at one particular rate.

It is very desirable to obtain and test a suitable dye. If a suitable dye is obtained, the flood front could be visually mapped at various times throughout the tests. The areal sweep efficiency would then be readily obtained by planimetering the area behind the flood front. It would then be possible to determine if the displacement efficiency correction, made in this report, is accurate. Possibly a correlation for obtaining displacement efficiency or a method of calculation could be devised. This, of course, presumes that the displacement efficiency calculation used here is incorrect.

Because of the correlation between the five-spot data run and the literature, the above investigations could best be carried out on a five-spot pattern. As there is an abundance of data on this pattern to be found in the literature, a ready means of comparison would then be available.

When the above problems have been overcome, nine-spot data for a variety of oil viscosities could be run with some assurance as to accuracy. If it is felt that data is to be obtained which is directly applicable to a drilled out field, consideration should be given to running data on a confined model. These remarks, of course, also apply to patterns other than the nine-spot which are deemed worthy of investigation.

CONCLUSIONS

FUNDAMENTAL RESERVOIR PROPERTIES

Capillary Pressure

The capillary pressure curve obtained indicates that good capillary pressure data may be obtained from the experimental procedure used. The results obtained were of the same magnitude as those of Leverett for an unconsolidated sand (see J-function comparison, Figure 5). This indicates that where time is a factor, or it is inconvenient to run capillary data, fairly accurate data may be obtained by utilizing the J-function correlation. This is not a universal correlation, however, and care must be taken to choose data which most closely corresponds to the rock type being investigated.

Wettability

The resistivity results do not agree with those which are anticipated by the Archie relationship. Archie's work involved a multitude of water wet specimens and must be accepted as authentic. The deviation experienced here may be interpretted to indicate that the system is not entirely water wet. It is possible that, during the course of the experiments, the wetting properties of the sand pack were undergoing a change from fully water wet to partially water wet.

Effective Permeability

The Ruska pump set-up results in very good effective permeability data. Since this type of information is not readily available for many porous media, the experimental technique may be readily utilized in obtaining such data. The poor comparison of the relative permeability curves to those of Leverett indicate that it is desirable to obtain this data for each unique system which is to be studied. If the data from the literature must be used, extreme care should be exercised in obtaining effective permeability curves which were run on systems very similar to those under consideration.

Critical Rate

When recovery of oil is considered as a function of rate, there is an optimum rate at which maximum recovery occurs for any given sand-fluid system. This is in contrast to the literature which suggests a maximum or critical above which recovery is rate independent.

This optimum rate suggests that there would also be an optimum pressure at which to conduct flood experiments. This, in turn, indicates an optimum rate and pressure for a field project.

MODEL WATER-FLOOD STUDIES

Other than the general shape of the curves, little comparison is apparent from the several sets of data processed for the pattern floods. However, a few general observations can be made.

1. Area much in excess of the unit pattern is swept when the flood is continued to high water-oil ratios. (The water-oil ratiocut off used was 20:1 in all cases).

2. At these high water-oil ratios, sufficient reservoir has been swept so that the isolated pattern no longer acts as if it were an infinite reservoir, and boundary effects influence the performance.

3. There is a maximum total sweep efficiency, areal sweep efficiency, and displacement efficiency for this type of system.

4. Breakthrough recoveries vary with the mobility ratio; and low breakthrough recoveries are followed by a much greater subordinate production.

5. Because the two floods run on the same sand-fluid system (but different models) did not compare, it appears that boundary effect was more pronounced and was felt earlier in the life of the flood for the smaller model.

6. For the three patterns run on the same sand-fluid system, the line drive was the most effective from the standpoints of high recovery to breakthrough, short subordinate production, and high ultimate areal sweep efficiency.

7. The most important factor in scaling an oil field reservoir model is the capillary pressure. Care should be used in choosing injection rates and operating pressures which are of sufficient magnitude to overcome capillary pressure gradients which may exist in the system.

8. High recoveries of oil (up to several times the unit pattern) can be obtained before water breakthrough. This is possibly the result of preferential imbibition allowing injection water to by-pass the producing well bores. Production by this method could possibly be utilized in a field prototype providing the production rates were high enough to result in the economic operation of the project.

9. The close proximity between the modified five-spot data (immiscible

77

flood) and that of Dyes et al (miscible flood) indicates that miscible data may be modified and utilized in the prediction of a water flood project if other data is not available.

      10. The method of re-establishing the initial saturations before each run may have altered the wetting properties of the bed. This in turn could have some influence on the performance of the water-flood tests.

REFERENCES CITED

1. Amyx, J.W., Bass, D.M. Jr., Whiting, R.L., "Petroleum Reservoir Engineering - Physical Properties", McGraw Hill, New York, (1960).

2. Archie, G.E., "Electrical Resistivity Log as an Aid in Determining Some Reservoir Characteristics", A.I.M.E. trans. (1942).

3. Brown, Harry W., "Capillary Pressure Investigations", A.I.M.E. trans. (1949).

4. Bruce, W.A., "Mathematical Aids in Reservoir Engineering", Carter Oil Company (limited publication).

5. Buckley, S.E., Leverett, M.C., "Mechanism of Fluid Displacement in Sands", A.I.M.E. trans. vol. 146, p. 117, (1942).

6. Caudle, B.H., Erickson, R.A., Slobod, R.L., "The Encroachment of Injected Fluids Beyond the Normal Well Pattern", A.I.M.E. trans. vol. 204, p. 79, (1955).

7. Craft, B.C., Hawkins, M.F., "Applied Petroleum Reservoir Engineering", Prentice Hall, Englewood Cliffs, N.J., (1959).

8. Craig, F.F. Jr., Geffen, T.M., Morse, R.A., "Oil Recovery of Pattern Gas or Water Injection Operations from Model Tests", A.I.M.E. trans. vol. 204, p. 7, (1955).

9. Dalton, R.L. Jr., Rapoport, L.A., Carpenter, C.W. Jr., "Laboratory Studies of Pilot Waterfloods", Jour. Pet. Tech., p. 24, Feb. (1960).

10. Dyes, A.B., Caudle, B.H., Erickson, R.A., "Oil Production After Breakthrough as Influenced by Mobility Ratio", A.I.M.E. trans. vol. 201, p. 81, (1954).

11. Elmdahl, B.A., "Core Analysis and Some Reservoir Rock Characteristics", The Mines Magazine, Oct. (1957).

12. Flock, D.L., "Drilling Mud Filtration and Its Effect on the Electrical Resistivity of Porous Rocks", unpublished manuscript, Ph.D. thesis, Agricultural and Mechanical College of Texas, (1956).

13. Jones-Parra, J., Calhoun, John C. Jr., "Computation of a Linear Flood by the Stabilized Zone Method", A.I.M.E. trans. vol. 198, p. 335, (1953).

14. Leverett, M.C., "Flow of Oil Water Mixtures Through Unconsolidated Sands", A.I.M.E. trans. (1938).

15. Leverett, M.C., "Capillary Behavior in Porous Solids", A.I.M.E. trans. (1941).

16. Mattax, C.C., Kyte, J.R., "Imbibition Oil Recovery from Fractured Water-Drive Reservoirs", A.I.M.E. tech. paper No. SPE-187, Presented at Dallas meeting, Oct. 8-11, (1961).

17. Muskat, M., "Physical Principals of Oil Production", McGraw-Hill, New York, (1959).

18. Neilson, I.D.R., "The Effect of a Free Gas Saturation on the Sweep Efficiency of an Isolated Inverted Five-Spot", unpublished manuscript, M.Sc. thesis, University of Alberta, (1960).

19. Pirson, S.J., "Oil Reservoir Engineering", 2nd edition, McGraw-Hill, New York, (1958).

20. Purcell, W.R., "Capillary Pressures - Their Measurement Using Mercury and Calculation of Permeability Therefrom", A.I.M.E. trans., (1949).

21. Rapoport, L.A., Leas, W.J., "Properties of Linear Waterfloods", A.I.M.E. trans. vol. 109, p. 139, (1953).

22. Rose, Walter, Bruce, W.A., "Evaluation of Capillary Characteristics in Reservoir Rocks", A.I.M.E. trans. (1949).

23. Scheidegger, A.E., "General Spectral Theory for the Onset of Instabilities in Displacement Processes in Porous Media", A.I.M.E. tech. paper No. 1551-G, presented at Denver meeting, Oct. 2-5, (1960).

24. Slobod, R.L., and Caudle, B.H., "X-ray Shadowgraph Studies of Areal Sweepout Efficiencies", A.I.M.E. trans., vol. 195, p. 265, (1952).

25. Stiles, W.E., "Use of Permeability Distribution in Waterflood Calculations", A.I.M.E. trans. vol. 186, p. 9 (1949).

26. Welge, H.J., "A Simplified Method of Computing Oil Recovery by Gas or Water Drive", A.I.M.E. trans. vol. 195, (1952).

27. Wykoff, R.D., Botset, H.G., Muskat, M., "The Mechanics of Porous Flow Applied to Water-Flooding Problems", vol. 103, p. 219, A.I.M.E. trans., (1933).

APPENDIX

TABLE 1

CAPILLARY PRESSURE CORE: CALIBRATION DATA

Saturation	Segment 1-2		Segment 11-12		Segments 2-11	
	R	Ro/R	R	Ro/R	R	Ro/R
100.0	194	1.0000	181	1.0000	1,494	1.0000
98.5	317	0.6120	190	0.9526	1,588	0.9408
95.3	331	0.5861	200	0.9050	1,646	0.9077
88.4	376	0.5160	300	0.6033	1,708	0.8747
83.7	380	0.5105	620	0.2919	1,748	0.8547
77.1	369	0.5257	1,650	0.1097	2,123	0.7037
69.5	600	0.3233	2,900	0.0624	2,705	0.5523
50.5	1,550	0.1252	7,900	0.0229	6,540	0.2284
58.0	770	0.2519	3,490	0.0519	4,620	0.3234
40.2	1,630	0.1190	7,190	0.0252	13,480	0.1108
32.6	1,400	0.1386	9,400	0.0193	22,240	0.0672
26.4	2,350	0.0826	29,000	0.0062	30,550	0.0489
25.6	3,600	0.0539	138,000	0.0013	29,920	0.0499

TABLE 2

RESISTIVITY READINGS AFTER DRAINAGE AND CONVERSION

TO WATER SATURATIONS

Segment	Resistivity R, ohms	Ro/R	Saturation (From Fig. 5)
11-12	5,250,000	0.0000	0.0
10-11	15,323	0.0106	6.1
9-10	9,100	0.0176	11.0
8-9	3,650	0.0430	23.8
7-8	1,870	0.0893	35.8
6-7	800	0.2100	50.0
5-6	355	0.4366	64.1
4-5	395	0.4304	63.9
3-4	300	0.5800	71.0
2-3	235	0.7702	79.8
1-2	285	0.6807	99.4

TABLE 3

LEVERETT'S J-FUNCTION: CALCULATION OF THE CONSTANT

FOR THE UNCONSOLIDATED SANDSTONE

$$J = \frac{\Delta\rho \; g \; h}{\gamma \cos \theta} \sqrt{\frac{k}{\phi}} \; ; \; \text{all terms are constant except h}$$

$$\text{constant} = \frac{\Delta\rho \; g}{\gamma \cos \theta} \sqrt{\frac{k}{\phi}}$$

$\rho w = 0.998$ gm/cm^2 (hydrometer reading)

$$= \frac{0.997 \times 980}{73.0} \left[\frac{40.7}{1.013 \times 10^8 \times 0.318} \right]^{1/2}$$

$\rho a = 0.001$ gm/cm^2 (p. N.G.S.M.A. converted to C.G.S. units).

$$= 150.444834 \times 10^{-4}$$

$\therefore \; \Delta\rho = 0.997$ gm/cm^2

$g = 980$ cm/sec^2

$K = 40.7$ Darcies (table 5)

$$= \frac{40.7}{1.013 \times 10^8} \; \text{cm}^2$$

$\gamma = 73.0$ dynes/cm (Fig. 40)

$\cos \theta = 1.0$ (sand is water wet)

$\phi = 0.318$

TABLE 4

CONVERTING CAPILLARY PRESSURE INTO

THE J-FUNCTION

Segment (1)	Saturation (2)	Capillary Pressure		J-Function (4) x 150.44 x 10^{-4} (5)
		Inches H_2O (3)	CM H_2O (4)	
11-12	0.0	13.688	34.76752	0.52306
10-11	6.1	12.375	31.43250	0.47289
9-10	11.0	11.125	28.25750	0.42512
8-9	23.8	9.875	25.0825	0.37735
7-8	35.8	8.625	21.9075	0.32959
6-7	50.0	7.375	18.7325	0.28182
5-6	64.1	6.125	15.5575	0.23405
4-5	63.9	4.875	12.3825	0.18629
3-4	71.0	3.625	9.2075	0.13852
2-3	79.8	2.375	6.0325	0.09076
1-2	99.4	0.875	2.225	0.03347

TABLE 5

CALCULATION OF ABSOLUTE AND

EFFECTIVE PERMEABILITIES

Darcies Law: $\quad K = \dfrac{Q\mu L}{A\Delta P}$;   where   Q is in cc/sec.
  μ is in cp
  L is in cm.
  A is in sq. cm.
  ΔP is in atmos.
  K is in Darcies

Core and Fluid Characteristics

μ_a = 1.00 cp
μ_o = 1.49 cp
 L = 29.5 in.
 d = 1.5 in.

$\text{psi} = \dfrac{\text{"Hg}}{2.036}$

$\text{atmos} = \dfrac{\text{psi}}{14.65}$

$\text{cc/sec} = \dfrac{\text{cc/hr}}{3600}$

$\therefore \quad K = \dfrac{Q(\text{cc/hr})}{\Delta P(\text{"Hg})} \ \times \ \text{constant}$

For water, constant

$= \dfrac{1.00 \times 29.5 \times 2.54 \times 14.65 \times 2.036}{/4 \times (1.5)^2 \ \times \ (2.54)^2 \times 3600}$

$= 0.0545$

For oil, constant

$= \dfrac{1.49 \times 29.5 \times 2.54 \times 14.65 \times 2.036}{/4 \ \times \ (1.5)^2 \times (2.54)^2 \times 3600}$

$= 0.0812$

Absolute Permeability

(1)	(2)	$(3) K = \dfrac{(1)}{(2)} \times 0.0545$
Q	ΔP	
cc/hr	"Hg	Darcies
560	0.71	43.0
400	0.58	37.6
2285	2.91	41.6
	Mean	40.7 Darcies

TABLE 5 (con't)

EFFECTIVE PERMEABILITY

(Run	(1) Water Rate cc/hr	(2) Oil Rate cc/hr	(3) ΔP "Hg	(4) $K_w = \frac{(1)}{(3)} \times .0545$ Darcies	(5) $K_o = \frac{(2)}{(3)} \times .0812$ Darcies
0	840	0	2.52	18.18	0.000
1	560	112	3.36	9.07	2.71
2	560	140	4.27	7.13	2.66
3	560	187	5.53	5.51	2.75
4	560	280	6.02	5.06	3.78
5	560	373	6.10	5.00	4.96
6	560	560	7.28	4.19	6.25
7	373	560	6.35	3.20	7.17
8	280	560	5.76	2.65	7.92
9	187	560	4.56	2.23	9.98
10	140	560	4.20	1.81	10.82
11	112	560	3.82	1.60	11.91
12	0	560	2.36	0.00	19.28

TABLE 6

EFFECTIVE PERMEABILITY TESTS: CALCULATION OF

FLUID SATURATIONS

Run No.	(1) Oil Injected To Core cc	(2) Oil in Core cc	(3) Oil in Core as Fraction of Total Pore Space (2)/29.010
0	0.0	41.0	0.141
1	53.6	94.6	0.326
2	14.5	109.1	0.376
3	7.0	116.1	0.400
4	18.1	134.2	0.462
5	1.2	135.4	0.466
6	14.3	149.7	0.515
7	15.3	165.0	0.568
8	11.8	176.8	0.609
9	- 1.4	175.4	0.605
10	11.1	186.5	0.644
11	10.5	197.0	0.679
12	48.5	245.5	0.845

connate water = 44.6 cc.

TABLE 7

CALCULATION OF RELATIVE PERMEABILITIES

Absolute permeability equals 40.7 Darcies; effective permeability to water at the residual oil saturation = 18.2 Darcies; effective permeability to oil at the connate water saturation = 19.3 Darcies.

(1) Run No.	(2) Effective Water Perm. to Darcies	(3) Effective Permeability to Oil Darcies	(4) Relative Perm. to Water	(5) Relative Perm. to Oil	(6) Relative Perm. to Water	(7) Relative Perm. to Oil
1	9.07	2.71	0.223	0.067	0.498	0.141
2	7.13	2.66	0.175	0.065	0.392	0.138
3	5.51	2.75	0.135	0.067	0.303	0.143
4	5.06	3.78	0.124	0.093	0.278	0.196
5	5.00	4.96	0.123	0.122	0.275	0.255
6	4.19	6.25	0.103	0.153	0.230	0.324
7	3.20	7.17	0.079	0.176	0.176	0.372
8	2.65	7.92	0.065	0.195	0.146	0.411
9	2.23	9.98	0.055	0.245	0.123	0.517
10	1.81	10.82	0.044	0.266	0.100	0.562
11	1.60	11.91	0.039	0.293	0.088	0.618
12	0.00	19.28	0.000	0.473	0.000	1.000
13	18.18	0.00	0.446	0.000	1.000	0.000

(4) K absolute = 40.7
i.e. (5)/40.7

(5) K absolute = 40.7
i.e. (6)/40.7

(6) K effective = 18.2
i.e. (5)/18.2

(7) K effective = 19.3
i.e. (6)/19.3

88

TABLE 8

EXPERIMENTAL FRACTIONAL-FLOW DATA

(1) Run No.	(2) Water Rate cc/hr	(3) Oil Rate cc/hr	(4) Total cc/hr	(5) Fraction of Water Flowing	(6) Oil in Core Fraction of Total Pore Space	(7) Water Sat'n 1.0 - (6)
1	560	112	672	.834	.326	.674
2	560	140	700	.800	.376	.624
3	560	187	747	.750	.400	.600
4	560	280	840	.667	.462	.538
5	560	373	933	.600	.466	.534
6	560	560	1120	.500	.515	.485
7	373	560	933	.400	.568	.432
8	280	560	840	.333	.609	.391
9	187	560	747	.250	.605	.395
10	140	560	700	.200	.644	.356
11	112	560	672	.167	.679	.321
12	0	560	560	.000	.845	.155
13	840	0	840	1.000	.154	.846

TABLE 9

FRACTIONAL-FLOW CALCULATIONS FOR

THREE OIL VISCOSITIES

$$f_W = \frac{1}{1 + \frac{k_O}{k_W} \frac{\mu_W}{\mu_O}}$$

(1)
$$\frac{\mu_W}{\mu_O} = \frac{1.000}{1.49} = 0.67114$$

(2)
$$\frac{\mu_W}{\mu_O} = \frac{0.860}{0.9064} = 0.94881$$

(3)
$$\frac{\mu_W}{\mu_O} = \frac{0.860}{5.107} = 0.16840$$

(1) S_W	(2) K_W from Fig. 8	(3) K_O from Fig. 8	(4) K_O/K_W	(5) (4) x $\frac{\mu_W}{\mu_O}$(1)	(6) (4) x $\frac{\mu_W}{\mu_O}$(2)
0.20	0.25	16.75	67.00000	44.96638	63.57027
0.30	1.35	12.30	9.11111	6.11483	8.64471
0.40	2.75	8.50	3.09091	2.07443	2.93269
0.50	4.40	5.50	1.25000	0.83893	1.18601
0.60	6.50	3.35	0.51538	0.34589	0.48900
0.70	9.45	1.76	0.18624	0.12499	0.17671
0.72	10.15	1.55	0.15271	0.10249	0.14489
0.74	10.90	1.25	0.11468	0.07697	0.10881
0.76	11.85	1.00	0.08439	0.05664	0.08007
0.78	12.85	0.75	0.05837	0.03917	0.05538
0.80	14.20	0.50	0.03521	0.02363	0.03341
0.82	15.60	0.30	0.01923	0.01291	0.01825
0.84	17.20	0.10	0.00581	0.00390	0.00551

(7) (4) x $\frac{\mu_W}{\mu_O}$(3)	(8) $f_W = \frac{1}{1 + (5)}$	(9) $f_W = \frac{1}{1 + (6)}$	(10) $f_W = \frac{1}{1 + (7)}$
11.28280	0.02176	0.01549	0.08141
1.53431	0.14055	0.10368	0.39458
0.39804	0.32526	0.25428	0.65767
0.21050	0.54379	0.45745	0.82610
0.08679	0.74300	0.67159	0.92014
0.03136	0.88890	0.84983	0.96959
0.02572	0.90704	0.87345	0.97492
0.01931	0.92853	0.90187	0.98106
0.01421	0.94640	0.92587	0.98599
0.00983	0.96231	0.94753	0.99027
0.00593	0.97692	0.96767	0.99410
0.00324	0.98724	0.982077	0.99677
0.00098	0.99612	0.99452	0.99902

TABLE 10

PRODUCTION HISTORY OF THE SEVERAL

CRITICAL RATE TESTS

Oil Production Instantaneous c.c.	Cumulative cc.	Cumulative Fraction of Pore Space	Producing Water-Oil Ratio	Mid-Point Frac. of Pore Space (i.e. points Plotted on Fig. 11)
RUN NO. 1	Rate = 10 cc/hr			
60.0	60.0	0.207	0.0	0.207
82.5	142.5	0.491	0.212	0.491
8.9	151.4	0.522	3.49	0.507
5.6	157.0	0.541	9.00	0.532
2.0	159.0	0.548	10.4	0.544
2.5	161.5	0.556	12.8	0.552
2.2	163.7	0.564	40.4	0.560
RUN NO. 2	Rate = 40 cc/hr			
104.3	104.3	0.360	0.0	0.360
30.0	134.3	0.463	0.033	0.463
9.1	143.4	0.495	1.09	0.479
12.8	156.2	0.538	3.27	0.517
6.4	162.6	0.560	6.93	0.549
4.8	167.4	0.576	11.52	0.568
2.6	170.0	0.586	23.2	0.581
RUN NO. 3	Rate = 100 cc/hr			
98.8	98.8	0.341	0.0	0.341
42.5	141.3	0.487	0.0	0.487
17.5	158.8	0.546	2.14	0.517
7.0	165.8	0.572	9.43	0.559
2.9	168.7	0.581	25.7	0.577
1.0	169.7	0.585	30.8	0.583
RUN NO. 4	Rate = 200 cc/hr			
100.0	100.0	0.345	0.0	0.345
48.4	148.4	0.511	0.0	0.511
10.5	158.9	0.547	1.81	0.529
3.6	162.5	0.560	7.34	0.554
2.6	165.1	0.569	14.38	0.564
1.8	166.9	0.575	21.2	0.572

TABLE 10 (cont'd.)

Oil Production Instantaneous	Cumulative		Producing Water-Oil Ratio	Mid-Point Frac. of Pore Space (i.e. points Plotted on Fig. 11)
	cc.	Fraction of Pore Space		
RUN NO. 5	Rate = 320 cc/hr			
100.0	100.0	0.345	0.0	0.345
49.5	149.5	0.525	0.0	0.525
6.8	156.3	0.539	0.442	0.532
3.4	159.7	0.550	1.94	0.545
2.3	162.0	0.558	3.34	0.554
1.8	163.8	0.564	10.10	0.561
3.2	167.0	0.576	11.3	0.570
0.8	167.8	0.578	24.0	0.577
0.0	167.8	0.578		0.577
RUN NO. 6	Rate = 560 cc/hr			
100.0	100.0	0.345	0.0	0.345
42.0	142.0	0.489	0.0	0.489
7.8	149.8	0.576	0.334	0.503
4.6	154.4	0.532	1.17	0.524
2.2	156.6	0.539	3.54	0.535
1.7	158.3	0.546	4.94	0.542
1.3	159.6	0.550	6.76	0.548
1.1	160.7	0.553	8.18	0.551
1.0	161.7	0.557	19.0	0.555
1.4	163.1	0.562	20.4	0.559
0.8	163.9	0.564	24.3	0.563
0.6	164.5	0.567	49.0	0.566
0.6	165.1	0.569	66.0	0.568
RUN NO. 7	Rate = 840 cc/hr			
76.6	76.6	0.2645	0.0	0.264
48.5	125.1	0.431	0.309	0.348
35.1	160.2	0.553	0.413	0.492
1.6	161.8	0.558	30.1	0.555
2.5	164.3	0.566	39.0	0.562
2.4	166.7	0.575	40.9	0.570
0.8	167.5	0.578	62.5	0.576
0.7	168.2	0.580	70.8	0.579
0.2	168.4	0.581	234.0	0.580

TABLE   10 (cont'd.)

Oil Production Instantaneous	Cumulative		Producing Water-Oil Ratio	Mid-Point Frac. of Pore Space (i.e. points Plotted on Fig. 11)
	cc.	Fraction of Pore Space		
RUN NO. 8	Rate = 40 cc/hr			
100.0	100.0	0.345	0.0	0.345
41.2	141.2	0.487	0.0	0.487
12.3	153.5	0.532	1.71	0.509
7.3	160.8	0.554	5.82	0.543
2.7	163.5	0.564	9.55	0.559
1.7	165.2	0.570	11.78	0.567
1.8	167.0	0.576	19.22	0.573
1.8	168.8	0.582	99.5	0.579
0.8	169.6	0.585	259.	0.583

TABLE 11

GEOMETRIC AND RESERVOIR PROPERTIES OF

THE TWO MODELS

Large Model	Small Model	
60 inches	32 inches	Length
1/2 inch	1/4 inch	Thickness
24 inches	8 inches	Length (unit area)
22.4%	22.4% (low visc. oil 17.6% high visc. oil	Connate water Saturation
34.8%	34.8	Porosity
1273 cc.	70.8 cc. low visc. oil 82.4 high visc. oil	Oil in place of unit area

TABLE 12

CALCULATION OF DISPLACEMENT EFFICIENCY

FROM FRACTIONAL-FLOW CURVES

LOW VISCOSITY OIL

(1) W.O.R.	(2) $f_W = \dfrac{\text{W.O.R.}}{1 + \text{W.O.R.}}$	(3) S_W (From Fig. 23)	(4) $S_W - 0.156$
0.0	0.0	0.796	0.640
0.2	0.1668	0.817	0.661
0.4	0.286	0.830	0.674
0.8	0.445	0.841	0.685
1.2	0.545	0.843	0.687
1.8	0.643	0.845	0.689
2.4	0.706	0.846	0.690
3.0	0.750	0.846	0.690
4.0	0.800	0.846	0.690

(5) Displacement Efficiency $\dfrac{(4)}{1 - 0.156}$
0.759
0.785
0.799
0.812
0.815
0.816
0.818
0.818
0.818

95

TABLE 12 (cont'd.)

HIGH VISCOSITY OIL

(1) W.O.R.	(2) $f_w = \dfrac{W.O.R.}{1 + W.O.R.}$	(3) S_w (From Fig. 23)	(4) $S_w - 0.156$	(5) $\dfrac{(4)}{1 - 0.156}$
0.0	0.0	0.514	0.358	0.424
0.2	0.1668	0.564	0.408	0.484
0.4	0.286	0.602	0.446	0.529
0.8	0.445	0.660	0.504	0.596
1.2	0.545	0.698	0.542	0.642
1.8	0.643	0.742	0.586	0.694
2.4	0.706	0.761	0.605	0.717
3.0	0.750	0.780	0.624	0.730
4.0	0.800	0.803	0.647	0.766
6.0	0.858	0.826	0.670	0.794
8.0	0.889	0.840	0.684	0.810
10.0	0.908	0.846	0.690	0.818
18.0	0.947	0.846	0.690	0.818

TABLE 13

CALCULATION OF BREAKTHROUGH MOBILITY RATIOS

$$M = \frac{K_O}{K_W} \frac{\mu_W}{\mu_O}$$

LOW VISCOSITY OIL

$\dfrac{\mu_W}{\mu_O}$ = 0.94881

at B.T., S_W = 0.796
K_W = 14.80

K_O = 19.28

$$M = \frac{19.28}{14.80} \times 0.94881$$

$$= 1.235$$

HIGH VISCOSITY OIL

$\dfrac{\mu_W}{\mu_O}$ = 0.16840

at B.T., S_W = 0.514
K_W = 4.65

K_O = 19.28

$$M = \frac{19.28}{4.65} \times 0.16840$$

$$= 0.697$$

TABLE 14

CONFINED FIVE-SPOT FLOOD: PRODUCTION HISTORY

(1) Cumulative Oil Prod'n.	(2) Cumulative Water Prod'n.	(3) Total Cum. Prod'n.	(4) Instantaneous Oil Production	(5) Instantaneous Water Prod'n.	(6) Instantaneous Water-Oil Ratio
200.5	0.0	200.5	200.5	0.0	0.000
400.5	0.0	400.5	200.0	0.0	0.000
601.5	0.5	602.0	201.0	0.5	0.002
636.0	6.0	642.0	34.5	5.5	0.159
667.0	15.0	682.0	31.0	9.0	0.281
699.0	23.0	722.0	32.0	8.0	0.250
733.0	29.0	762.0	34.0	6.0	0.176
763.0	39.0	802.0	30.0	10.0	0.333
790.5	51.5	842.0	27.5	12.5	0.463
817.5	64.5	882.0	27.0	13.0	0.473
841.5	80.5	922.0	24.0	16.0	0.667
862.5	99.5	962.0	21.0	19.0	0.905
880.5	121.5	1002.0	18.0	22.0	1.222
896.0	146.0	1042.0	15.5	24.5	1.581
905.5	176.5	1082.0	9.5	30.5	3.211
916.0	206.0	1122.0	10.5	29.5	2.810
922.5	239.5	1162.0	6.5	33.5	5.154
925.5	276.5	1202.0	3.0	37.0	12.333
929.0	313.0	1242.0	3.5	36.5	10.429
931.0	351.0	1282.0	2.0	38.0	19.000
934.5	387.5	1322.0	3.5	36.5	10.429
935.0	427.0	1362.0	0.5	39.5	79.000
936.5	465.5	1402.0	1.5	38.5	25.667

TABLE 15

CONFINED FIVE-SPOT FLOOD: CALCULATION OF TOTAL SWEEP

EFFICIENCY (E_s), AREAL SWEEP EFFICIENCY (E_{as}), AND

THE RATIO OF WATER INJECTED TO WATER

INJECTED TO BREAKTHROUGH (Q/Q_{bt})

(1) Water-Oil Ratio	(2) Cum. Oil Production (From Fig. 21) cc	(3) Cum. Water Injected (From Fig. 21) cc	(4) E_s = Oil Rec./ Oil in Place = (2)/1162	(5) Q/Q_{bt} = (3)/600	(6) Displacement Efficiency, E_d (From Fig. 19)	(7) Areal Sweep Efficiency, E_{as} (4)/(6)
0.0	600	600	0.516	1.000	0.759	0.680
0.2	725	730	0.624	1.218	0.785	0.795
0.4	788	821	0.678	1.370	0.799	0.849
0.8	848	917	0.728	1.530	0.812	0.897
1.2	869	975	0.748	1.625	0.815	0.917
1.8	888	1015	0.765	1.690	0.816	0.937
2.4	900	1062	0.774	1.770	0.818	0.946
3.0	908	1090	0.781	1.818	0.818	0.955
4.0	917	1121	0.789	1.870	0.818	0.964
6.0	923	1154	0.794	1.925	0.818	0.970
8.0	926	1180	0.796	1.968	0.818	0.973
10.0	928	1207	0.799	2.01	0.818	0.976
18.0	936	1317	0.805	2.19	0.818	0.984

TABLE 15 (cont'd.)

CORRECTING EFFICIENCIES TO A COMMON DATUM

(8) E_s Transposed	(9) Pseudo E_{as} (8)/(6)	(10) E_{as} Transposed (9) x $\frac{71.5}{0.943}$
0.715	0.943	0.715
0.823	1.048	0.795
0.877	1.098	0.832
0.927	0.142	0.866
0.947	1.162	0.881
0.964	1.180	0.895
0.973	1.189	0.900
0.980	1.198	0.908
0.988	1.208	0.915
0.993	1.213	0.920
0.995	1.215	0.921
0.998	1.220	0.926
1.004	1.227	0.929

TABLE 16

ISOLATED FIVE-SPOT FLOOD: PRODUCTION HISTORY

(1) Cum. Oil Prod'n.	(2) Cum. Water Production	(3) Total Cum. Production	(4) Instantaneous Oil Prod'n.	(5) Instantaneous Water Prod'n.	(6) Instantaneous Water-Oil Ratio
200.0	0.0	200.0	200.0	0.0	0.000
400.0	0.0	400.0	200.0	0.0	0.000
498.0	2.0	500.0	98.0	2.0	0.020
518.0	2.0	520.0	20.0	0.0	0.000
536.0	4.0	540.0	18.0	2.0	0.111
555.5	4.5	560.0	19.5	0.5	0.026
574.0	6.0	580.0	18.5	1.5	0.081
590.0	10.0	600.0	16.0	4.0	0.250
627.5	32.5	660.0	37.5	22.5	0.600
648.0	52.0	700.0	20.5	19.5	0.951
707.0	153.0	860.0	59.0	101.0	1.712
719.0	241.0	960.0	12.0	88.0	7.333
723.5	336.5	1060.0	4.5	95.5	21.222
730.5	469.5	1200.0	6.0	133.0	22.167

TABLE 17

ISOLATED FIVE-SPOT FLOOD: CALCULATION OF TOTAL

SWEEP EFFICIENCY (E_s), AREAL SWEEP EFFICIENCY (E_{as}), AND THE RATIO OF

WATER INJECTED TO WATER INJECTED TO BREAKTHROUGH (Q/Q_{bt})

(1) Water-Oil Ratio	(2) Cum. Oil Production (Fig. 24)	(3) Cum. Water Injected Fig. 24)	(4) E_s = Oil Rec./ Oil in Place = (2)/70.8	(5) Q/Q_{bt} = (4)/520
0.0	520	520	7.35	1.000
0.2	578	580	8.16	1.117
0.4	602	620	8.50	1.192
0.8	628	682	8.86	1.312
1.2	644	728	9.10	1.402
1.8	661	771	9.34	1.482
2.4	672	802	9.49	1.542
3.0	681	826	9.62	1.590
4.0	692	860	9.78	1.655
6.0	706	908	9.96	1.748
8.0	715	941	10.10	1.810
10.0	720	973	10.18	1.872
18.0	721	1082	10.20	2.080

(6) Displacement Efficiency, E_d (Fig. 19)	(7) Actual E_{as} Areal Sweep Efficiency	(8) E_s by assuming E_s (h) (4) x $\frac{71.5}{735}$	(9) E_{as} x $\frac{71.5}{968}$
0.759	9.68	.715	.715
0.785	10.39	.794	.766
0.799	10.64	.828	.786
0.812	10.90	.862	.805
0.815	11.16	.885	.824
0.816	11.45	.908	.846
0.818	11.59	.923	.855
0.818	11.75	.935	.868
0.818	11.95	.951	.883
0.818	12.18	.969	.900
0.818	12.33	.982	.911
0.818	12.43	.990	.918
0.818	12.46	.992	.920

TABLE 18

LINE DRIVE FLOOD: PRODUCTION HISTORY

(1) Cum. Oil	(2) Cum. Water	(3) Total Cum. Prod'n.	(4) Inst. Oil	(5) Inst. Water	(6) Inst. W.O.R.
ALL WELLS					
300.0	0.0	300.0	300.0	0.0	0.000
600.0	0.0	600.0	300.0	0.0	0.000
686.0	4.0	690.0	86.0	4.0	0.046
711.5	8.5	720.0	25.5	4.5	0.176
756.5	23.5	780.0	45.0	15.0	0.333
781.5	58.5	840.0	25.0	35.0	1.400
797.0	103.0	900.0	15.5	44.5	2.871
807.5	152.5	960.0	10.5	49.5	4.714
815.0	205.0	1020.0	7.5	52.5	7.000
820.0	260.0	1080.0	5.0	55.0	11.000
823.5	316.5	1140.0	3.5	56.5	16.143
825.5	374.5	1200.0	2.0	58.0	29.000
FIRST LINE OF WELLS:					
150.0	0.0	150.0	150.0	0.0	0.000
300.0	0.0	300.0	300.0	0.0	0.000
341.0	4.0	345.0	41.0	4.0	0.098
354.0	6.0	360.0	13.0	2.0	0.154
375.0	15.0	390.0	21.0	9.0	0.429
385.0	35.0	420.0	10.0	20.0	2.000
393.0	57.0	450.0	8.0	22.0	2.750
396.5	83.5	480.0	3.5	26.5	7.571
400.5	109.5	510.0	4.0	26.0	6.500
402.5	137.5	540.0	2.0	27.5	13.750
403.5	166.5	570.0	1.0	29.5	29.500
404.5	195.5	600.0	1.0	29.0	29.000
SECOND LINE OF WELLS:					
150.0	0.0	150.0	150.0	0.0	0.000
300.0	0.0	300.0	150.0	0.0	0.000
345.0	0.0	345.0	45.0	0.0	0.000
357.5	2.5	360.0	12.5	2.5	0.200
382.5	8.5	390.0	25.0	6.0	0.240
396.5	23.5	420.0	14.0	15.0	1.071
404.0	46.0	450.0	7.5	22.5	3.000
411.0	69.0	480.0	7.0	23.0	3.286
414.5	95.5	510.0	3.5	26.5	7.571
417.0	123.0	540.0	2.5	27.5	11.000
420.0	150.0	570.0	3.0	27.0	9.000
421.0	179.0	600.0	1.0	29.0	29.000

TABLE 19

LINE DRIVE FLOOD: CALCULATION OF TOTAL SWEEP

EFFICIENCY (E_s), AREAL SWEEP EFFICIENCY (E_{as}) AND

THE RATIO OF WATER INJECTED TO WATER

INJECTED TO BREAKTHROUGH (Q/Q_{bt})

(1) Water -Oil Ratio	(2) Cumulative Oil Production (Fig. 27)	(3) Cumulative Water Injected (Fig. 27)	(4) E_s = Oil Recovery/ Oil in Place (2)/70.8
0.0	695	695	9.82
0.2	720	723	10.18
0.4	735	746	10.39
0.8	756	781	10.69
1.2	767	807	10.85
1.8	777	837	10.98
2.4	785	862	11.09
3.0	792	885	11.18
4.0	799	9.8	11.29
6.0	810	965	11.44
8.0	815	1007	11.50
10.0	818	1039	11.55
18.0	823	1148	11.63

(5) Q/Q_{bt} = (3)/695	(6) Displacement Efficiency Ed, (Fig. 19)	(7) E_{as} Areal Sweep Eff. (4)/(6)
1.000	0.759	12.94
1.040	0.785	12.98
1.074	0.799	13.00
1.124	0.812	13.17
1.162	0.815	13.22
1.204	0.816	13.45
1.240	0.818	13.55
1.273	0.818	13.66
1.322	0.818	13.80
1.388	0.818	14.00
1.448	0.818	14.06
1.495	0.818	14.12
1.651	0.818	14.22

104

TABLE 20

NINE-SPOT FLOOD NO. 2-1: TOTAL PRODUCTION HISTORY

(1) Cumulative Oil Prod'n.	(2) Cumulative Water Prod'n.	(3) Total Cum. Production	(4) Instantaneous Oil Prod'n.	(5) Instantaneous Water Prod'n.	(6) Instantaneous Water-oil Ratio
201.1 cc	9.0 cc	210.1 cc	201.0 cc	9.0 cc	0.045
323.4	9.0	332.4	122.3	0.0	0.000
415.3	9.0	424.3	91.9	0.0	0.000
615.7	12.0	627.7	200.4	3.0	0.015
819.1	16.0	835.1	203.4	4.0	0.020
1033.1	23.0	1056.1	214.0	7.0	0.033
1250.7	29.0	1279.7	217.6	6.0	0.028
1432.2	39.5	1471.7	181.5	10.5	0.058
1595.4	51.9	1647.3	163.2	12.4	0.076
1784.7	101.7	1886.4	189.3	49.8	0.263
2046.4	192.6	2238.6	261.7	90.9	0.347
2221.2	265.4	2486.6	174.8	72.8	0.416
2420.3	422.3	2842.6	199.1	156.9	0.788
2571.4	555.6	3127.0	151.1	133.3	0.882
2827.3	747.7	3575.0	255.9	192.1	0.751
3009.9	946.2	3956.1	182.6	198.5	1.087
3135.8	1196.5	4332.3	125.9	250.3	1.988
3191.0	1522.6	4713.6	55.2	326.1	5.908
3235.7	1883.1	5118.8	44.7	360.5	8.065
3273.2	2266.5	5539.7	37.5	383.4	10.224
3299.0	2631.3	5930.3	25.8	364.8	14.140

TABLE 21

NINE-SPOT FLOOD NO. 2-1: PRODUCTION HISTORY, DIRECT OFFSET WELLS

(1) Cumulative Oil Prod'n.	(2) Cumulative Water Prod'n.	(3) Total Cum. Prod'n.	(4) Instantaneous Oil Prod'n.	(5) Instantaneous Water Prod'n.	(6) Instantaneous Water-oil Ratio
90.3	0.0	90.3	90.3	0.0	0.000
141.9	0.0	141.9	51.6	0.0	0.000
182.2	0.0	182.2	40.3	0.0	0.000
265.5	0.0	265.5	83.3	0.0	0.000
350.1	0.0	350.1	84.6	0.0	0.000
442.5	2.0	444.5	92.4	2.0	0.022
518.6	4.0	522.6	76.1	2.0	0.026
601.2	7.0	608.2	82.6	3.0	0.036
675.3	10.0	685.3	74.1	3.0	0.040
774.1	16.8	790.9	98.8	6.8	0.069
905.8	30.0	935.8	131.7	13.2	0.100
986.0	46.1	1032.1	80.2	16.1	0.201
1091.4	66.8	1158.2	105.4	20.7	0.196
1170.0	91.2	1261.2	78.6	24.4	0.310
1286.7	137.8	1424.5	116.7	46.6	0.399
1351.9	209.5	1561.4	65.2	71.7	1.100
1390.9	323.3	1714.2	39.0	113.8	2.918
1409.3	460.1	1869.4	18.4	136.8	7.435
1425.4	624.4	2049.8	16.1	164.3	10.205
1438.4	790.3	2228.7	13.0	165.9	12.762
1447.7	942.9	2390.6	9.3	152.6	16.409

TABLE 22

NINE-SPOT FLOOD NO. 2-1: PRODUCTION HISTORY, DIAGONAL OFFSET WELLS

(1) Cumulative Oil Production	(2) Cumulative Water Prod'n.	(3) Total Cum. Prod'n.	(4) Instantaneous Oil Prod'n.	(5) Instantaneous Water Prod'n.	(6) Instantaneous Water-oil Ratio
110.8	9.0	119.8	110.8	9.0	0.081
181.5	9.0	190.5	70.7	0.0	0.000
233.1	9.0	242.1	51.6	0.0	0.000
350.2	12.0	362.2	117.1	3.0	0.026
469.0	16.0	485.0	118.8	4.0	0.034
590.6	21.0	611.6	121.6	5.0	0.041
732.1	25.0	757.1	141.5	4.0	0.028
831.0	32.5	863.5	98.9	7.5	0.076
920.1	41.9	962.0	89.1	9.4	0.105
1010.6	84.9	1095.0	90.5	43.0	0.475
1140.6	162.6	1303.2	130.0	77.7	0.598
1235.2	219.3	1454.5	94.6	56.7	0.599
1328.9	355.5	1684.4	93.7	136.2	1.454
1401.4	464.4	1865.8	72.5	108.9	1.502
1540.6	609.9	2150.5	139.2	145.5	1.045
1658.0	736.7	2394.7	117.4	126.8	1.080
1744.9	873.2	2618.1	86.9	136.5	1.571
1781.7	1062.5	2844.2	36.8	189.3	5.144
1810.3	1258.7	3069.0	28.6	196.2	6.860
1834.8	1476.2	3311.0	24.5	217.5	8.878
1851.3	1688.4	3539.7	16.5	212.2	12.861

TABLE   23

NINE-SPOT FLOOD NO. 2-1:   CALCULATION OF TOTAL SWEEP EFFICIENCY (E_s),

AREAL SWEEP EFFICIENCY (E_{as}), AND THE RATIO OF WATER

INJECTED TO WATER INJECTED TO BREAKTHROUGH (Q/Q_{bt})

(1) Water- Oil Ratio	(2) Cum. Oil Production (Figs. 31 and 32)	(3) Cum. Water Injected (Figs. 31 and 32)	(4) E_s = Oil Rec./ Oil in Place = (2)/1426
0.000	800 cc	800 cc	0.562
0.008	950	1040	0.666
0.016	990	1140	0.695
0.020	1030	1200	0.722
0.032	1140	1290	0.800
0.040	1200	1350	0.842
0.048	1260	1410	0.884
0.060	1330	1500	0.933
0.080	1430	1620	1.003
0.100	1510	1720	1.060
0.14	1610	1890	1.130
0.18	1710	2040	1.200
0.22	1800	2180	1.262
0.24	1830	2240	1.284
0.28	1900	2380	1.332
0.32	1980	2500	1.390
0.35	2020	2590	1.417
0.40	2100	2720	1.473
0.45	2180	2840	1.530
0.50	2250	2950	1.578
0.55	2320	3070	1.628
0.60	2400	3170	1.683
0.65	2470	3270	1.731
7.70	2540	3360	1.780
0.75	2610	3440	1.830
0.80	2670	3520	1.872
0.85	2720	3580	1.907
0.90	2770	3640	1.942
0.95	2840	3680	1.991
1.00	2850	3720	2.000

108

TABLE 23 (Cont'd.)

(1) Water- Oil Ratio	(2) Cum. Oil Production (Figs. 31 and 32)	(3) Cum. Water Injected (Figs. 31 and 32)	(4) E_s = Oil Rec./ Oil in Place = (2)/1426
1.2	2920	3810	2.05
1.8	3015	4030	2.12
2.4	3070	4160	2.15
3.0	3100	4280	2.18
4.0	3120	4430	2.19
6.0	3170	4670	2.22
8.0	3210	4970	2.26
10.0	3240	5280	2.27
18.0	3300	6010	2.32

TABLE 23 (Cont'd.)

(5) Q/Q_{bt} = (3)/800	(6) Displacement Eff., Ed (Fig. 25)	(7) Areal Sweep Efficiency, E_{as} (4)/(6)
1.00	0.759	0.740
1.30	0.7615	0.875
1.426	0.7620	0.913
1.500	0.7625	0.947
1.612	0.7645	1.047
1.688	0.7660	1.100
1.762	0.7675	1.152
1.876	0.769	1.214
2.025	0.774	1.298
2.150	0.775	1.368
2.365	0.779	1.450
2.550	0.784	1.530
2.725	0.787	1.605
2.800	0.789	1.628
2.975	0.792	1.682
3.125	0.795	1.749
3.24	0.797	1.778
3.40	0.7995	1.845
3.55	0.802	1.908
3.69	0.804	1.963
3.84	0.806	2.02
3.96	0.807	2.09
4.08	0.8085	2.14
4.20	0.8095	2.20
4.30	0.8105	2.26
4.40	0.8115	2.31
4.47	0.8120	2.35
4.55	0.8130	2.39
4.60	0.8135	2.45
4.65	0.8140	2.46
4.76	0.815	2.52
5.05	0.817	2.60
5.20	0.818	2.63
5.35	0.818	2.66
5.55	0.818	2.68
5.85	0.818	2.72
6.22	0.818	2.76
6.61	0.818	2.78
7.52	0.818	2.84

TABLE 24

NINE-SPOT FLOOD NO. 2-2: PRODUCTION HISTORY

(1) Cum. Oil Prod'n.	(2) Cum. Water Prod'n.	(3) Total Cum. Production	(4) Instantaneous Oil Prod'n.	(5) Instantaneous Water Prod'n.	(6) Instantaneous Water-oil Ratio
ALL WELLS					
641.2	4.5	645.7	641.2	4.5	0.007
704.2	21.5	725.7	63.0	17.0	0.270
741.2	64.5	805.7	37.0	43.0	1.162
779.2	116.5	895.7	28.0	52.0	1.857
786.2	179.5	965.7	17.0	63.0	3.706
796.2	249.5	1045.7	10.0	70.0	7.000
802.7	325.0	1127.7	6.5	75.5	11.615
811.0	396.7	1207.7	8.3	71.7	8.639
817.7	472.0	1289.7	6.7	75.3	11.239
DIRECT OFFSET WELLS					
316.8	4.0	320.8	316.8	4.0	0.013
343.3	17.5	360.8	26.5	13.5	0.509
353.3	47.5	400.8	10.0	30.0	3.000
360.8	80.8	440.8	7.5	32.5	4.333
363.3	117.5	480.8	2.5	37.5	15.000
365.8	278.0	643.8	2.5	160.5	64.200
DIAGONAL OFFSET WELLS					
324.4	0.5	324.9	324.4	0.5	0.002
360.9	4.0	364.9	36.5	3.5	0.096
387.9	17.0	404.9	27.0	13.0	0.481
408.4	36.5	444.9	20.5	19.5	0.951
422.9	62.0	484.9	14.5	25.5	1.759
432.9	92.0	524.9	10.0	30.0	3.000
439.4	126.5	565.9	6.5	34.5	5.308
446.4	159.5	605.9	7.0	33.0	4.714
451.9	194.0	645.9	5.5	34.5	6.273

TABLE 25

NINE-SPOT FLOOD NO. 2-2: CALCULATION OF E_s, E_{as} AND Q/Q_{bt}

(1) Water-Oil Ratio	(2) Cum. Oil Production	(3) Cum. Water Injected	(4) E_s, Oil Rec./ Oil in Place (2)/70.8	(5) Q/Q_{bt} = (3)/640
0.0	640	640	9.04	1.000
0.2	672	691	9.49	1.080
0.4	688	723	9.72	1.130
0.8	710	774	10.03	1.210
1.2	726	813	10.26	1.271
1.8	745	862	10.52	1.348
2.4	757	902	10.70	1.410
3.0	767	939	10.83	1.468
4.0	778	989	11.00	1.545
6.0	790	1066	11.16	1.665
8.0	796	1129	11.24	1.762
10.0	803	1182	11.35	1.849
18.0	812	1272	11.48	1.990

(6) Displacement Efficiency Ed, (Fig. 25)	(7) Actual E_{as} Areal Sweep Efficiency (4)/(6)	(8) E_s, assuming $E_{so} = .740$ (4) x $\frac{.740}{9.04}$	(9) E_{as}, assuming $E_{aso} = .740$ (7) x $\frac{.740}{11.90}$
0.759	11.90	0.740	0.740
0.785	12.09	0.777	0.751
0.799	12.18	0.796	0.757
0.812	12.36	0.822	0.768
0.815	12.59	0.840	0.783
0.816	12.90	0.862	0.802
0.818	13.09	0.876	0.814
0.818	13.24	0.888	0.824
0.818	13.45	0.901	0.836
0.818	13.63	0.914	0.848
0.818	13.75	0.921	0.855
0.818	13.88	0.930	0.864
0.818	14.04	0.940	0.874

TABLE 26

NINE-SPOT FLOOD NO. 2-3: TOTAL PRODUCTION HISTORY

(1) Cumulative Oil Prod'n.	(2) Cumulative Water Prod'n.	(3) Total Cum. Prod'n.	(4) Instantaneous Oil Prod'n.	(5) Instantaneous Water Prod'n.	(6) Instantaneous Water-oil Ratio
397.5	2.5	400.0	397.5	2.5	0.006
435.0	5.0	440.0	37.5	2.5	0.043
472.5	7.5	480.0	37.5	2.5	0.043
509.0	11.0	520.0	36.5	3.5	0.096
546.5	13.5	560.0	37.5	2.5	0.043
576.0	24.0	600.0	29.5	10.5	0.356
598.0	42.0	640.0	22.0	18.0	0.818
614.0	66.0	680.0	16.0	24.0	1.500
632.0	88.0	720.0	18.0	22.0	1.222
647.5	112.5	760.0	15.5	24.5	1.581
653.5	128.5	782.0	6.0	16.0	2.667
664.5	157.5	822.0	11.0	29.0	2.636
675.0	187.0	862.0	10.5	29.5	2.809
685.5	216.5	902.0	10.5	29.5	2.809
695.5	246.5	942.0	10.0	30.0	3.000
706.0	276.0	982.0	10.5	29.5	2.809
723.0	339.0	1062.0	17.0	63.0	3.706
728.0	374.0	1102.0	5.0	35.0	7.000
734.5	407.5	1142.0	6.5	33.5	5.154
738.0	444.0	1182.0	3.5	36.5	10.429
743.5	578.5	1262.0	5.5	74.5	13.545
750.0	592.0	1342.0	6.5	73.5	11.308
759.0	663.0	1422.0	9.0	71.0	7.889
764.0	738.0	1502.0	5.0	75.0	15.000
764.5	817.5	1582.0	0.5	79.5	159.000

TABLE 27

NINE-SPOT FLOOD NO. 2-3: PRODUCTION HISTORY, DIRECT OFFSET WELLS

(1) Cumulative Oil Prod'n.	(2) Cumulative Water Prod'n.	(3) Total Cum. Prod'n.	(4) Instantaneous Oil Prod'n.	(5) Instantaneous Water Prod'n.	(6) Instantaneous Water-oil Ratio
197.5	2.5	200.0	197.5	2.5	0.013
215.0	5.0	220.0	17.5	2.5	0.143
232.5	7.5	240.0	17.5	2.5	0.143
249.0	11.0	260.0	16.5	3.5	0.212
266.5	13.5	280.0	17.5	2.5	0.143
276.0	24.0	300.0	9.5	10.5	1.105
282.5	37.5	320.0	6.5	13.5	2.077
290.0	50.0	340.0	7.5	12.5	1.667
295.5	64.5	360.0	5.5	14.5	2.636
302.0	87.5	389.5	6.5	23.0	3.538
305.5	104.0	409.5	3.5	16.5	4.712
308.0	121.5	429.5	2.5	17.5	7.000
312.0	137.5	449.5	4.0	16.0	4.000
316.5	153.0	469.5	4.5	15.5	3.444
319.5	170.0	489.5	3.0	17.0	5.667
326.0	203.5	529.5	6.5	33.5	5.154
327.0	222.5	549.5	1.0	19.0	19.000
329.0	260.5	589.5	2.0	38.0	19.000
330.5	299.0	629.5	1.5	38.5	25.667
332.0	337.5	669.5	1.5	38.5	25.667
334.0	375.5	709.5	2.0	38.0	19.000
335.5	414.0	749.5	1.5	38.5	25.667
336.0	453.5	789.5	0.5	39.5	79.000

114

TABLE 28

NINE-SPOT FLOOD NO. 2-3:   PRODUCTION HISTORY, DIAGONAL OFFSET WELLS

(1) Cumulative Oil Prod'n.	(2) Cumulative Water Prod'n.	(3) Total Cum. Prod'n.	(4) Instantaneous Oil Prod'n.	(5) Instantaneous Water Prod'n.	(6) Instantaneous Water-oil Ratio
200.0	0.0	200.0	200.0	0.0	0.000
220.0	0.0	220.0	20.0	0.0	0.000
240.0	0.0	240.0	20.0	0.0	0.000
260.0	0.0	260.0	20.0	0.0	0.000
280.0	0.0	280.0	20.0	0.0	0.000
300.0	0.0	300.0	20.0	0.0	0.000
315.5	4.5	320.0	15.5	4.5	0.290
324.0	16.0	340.0	8.5	11.5	1.353
336.5	23.5	360.0	12.5	7.5	0.600
345.5	34.5	380.0	9.0	11.0	1.222
351.5	41.0	392.5	6.0	6.5	1.083
359.0	53.5	412.5	7.5	12.5	1.667
367.0	65.5	432.5	8.0	12.0	1.500
373.5	79.0	452.5	6.5	13.5	2.077
379.0	93.5	472.5	5.5	14.5	2.636
386.5	106.0	492.5	7.5	12.5	1.667
397.0	135.5	532.5	10.5	29.5	2.809
401.0	151.5	552.5	4.0	16.0	4.000
405.5	167.0	572.5	4.5	15.5	3.444
409.0	183.5	592.5	3.5	16.5	4.714
413.0	219.5	632.5	4.0	36.0	9.000
418.0	254.5	672.5	5.0	35.0	7.000
425.0	287.5	712.5	7.0	33.0	4.714
428.5	324.0	752.5	3.5	36.5	10.429
428.5	364.0	792.5	0.0	40.0	inf.

TABLE 29

NINE-SPOT FLOOD NO. 2-3:   CALCULATION OF

E_s, E_{as} AND Q/Q_{bt}

(1) Water-Oil Ratio	(2) Cum. Oil Prod'n. (Fig. 30)	(3) Cum. Water Injected (Fig. 30)	(4) E_s Oil Rec. ÷ Oil in Place (2)/70.8
0.0	500	500	7.06
0.2	530	535	7.49
0.4	576	581	8.14
0.8	613	656	8.66
1.2	640	713	9.04
1.8	666	776	9.41
2.4	687	848	9.70
3.0	701	900	9.90
4.0	720	976	10.18
6.0	742	1081	10.48
8.0	752	1162	10.62
10.0	756	1238	10.68
18.0	760	1488	10.73

(5) Q/Q_{bt} = (3)/500	(6) Displacement Efficiency Ed, (Fig. 25)	(7) Actual E_{as}, Areal Sweep Effic. (4)/(6)	(8) E_s, assuming E_{so} = 0.740 (4) x $\frac{.740}{7.06}$	(9) E_{as}, assuming E_{aso} = 0.740 (7) x $\frac{.740}{9.31}$
1.000	0.759	9.31	0.740	0.740
1.070	0.785	9.54	0.784	0.758
1.162	0.799	10.19	0.853	0.809
1.311	0.812	10.67	0.908	0.846
1.428	0.815	11.09	0.946	0.880
1.552	0.816	11.53	0.986	0.916
1.698	0.818	11.86	1.017	0.942
1.800	0.818	12.10	1.038	0.961
1.952	0.818	12.43	1.067	0.988
2.165	0.818	12.81	1.098	0.018
2.325	0.818	13.00	1.113	1.033
2.475	0.818	13.06	1.120	1.038
2.975	0.818	13.13	1.124	1.043

TABLE 30

FLOOD NO. 2-4: TOTAL PRODUCTION

Total Cum. Production	Cum. Wtr. Production	Cum. Oil Production	Inst. Oil Prod'n.	Inst. Wtr. Production	Inst. W.O.R.
40.0	tr.	40.0	40.0	tr.	0.000
80.0	1.0	79.0	39.0	1.0	0.026
120.0	7.0	113.0	34.0	6.0	0.176
160.0	17.0	143.0	30.0	10.0	0.333
200.0	29.5	170.5	27.5	12.5	0.454
240.0	46.5	193.5	23.0	17.0	0.739
320.0	80.0	240.0	46.5	33.5	0.720
400.0	124.0	276.0	36.0	44.0	1.222
480.0	165.0	315.0	39.0	41.0	1.051
560.0	215.5	344.5	29.5	50.5	1.712
640.0	267.5	372.5	28.0	52.0	1.857
720.0	316.5	403.5	31.0	49.0	1.581
800.0	376.0	424.0	20.5	59.5	2.902
880.0	415.0	465.0	41.0	39.0	0.951
960.0	467.5	492.5	27.5	52.5	1.909
1040.0	524.5	515.5	23.0	57.0	2.478
1120.0	582.0	538.0	22.5	57.5	2.555
1200.0	638.0	562.0	24.0	56.0	2.333
1280.0	693.0	587.0	25.0	55.0	2.200
1360.0	750.5	609.5	22.5	57.5	2.555
1440.0	808.5	631.5	22.0	58.0	2.636
1520.0	866.5	653.5	22.0	58.5	2.659
1600.0	927.0	673.0	19.5	60.0	3.077
1680.0	980.5	699.5	26.5	53.5	2.019
1760.0	1036.5	723.5	24.0	56.0	2.333
1840.0	1100.0	740.0	16.5	63.5	3.848
1920.0	1162.5	757.5	17.5	62.5	3.571
2000.0	1223.0	777.0	19.5	60.5	3.103
2080.0	12825	797.5	20.5	59.5	2.902
2160.0	1343.0	817.0	19.5	60.5	3.103
2240.0	1404.5	835.5	18.5	61.5	3.324
2320.0	1467.0	853.0	17.5	62.5	3.571
2400.0	1531.0	869.0	16.0	64.0	4.000
2520.0	1625.0	895.0	26.0	94.0	3.615
2640.0	1722.5	917.5	22.5	97.5	4.333
2720.0	1789.5	930.5	13.0	67.0	5.154
2800.0	1856.5	943.5	13.0	67.0	5.154

TABLE 30 (Cont'd.)

Total Cum. Production	Cum. Wtr. Production	Cum. Oil Production	Inst. Oil Prod'n.	Inst. Wtr. Production	Inst. W.O.R.
2880.0	1924.0	956.0	12.5	67.5	5.400
2960.0	1991.0	969.0	13.0	67.0	5.154
3040.0	2061.0	979.0	10.0	70.0	7.000
3120.0	2134.5	985.5	6.5	73.5	11.308
3200.0	2207.0	993.0	7.5	72.5	9.667
3280.0	2278.5	1001.5	8.5	71.5	8.412
3360.0	2350.5	1009.5	8.0	72.0	9.000
3440.0	2424.0	1016.0	6.5	73.5	11.308
3520.0	2500.0	1020.0	4.0	76.0	19.000
3600.0	2575.5	1024.5	4.5	75.5	16.778
3680.0	2651.5	1028.5	4.0	76.0	19.000
3760.0	2726.5	1033.5	5.0	75.0	15.000
3840.0	2801.5	1038.5	5.0	75.0	15.000
3920.0	2877.5	1042.5	4.0	76.0	19.000
4000.0	2954.0	1046.0	3.5	76.5	21.857

TABLE 31

NINE-SPOT FLOOD NO. 2-4:   DIRECT OFFSET WELLS

Total Cum. Production	Cum. Wtr. Production	Cum. Oil Production	Inst. Oil Production	Inst. Wtr. Production	Inst. W.O.R.
20.0	tr.	20.0	20.0	tr.	0.000
40.0	1.0	39.0	19.0	1.0	0.053
60.0	7.0	53.0	14.0	6.0	0.429
80.0	15.0	65.0	12.0	8.0	0.667
100.0	25.5	74.5	9.5	10.5	1.105
120.0	38.0	82.0	7.5	12.5	1.667
160.0	63.0	97.0	15.0	25.0	1.667
200.0	91.5	108.5	11.5	28.5	2.478
240.0	116.5	123.5	15.0	25.0	1.667
280.0	145.0	135.0	11.5	28.0	2.478
320.0	173.0	147.0	12.0	28.0	2.333
360.0	198.0	162.0	15.0	25.0	1.667
400.0	231.5	168.5	6.5	33.5	5.154
440.0	254.0	186.0	17.5	22.5	1.286
480.0	283.0	197.0	11.0	29.0	2.636
520.0	313.0	207.0	10.0	30.0	3.000
560.0	344.0	216.0	9.0	31.0	3.444
600.0	374.0	226.0	10.0	30.0	3.000
640.0	404.5	235.5	9.5	30.5	3.211
680.0	436.5	243.5	8.0	32.0	4.000
720.0	466.5	253.5	10.0	30.0	3.000
760.0	498.5	261.5	8.0	32.0	4.000
800.0	531.5	268.5	7.0	33.0	4.714
840.0	559.0	281.0	12.5	27.5	2.200
880.0	590.0	290.0	9.0	31.0	3.444
920.0	623.0	297.0	7.0	33.0	4.714
960.0	654.5	305.5	8.5	31.5	3.706
1000.0	687.0	313.0	7.5	32.5	4.333
1040.0	719.5	320.5	7.5	32.5	4.333
1080.0	750.5	329.5	9.0	31.0	3.444
1120.0	783.5	336.5	7.0	33.0	4.714
1160.0	817.0	343.0	6.5	33.5	5.154
1200.0	851.5	348.5	5.5	34.5	6.273
1260.0	901.0	359.0	10.5	49.5	4.714
1320.0	950.5	369.5	10.5	49.5	4.714
1360.0	985.5	374.5	5.0	35.0	4.000
1400.0	1021.5	378.5	4.0	36.0	9.000

119

TABLE   31 (Cont'd.)

Total Cum. Production	Cum. Wtr. Production	Cum. Oil Production	Inst. Oil Production	Inst. Wtr. Production	Inst. W.O.R.
1440.0	1056.0	384.0	5.5	34.5	6.273
1480.0	1091.0	389.0	5.0	35.0	7.000
1520.0	1126.5	393.5	4.5	33.5	7.889
1560.0	1164.0	396.0	2.5	37.5	15.000
1600.0	1201.0	399.0	3.0	37.0	12.333
1640.0	1237.0	403.0	4.0	36.0	9.000
1680.0	1273.5	406.5	3.5	36.5	10.429
1720.0	1311.0	409.0	2.5	37.5	15.000
1760.0	1349.5	410.5	1.5	38.5	25.667
1800.0	1388.0	412.0	1.5	38.5	25.667
1840.0	1426.0	414.0	2.0	38.0	19.000
1880.0	1463.5	416.5	2.5	37.5	15.000
1920.0	1501.5	418.5	2.0	38.0	19.000
1960.0	1539.5	420.5	2.0	38.0	19.000
2000.0	1578.5	421.5	1.0	39.0	39.000

TABLE 32

NINE-SPOT FLOOD NO. 2-4:   DIAGONAL OFFSET WELLS

Total Cum. Production	Cum. Water Production	Cum. Oil Production	Inst. Oil Production	Inst. Wtr. Production	Inst. W.O.R.
20.0	tr.	20.0	20.0	tr.	0.000
40.0	tr.	40.0	20.0	tr.	0.000
60.0	tr.	60.0	20.0	tr.	0.000
80.0	2.0	78.0	18.0	2.0	0.111
100.0	4.0	96.0	18.0	2.0	0.111
120.0	8.5	111.5	15.5	4.5	0.290
160.0	17.0	143.0	31.5	8.5	0.270
200.0	32.5	167.5	24.5	15.5	0.633
240.0	48.5	191.5	24.0	16.0	0.667
280.0	70.5	209.5	18.0	22.0	1.222
320.0	94.5	225.5	16.0	24.0	1.500
360.0	118.5	241.5	16.0	24.0	1.500
400.0	144.5	255.5	14.0	26.0	1.857
440.0	161.0	279.0	23.5	16.5	0.702
480.0	184.5	295.5	16.5	23.5	1.424
520.0	211.5	308.5	13.0	27.0	2.077
560.0	238.0	322.0	13.5	26.5	1.963
600.0	264.0	336.0	14.0	26.0	1.857
640.0	288.5	351.5	15.5	24.5	1.581
680.0	314.0	366.0	14.5	25.5	1.759
720.0	342.0	378.0	12.0	28.0	2.333
760.0	368.5	392.0	14.0	26.5	1.893
800.0	395.5	404.5	12.5	27.0	2.160
840.0	421.5	418.5	14.0	26.0	1.857
880.0	446.5	433.5	15.0	25.0	1.667
920.0	477.0	443.0	9.5	30.5	3.211
960.0	508.0	452.0	9.0	31.0	3.444
1000.0	536.0	464.0	12.0	28.0	2.333
1040.0	563.0	477.0	13.0	27.0	2.077
1080.0	592.5	487.5	10.5	29.5	2.810
1120.0	621.0	499.0	11.5	28.5	2.478
1160.0	650.0	510.0	11.0	29.0	2.636
1200.0	679.5	520.5	10.5	29.5	2.810
1260.0	724.0	536.0	15.5	44.5	2.870
1320.0	772.0	548.0	12.0	48.0	4.000
1360.0	804.0	556.0	8.0	32.0	4.000
1400.0	835.0	565.0	9.0	31.0	3.444

TABLE 32 (Cont'd.)

Total Cum. Production	Cum. Water Production	Cum. Oil Production	Inst. Oil Production	Inst. Wtr. Production	Inst. W.O.R.
1440.0	868.0	572.0	7.0	33.0	4.714
1480.0	900.0	580.0	8.0	32.0	4.000
1520.0	934.5	585.5	5.5	34.5	6.273
1560.0	970.5	589.5	4.0	36.0	9.000
1600.0	1006.0	594.0	4.5	35.5	7.889
1640.0	1041.5	598.5	4.5	35.5	7.889
1680.0	1077.0	603.0	4.5	35.5	7.889
1720.0	1113.0	607.0	4.0	36.0	9.000
1760.0	1150.5	609.5	2.5	37.5	15.000
1800.0	1187.5	612.5	3.0	37.0	12.333
1840.0	1225.5	614.5	2.0	38.0	19.000
1880.0	1263.0	617.0	2.5	37.5	15.000
1920.0	1300.0	620.0	3.0	37.0	12.333
1960.0	1338.0	622.0	2.0	38.0	19.000
2000.0	1375.5	624.5	2.5	37.5	15.000

TABLE 33

NINE-SPOT FLOOD NO. 2-4: CALCULATION OF TOTAL SWEEP EFFICIENCY (E_s),

AREAL SWEEP EFFICIENCY (E_{as}) AND THE RATIO OF WATER

INJECTED TO WATER INJECTED TO BREAKTHROUGH (Q/Q_{bt}).

(1) Water-Oil Ratio	(2) Cum. Oil Production Fig. 33	(3) Cum. Water Injected Fig. 33	(4) E_s = oil rec./ Oil in Place = (2)/75.2	(5) Q/Q_{bt} = (3)/67
0.0	67 cc	67 cc	0.892	1.000
0.1	88	94	1.172	1.403
0.2	109	122	1.451	1.821
0.3	130	150	1.731	2.24
0.4	151	177	2.01	2.64
0.5	161	205	2.40	3.06
0.6	193	232	2.570	3.46
0.7	214	263	2.85	3.93
0.8	234	300	3.115	4.48
0.9	255	333	3.395	4.96
1.0	276	368	3.675	5.49
1.2	318	440	4.23	6.56
1.4	360	540	4.79	8.06
1.6	401	670	5.34	10.00
2.0	498	990	6.64	14.78
2.4	591	1390	7.86	20.75
2.8	740	1790	9.85	26.7
3.2	838	2085	11.17	31.15
3.6	866	2305	11.53	34.45
4.0	890	2480	11.85	37.00
6.0	969	2995	12.90	44.7
8.0	998	3260	13.30	48.6
12.0	1015	3375	13.52	50.4
20.0	1038	3930	13.82	65.6

TABLE 33 (Cont'd.)

(6) Displacement Efficiency Ed, (Fig. 20)	(7) Areal Sweep Efficiency $E_{as} = (4)/(6)$
0.424	2.10
0.450	2.60
0.479	3.03
0.502	3.43
0.527	3.815
0.545	4.41
0.562	4.58
0.580	4.92
0.592	5.26
0.605	5.61
0.618	5.94
0.640	6.62
0.660	7.25
0.678	7.88
0.698	9.51
0.716	10.98
0.728	13.52
0.744	15.02
0.752	15.38
0.761	15.58
0.794	16.25
0.802	16.58
0.804	16.86
0.804	17.20

DATA MODIFIED AFTER P. 2014,
HANDBOOK OF CHEMISTRY AND
PHYSICS, 38th EDITION, 1957

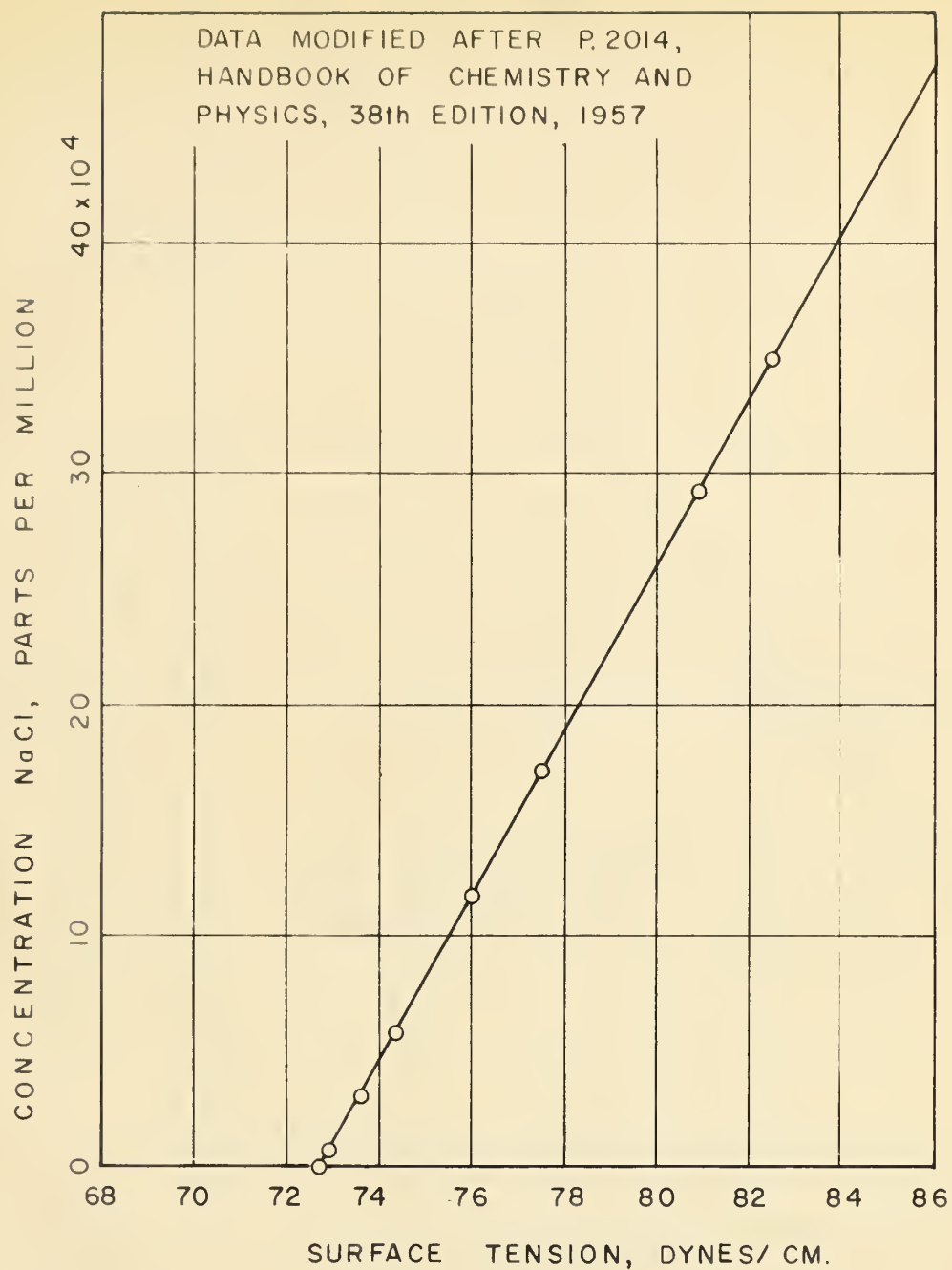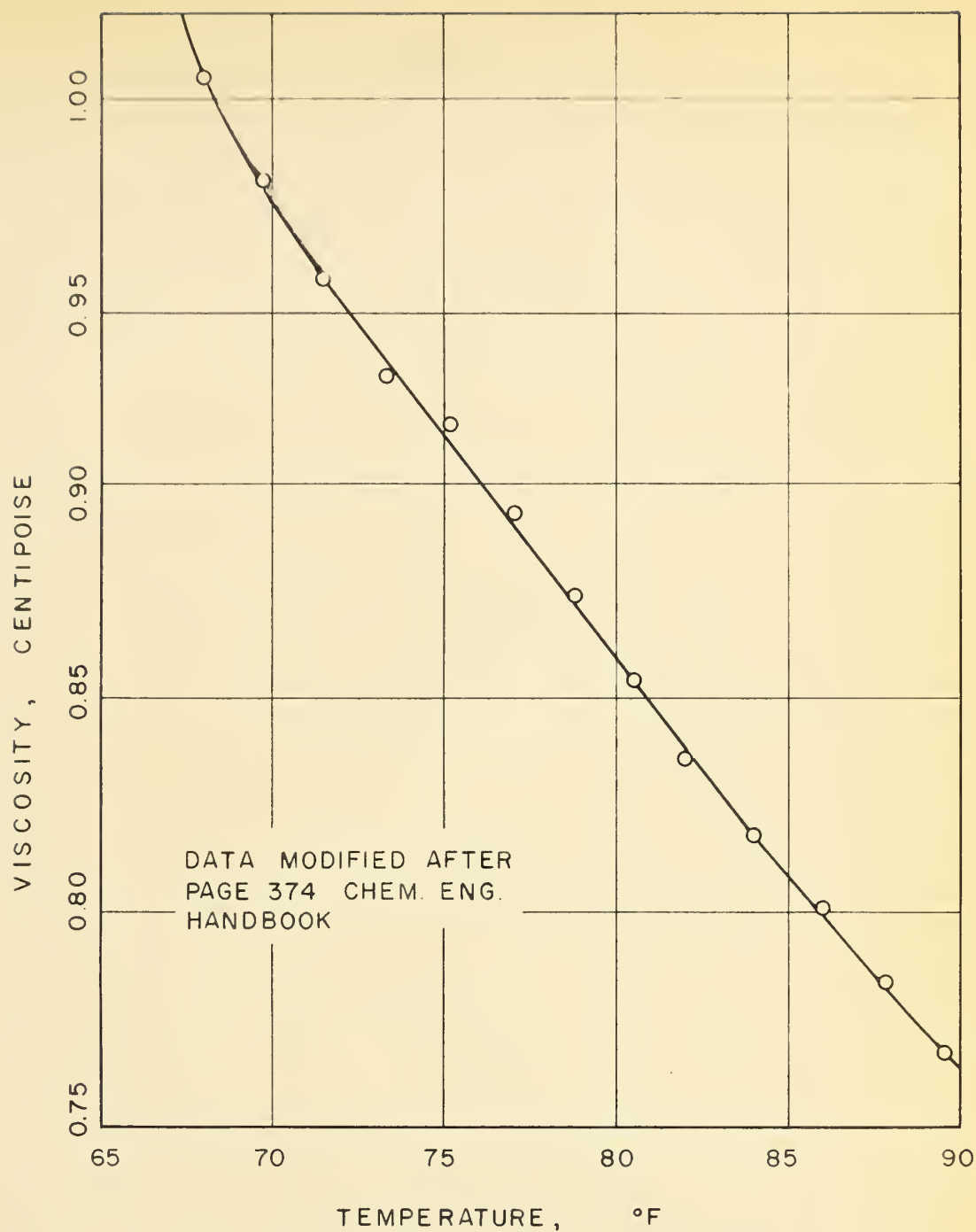FIG. 38   SURFACE   TENSION   OF   AN   NaCl
            BRINE   VERSUS   CONCENTRATION

FIG. 39   VISCOSITY OF WATER VERSUS
TEMPERATURE